

A METHODOLOGY FOR ACCURATE SIMULATION OF MOVABLE PARTS UNDER THE INFLUENCE OF ELECTROMAGNETIC FORCES

Christian Olivier van Staden

A dissertation submitted to the Faculty of Engineering and the Built Environment,
University of the Witwatersrand, Johannesburg, in fulfilment of the requirements for the
degree of Master of Science in Engineering.

Johannesburg, 2008

DECLARATION

I declare that this dissertation is my own, unaided work. It is being submitted for the degree of Master of Science in Engineering at the University of the Witwatersrand, Johannesburg. It has not been submitted before for any degree or examination at any other University.

Signature of Candidate

_____ day of _____ in the year _____

ABSTRACT

Many devices, for example contactors and solenoid actuated valves, rely on ferromagnetic components moving under the influence of electromagnetic force for their operation. The popularity of this technology stems from the fact that it is an elegant, cost effective and robust way to convert electrical energy into mechanical work. From a product design point of view it is very important to quantify the magnitude of the electromagnetic force and to predict the behaviour of ferromagnetic components under the influence of this force. In most cases these forces are estimated by means of first order calculations or Finite Element Methods. It is plausible, as this dissertation shows, that direct measurement can be used to replace or supplement theoretical methods to obtain these forces. However, limited previous work describing methods and techniques for the measurement of these electromagnetic forces, are available in the public domain. In general, prior work in this field [12] is very specialised and limited with respect to the range of forces that can be measured, and not easily adaptable to a product design environment.

This thesis proposes a novel piece of equipment for the measurement of electromagnetic forces acting on ferromagnetic components, and a method to predict product performance based on these measurements.

The measurement equipment, and product performance prediction, is described and evaluated for the case of low voltage hydraulic magnetic circuit breakers.

Low voltage hydraulic magnetic circuit breakers are a particularly interesting subject as it contains one source of electromagnetic force acting on two ferromagnetic components. The two ferromagnetic components have different equations of motion, with dramatically different damping coefficients. A further complication in the operation of hydraulic magnetic circuit breakers is that these ferromagnetic components can move separately or simultaneously. The motion of the components is influenced by the magnitude of the applied electromagnetic force and their position relative to each other. Low voltage hydraulic magnetic circuit breaker performance is subject to the combined motion of these two ferromagnetic components.

This work concludes that the method for measuring electromagnetic forces with the aim of predicting device performance is feasible, and that it produces good results where electromagnetic forces need to be known to high accuracies.

ACKNOWLEDGEMENTS

The author would like to thank and acknowledge the various persons without whom this work would not have been possible:

- Eldridge van Niekerk under whose guidance, this work and most of the work that forms the basis of this thesis has been conducted, either by himself or by others. His tutelage, guidance and efforts to make this thesis a reality were invaluable, and are well appreciated.
- Prof Willie Cronje for all his time, insightful discussions and advice.
- Hagen Niebering who laid a solid foundation in the field of mathematical modelling of hydraulic magnetic circuit breakers on which this work draws heavily.
- All other people involved in aiding to bring this work to fruition, the laboratory personnel for their endless testing to help evaluate this work and all who gave some of their time to make it possible for the thesis to be published.

TABLE OF CONTENTS

1. INTRODUCTION	13
1.1 FEM SIMULATIONS.....	13
1.2 ELECTROMAGNETIC FORCE MEASUREMENT.....	14
1.3 THESES OBJECTIVE	14
1.4 OUTLINE OF THE THESIS	15
1.4.1 CHAPTER 2 – LOW VOLTAGE CIRCUIT BREAKERS	15
1.4.2 CHAPTER 3 – FORCE MEASUREMENT EQUIPMENT.....	15
1.4.3 CHAPTER 4 – ACCURACY OF ELECTROMAGNETIC FORCE MEASUREMENTS	15
1.4.4 CHAPTER 5 – DC CIRCUIT BREAKER BEHAVIOUR PERFORMANCE PREDICTION.....	16
1.4.5 CHAPTER 6 – AC CIRCUIT BREAKER BEHAVIOUR PERFORMANCE PREDICTION	16
1.4.6 CHAPTER 7 – TEST METHOD AND EQUIPMENT.....	16
1.4.7 CHAPTER 8 – SUMMARY OF RESULTS	16
1.4.8 CHAPTER 9 – CONCLUSION.....	16
 2. LOW VOLTAGE CIRCUIT BREAKERS	 17
2.1 INTRODUCTION	17
2.1.1 TIME-DELAY CURVE	17
2.2 LOW VOLTAGE CIRCUIT BREAKER TECHNOLOGIES	18
2.2.1 THERMAL MAGNETIC CIRCUIT BREAKERS	18
2.2.2 HYDRAULIC MAGNETIC CIRCUIT BREAKERS.....	19
2.3 SENSING UNIT PERFORMANCE MEASURES	21
2.3.1 MUST-HOLD-POINT	21
2.3.2 MUST-TRIP-POINT.....	21
2.3.3 OVERLOAD CHARACTERISTICS	21
2.3.4 INSTANTANEOUS POINT	21
2.3.5 IMPULSE TOLERANCE	22
2.4. MUST-HOLD-POINT AND MUST-TRIP-POINT.....	22
2.4.1 FACTORS INFLUENCING THE CORE-PULL-IN POINT.....	23
2.4.2 FACTORS INFLUENCING THE ARMATURE RESPONSE POINT	23
2.5. OVERLOAD CHARACTERISTICS.....	23
2.6 INSTANTANEOUS REGION	23
2.7. PREDICTION OF SENSING UNIT BEHAVIOUR	24
2.8 CONCLUSION.....	24

3. FORCE MEASUREMENT EQUIPMENT	25
3.1 INTRODUCTION	25
3.2 PHYSICAL DESCRIPTION	25
3.3 FUNCTIONAL DESCRIPTION	27
3.3.1 LOAD MEASUREMENT PARAMETERS	27
3.3.2 LOAD CURRENT SETTINGS	28
3.3.3 POSITION THE CORE AND ARMATURE IN KNOWN POSITIONS	29
3.3.4 MEASUREMENT	30
3.3.5 SAVING OF RESULTS TO FILE	33
3.4 CONCLUSION	33
 4. ACCURACY OF ELECTROMAGNETIC FORCE MEASUREMENT	 34
4.1 INTRODUCTION	34
4.2 MEASUREMENT SENSITIVITY	34
4.3 MEASUREMENT SYSTEM REPEATABILITY	35
4.4 INFLUENCE OF LOAD CELL CALIBRATION ON MEASUREMENT ACCURACY	36
4.4.1 EFFECT OF LSB UNCERTAINTY	37
4.4.2 EFFECT OF DISCREET CALIBRATION POINTS	37
4.4.3 EFFECT OF CALIBRATION FACTOR ROUNDING	38
4.4.4 CUMULATIVE MEASUREMENT ERROR	38
4.5 CONTROL ACCURACY	38
4.5.1 CURRENT CONTROL AND REGULATION	39
4.5.1.1 <i>Current Control Sensitivity</i>	39
4.5.1.2 <i>Current Control Repeatability</i>	40
4.5.1.3 <i>Current Regulation</i>	40
4.5.2 CORE AND ARMATURE POSITION CONTROL	40
4.5.2.1 <i>Positioning Stages – Sensitivity, Repeatability & Accuracy</i>	41
4.5.2.2 <i>Positioning accuracy due to load cell deflection</i>	41
4.5.2.2 <i>Core Reference Position Inaccuracy</i>	42
4.5.2.3 <i>Armature Reference Position Inaccuracy</i>	42
4.5.2.4 <i>Effect of Load Cell Deflection during the Measurement Sequence</i>	43
4.6 TOTAL MEASUREMENT ERROR	44
4.7 CONCLUSION	44
 5. DC CIRCUIT BREAKER PERFORMANCE PREDICTION	 45
5.1 INTRODUCTION	45
5.2 MEASURED ELECTROMAGNETIC FORCES	45
5.3 CPP PREDICTION	46
5.3.1 SCALING OF ELECTROMAGNETIC FORCE MEASUREMENTS	47

5.3.2 MAXIMUM AND MINIMUM CPP PREDICTION	48
5.4 ARP CALCULATION	50
5.5 TIME-DELAY CALCULATION	51
5.5.1 DETERMINATION OF THE TRIP-GAP	52
5.5.2 EQUATIONS OF MOTION	53
5.6 CONCLUSION.....	53
6. AC CIRCUIT BREAKER PERFORMANCE PREDICTION	54
6.1 INTRODUCTION	54
6.2 ELECTROMAGNETIC FORCES	54
6.2.1 CALCULATION BASED ON DC MEASUREMENTS.....	54
6.2.2 HYSTERESIS LOSSES	55
6.2.3 EDDY CURRENT LOSSES.....	55
6.2.4 TEMPERATURE MEASUREMENT	55
6.3 CORE AND ARMATURE MOTION UNDER AC CONDITIONS	56
6.4 CONCLUSION.....	58
7. METHOD OF TESTING AND TEST EQUIPMENT	59
7.1 INTRODUCTION	59
7.2 DESCRIPTION OF THE TEST METHOD	59
7.2.1 DC TEST SETUP.....	59
7.2.2 AC TEST SETUP	60
7.3 CURRENT MEASUREMENT.....	60
7.4 MEASUREMENT UNCERTAINTIES.....	60
7.4.1 CURRENT MEASURING RESISTANCE CALIBRATION	61
7.4.2 OSCILLOSCOPE ACCURACY	61
7.4.3 TEST DYNAMICS	61
7.4.4.1 DC TEST DYNAMICS	61
7.4.4.2 AC TEST DYNAMICS	61
7.4.5 HUMAN INTERFACE.....	62
7.5 CONCLUSION.....	62
8. SUMMARY OF RESULTS.....	63
8.1 INTRODUCTION	63
8.2 TEST SAMPLE DESCRIPTION.....	63
8.3 ELECTROMAGNETIC FORCE MEASUREMENTS	64
8.3.1 MEASUREMENT REPEATABILITY.....	64
8.4 PREDICTED CORE MOVEMENT UNDER AC AND DC CONDITIONS	67
8.5 PREDICTED ARMATURE RESPONSE UNDER AC AND DC CONDITIONS	68

8.6 AC VS. DC TIME-DELAYS.....	69
8.7 CPP RESULTS.....	70
8.8 ARP RESULTS	72
8.9 TIME-DELAY RESULTS	72
8.10 CONCLUSION	76
9. SUMMARY AND CONCLUSION.....	77
9.1 INTRODUCTION	77
9.2 THE AIM	77
9.3 SUMMARY.....	77
9.4 SUMMARY OF RESULTS	78
9.5 POSSIBLE IMPROVEMENTS	78
9.6 CONCLUSION.....	78
APPENDIX A.....	81
A.1 INTRODUCTION	81
A.2 PREDICTION RESULTS	82
A.3 PREDICTED RESULTS COMPARED TO MEASUREMENTS	96

LIST OF FIGURES

Figure	Page
<i>Figure 2.1: Time-Delay curve example</i>	18
<i>Figure 2.2: Thermal Magnetic circuit breaker</i>	19
<i>Figure 2.3: The Current Sensing Unit of a Hydraulic Magnetic Circuit Breaker</i>	20
<i>Figure 3. 1: Load cell connection to core (some circuit breaker components omitted)</i>	26
<i>Figure 3.2: Image of FMA</i>	26
<i>Figure 3. 3: FMA subsections</i>	27
<i>Figure 3. 4: Subsection responsible for the loading of measurement parameters.</i>	28
<i>Figure 3. 5: Current setup procedure</i>	29
<i>Figure 3. 6: Reset core and armature to their default measurement starting positions.</i>	30
<i>Figure 3.7: Measurement sequence</i>	32
<i>Figure 4.1: Measurement Repeatability</i>	36
<i>Figure 4.2: Load Cell Deflection vs. Measured Force</i>	42
<i>Figure 5.1: Measured vs. Calculated Core Force Values</i>	48
<i>Figure 5.2: Armature motion at the ARP.</i>	50
<i>Figure 5. 3: Electromagnetic forces acting on the armature at different core gaps and currents.</i>	52
<i>Figure 6.1: Core temperature measurements</i>	56
<i>Figure 7.1: DC test setup</i>	59
<i>Figure 7.2: AC test setup</i>	60
<i>Figure 8.1: Output of the Matlab function ‘probplot’ applied to a set of core force measurements</i>	65
<i>Figure 8.2: AC and DC Core Movement</i>	67
<i>Figure 8.3: Armature response under AC conditions</i>	68
<i>Figure 8.4: Armature response under DC conditions</i>	69
<i>Figure 8.5: Monte Carlo Analysis on the CPP of 15A Circuit Breaker Compared to Measurement Results</i>	71
<i>Figure 8. 6: Monte Carlo Analysis on the CPP of 5A Circuit Breaker Compared to Measurement Result</i>	71
<i>Figure 8 7:2.5A Slow time-delay curve results</i>	73
<i>Figure 8.8: 2.5A Medium time-delay curve results</i>	74
<i>Figure 8 9: 2.5A Fast time-delay curve results</i>	75
<i>Figure A. 1: 2.5A Circuit Breaker Slow Time-Delay Curve Results</i>	96
<i>Figure A. 2: 4A Circuit Breaker Slow Time-Delay Curve Results</i>	97
<i>Figure A. 3: 5A Circuit Breaker Slow Time-Delay Curve Results</i>	98
<i>Figure A. 4: 12A Circuit Breaker Slow Time-Delay Curve Results</i>	99
<i>Figure A. 5: 12.5A Circuit Breaker Slow Time-Delay Curve Results</i>	100
<i>Figure A. 6: 15A Circuit Breaker Slow Time-Delay Curve Results</i>	101
<i>Figure A. 7: 2.5A Circuit Breaker Medium Time-Delay Curve Results</i>	102
<i>Figure A. 8: 4A Circuit Breaker Medium Time-Delay Curve Results</i>	103
<i>Figure A. 9: 5A Circuit Breaker Medium Time-Delay Curve Results</i>	104
<i>Figure A. 10: 12A Circuit Breaker Medium Time-Delay Curve Results</i>	105
<i>Figure A. 11: 12.5A Circuit Breaker Medium Time-Delay Curve Results</i>	106
<i>Figure A. 12: 15A Circuit Breaker Medium Time-Delay Curve Results</i>	107
<i>Figure A. 13: 2.5A Circuit Breaker Fast Time-Delay Curve Results</i>	108
<i>Figure A. 14: 4A Circuit Breaker Fast Time-Delay Curve Results</i>	109
<i>Figure A. 15: 12A Circuit Breaker Fast Time-Delay Curve Results</i>	110
<i>Figure A. 16: 12.5A Circuit Breaker Fast Time-Delay Curve Results</i>	111

LIST OF TABLES

Table	Page
<i>Table 3.1: Complete set of measurement data.....</i>	<i>31</i>
<i>Table 4.1: Segment of the load cell calibration data.....</i>	<i>37</i>
<i>Table 5.1: Measured electromagnetic force.....</i>	<i>46</i>
<i>Table 5.2: Published core spring data</i>	<i>49</i>
<i>Table 5.3: Maximum and Minimum Spring Force values</i>	<i>49</i>
<i>Table 8.1: 100% I_n Measurement Results of a 12A C-Frame Sample.....</i>	<i>66</i>
<i>Table 8. 2: 95% Confidence interval calculated from Table 2.....</i>	<i>66</i>
<i>Table 8.3: AC and DC ARP results</i>	<i>72</i>

DEFINITIONS AND SYMBOLS

I_n	- Circuit Breaker nominal (Rated) current
I	- Current
Φ	- Magnetic flux
μ_0	- Permittivity constant of a vacuum
B	- Magnetic induction
\mathcal{A}	- Air gap Area
T_m	- Electromagnetic torque
T_s	- Spring Torque
F_m	- Electromagnetic force
F_s	- Spring Force
k_a	- Lumped friction coefficient
θ	- Armature angle
m	- Mass of component
t	- Time
L_1	- Compression spring length
L_2	- Compression spring length
F_1	- Spring force at L_1
F_2	- Spring force at L_2
k	- Spring rate
x	- Core gap
k_v	- Viscous friction coefficient
f	- Frequency
F_{AC}	- AC electromagnetic force
F_{DC}	- DC electromagnetic force
P_b	- Hysteresis losses
v_c	- Linear velocity of the core
v_a	- Rotational velocity of the armature
L	- Inductance
R	- Resistance
σ	- Standard deviation
N	- Number of samples
μ	- Sample mean
I_{CPP}	- Core-pull-in-point current

ACRONYMS

FEM	- Finite Element Method
BEM	- Boundary Element Method
DC	- Direct Current
AC	- Alternating Current
MMF	- Magnetomotive Force
IEC	- International Electrotechnical Commission
CPP	- Core Pull in Point
ARP	- Armature Response Point
FMA	- Force Measurement Apparatus
PC	- Personal Computer
gf	- Grams of force
A/D	- Analogue to Digital Converter
EMI	- Electromagnetic Interference
MSB	- Most Significant Bit
LSB	- Least Significant Bit
RAM	- Random Access Memory
SMPS	- Switch Mode Power Supply
RMS	- Root Mean Square
EMI	- Electromagnetic Interference

CHAPTER 1

INTRODUCTION

Many engineering applications require the transformation of electrical energy into mechanical (potential or kinetic) energy. A simple example of such a system is a solenoid coil enclosing a ferromagnetic core. When electrical energy is applied to the coil it manifests itself as electromagnetic force acting on the ferromagnetic core. Predicting the movement of the ferromagnetic core under the influence of the electromagnetic force is a crucial part of the design process for equipment based on the plunger action of the solenoid. In order to accurately achieve this, the electromagnetic force acting on the core needs to be known.

1.1 FEM Simulations

The most common method for obtaining the electromagnetic force acting on ferromagnetic components, as a result of the close proximity of a current carrying conductor, is by means of FEM (Finite Element Method) or BEM (Boundary Element Method) simulations. Various software packages are commercially available for this purpose.

The major advantage of packages of this nature is that no physical model is needed. This allows the designer to form an idea of the electromagnetic forces that will act on the ferromagnetic components during the concept design phase. For this purpose these tools are ideal. The results, however, are only as good as the modelling process, which can be difficult.

In order to obtain very accurate results from electromagnetic simulations the geometry of the ferromagnetic components as well as the current carrying conductors need to be modelled in detail. In addition the magnetic properties (BH-curve) of the ferromagnetic components need to be known and incorporated into the model to be solved. These two criteria complicate the modelling and simulation process when high accuracy is required.

When the geometrical complexity is increased the modelling and simulation time is increased dramatically. Including the electromagnetic (non-linear) material properties in the model will further increase the simulation time. For these reasons it can be argued that, when very accurate electromagnetic force values are required FEM or BEM simulations are not the optimal method.

1.2 Electromagnetic Force Measurement

An alternative to calculating the electromagnetic forces using Finite Element Methods is to measure the forces acting on the ferromagnetic components. Measuring the forces effectively eliminates all the problems mentioned previously.

Measuring forces on a physical sample eliminates the need for an accurate modelling process as well as eliminating the disadvantage of long simulation times.

There are, however, implied drawbacks in measuring electromagnetic forces. Firstly, a sample to be measured is always needed, which transfers the effort of the modelling process to the manufacture of a sample to be measured. Secondly, specialized equipment for measuring the electromagnetic forces is needed. In addition the equipment for measuring the electromagnetic forces will by its very nature be customised and closely matched to the system it is designed to measure, losing the advantage of generality offered by the commercial simulation packages. Thus, the measurement of electromagnetic forces is only a viable option in very specific cases. For these reasons the measurement of electromagnetic forces is not generally employed. Measurement is however applicable in cases where the electromagnetic force needs to be known at a large number of component positions and currents. When needing this amount of electromagnetic data FEM simulations are eliminated as a solution, due to the time they would take.

1.3 Theses Objective

This thesis evaluates the accuracy and the usability of a method for the prediction of the movement of ferromagnetic components under the influence of electromagnetic forces based on static electromagnetic force measurements. This will be done by means of a practical example. The ideal case study for this purpose is the sensing unit of low voltage hydraulic magnetic circuit breakers. These circuit breakers consist of two ferromagnetic parts that move due to electromagnetic forces acting upon them, and the design process for these products leans very heavily on the accurate prediction of the movement of both

components [1]. The prediction of these motions in turn requires accurate values for the electromagnetic forces acting upon them.

This thesis covers the DC measurement of the electromagnetic forces acting on the ferromagnetic components and the prediction of the dynamic behaviour of the components based on these static measurements. The behaviour of the ferromagnetic components is related back to the performance measures for the circuit breakers. The method is evaluated based on the success in predicting the performance of the hydraulic magnetic circuit breaker using the electromagnetic force measurements. This evaluation process is done for two cases:

1. Static, direct current measurements are used to predict the DC behaviour of hydraulic magnetic circuit breakers.
2. Static, direct current measurements are used to predict the AC behaviour of this type of circuit breaker.

1.4 Outline of this Thesis

1.4.1 Chapter 2 – Low Voltage Circuit Breakers

This section covers the theory of operation of low voltage circuit breakers and the variables governing their performance. Both hydraulic magnetic and thermal magnetic low voltage circuit breakers are discussed, with specific emphasis on low voltage circuit breakers of the hydraulic magnetic type.

1.4.2 Chapter 3 – Force Measurement Equipment

The equipment designed and built for the measurement of electromagnetic forces acting on low voltage hydraulic magnetic circuit breaker components is described. The measurement equipment is described in terms of its basic operation, its various subsystems and their function and the sequence of electromagnetic force measurements it will perform.

1.4.3 Chapter 4 – Accuracy of Electromagnetic Force Measurements

The measurement equipment is described in terms of its measurement accuracy. The components and parameters influencing the measurement accuracy are discussed and the impact on the measurement accuracy of each of these is quantified. Lastly the cumulative effect of all these combined sources of measurement error is calculated.

1.4.4 Chapter 5 – DC Circuit Breaker Behaviour Performance Prediction

The proposed method for predicting DC hydraulic magnetic circuit breaker behaviour, based on the electromagnetic force measurements, is discussed. This entails solving the equations of motion for the components moving under influence the measured forces.

1.4.5 Chapter 6 – AC Circuit Breaker Behaviour Performance Prediction

Most hydraulic magnetic circuit breakers in the market are AC devices. Thus, a method for the prediction of AC hydraulic magnetic circuit breaker behaviour, based on DC electromagnetic force measurements, is described. Additional complications due to AC excitation, like hysteresis losses and the oscillating movement of components under the influence of time varying nature of force, is discussed. In addition the modifications to the DC circuit breaker behaviour prediction method to accommodate these complications are highlighted.

1.4.6 Chapter 7 – Method of Testing and Test Equipment

The test equipment and procedures for testing the time-delay characteristics of low voltage circuit breakers are described. Factors influencing the accuracy of these test results are highlighted and their effects quantified.

1.4.7 Chapter 8 – Summary of Results

The results obtained are discussed and evaluated. These results discussed are:

1. Electromagnetic force measurement results.
2. Predicted and measured circuit breaker performance for both AC and DC circuit breakers.

1.4.8 Chapter 9 – Summary and Conclusion

Lastly a summary of the objective and outcome of the work, described in this thesis, is given and a conclusion is drawn regarding the successfulness of the measurement equipment and the circuit breaker performance prediction method. This section also proposes possible future work and improvements.

CHAPTER 2

LOW VOLTAGE CIRCUIT BREAKERS

2.1 Introduction

Low voltage circuit breakers serve as electrical fault protection devices for low voltage (supply voltage of less than 1000V) electrical systems. The function of low voltage circuit breakers, regardless of the type of technology used is the protection of electrical cables. Electrical cables account for a big portion of the cost of an electrical installation and cable failure can lead to catastrophic events, like fire and loss of life. In addition to protection of electrical cables, a very important aspect of a circuit protection device is not to trip unless absolutely necessary. The premature tripping of a circuit breaker (also known as nuisance tripping) should be avoided at all times, as it disrupts processes and causes inconvenience. Nuisance tripping is avoided by controlling the time it takes for a circuit breaker to trip under different fault conditions [1].

2.1.1 Time-Delay Curve

Low voltage circuit breakers evaluate an electrical fault based on two variables, the magnitude of the over current, and the time it has been present for. Low over currents e.g. 125% of the nominal circuit breaker current (also expressed as $1.25I_n$), are allowed to persist for much longer than high over currents (e.g. $6I_n$). A graph that relates the time for the circuit breaker to trip to the magnitude of the over current is called a time-delay curve.

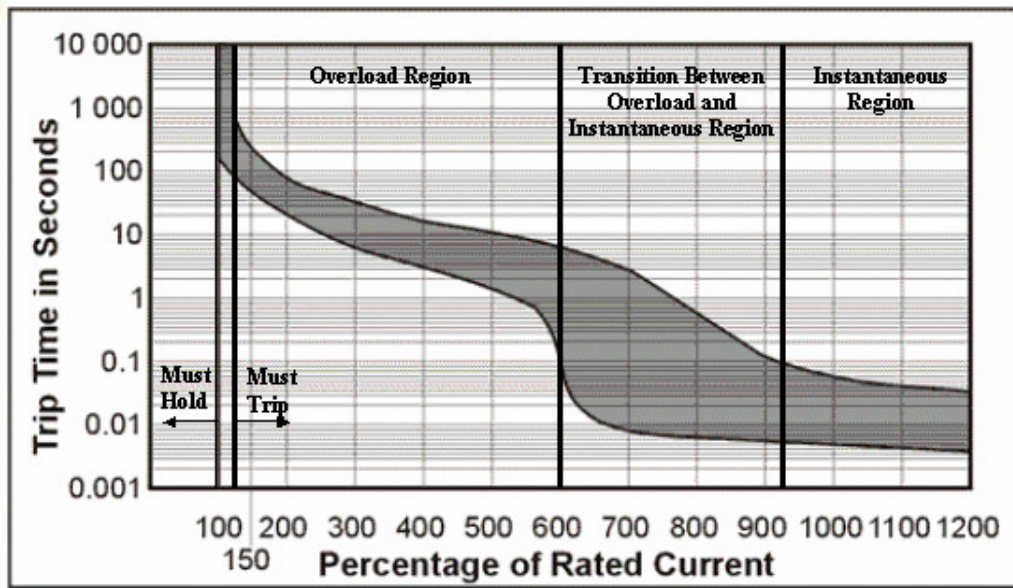


Figure 2.1: Example of Time-Delay Curve Showing Upper and Lower Tolerances Limits

Figure 2.1 shows a typical example of such a graph.

2.2 Low Voltage Circuit Breaker Technologies

Low voltage circuit breakers can be divided into two main types based on the technology they employ. These two types are known as thermal magnetic circuit breakers and hydraulic magnetic circuit breakers.

2.2.1 Thermal Magnetic Circuit Breakers

In a thermal magnetic circuit breaker the path conducting current between the terminals of the circuit breaker is in very close proximity to, or includes a bimetal strip. The bimetal strip is fixed at only one end with the other end free to move. As the current heats the bimetal, it deforms, causing a displacement of the free end. This displacement is the actuating effect that disengages the circuit breaker mechanism and trips the circuit breaker. The higher the current, the shorter the time needed to cause a large enough displacement to actuate the mechanism. At very high currents where, due to heat transfer constraints, the bimetal actuator is unable to trip the circuit breaker within a sufficiently short time, a solenoid plunger (also referred to as a magnetic trip) will actuate the mechanism.

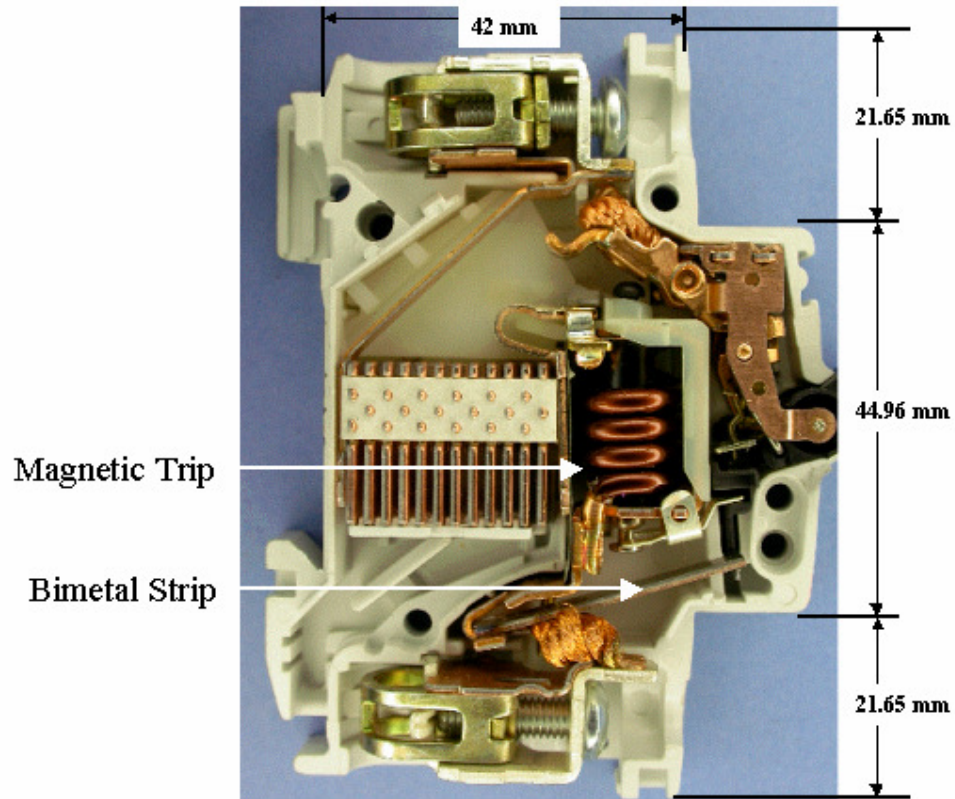


Figure 2.2: Thermal Magnetic Circuit Breaker

2.2.2 Hydraulic Magnetic Circuit Breakers

Hydraulic magnetic circuit breakers do not rely on temperature effects to actuate the circuit breaker mechanism. This type of circuit breaker will react to the electromagnetic flux generated by a solenoid coil that carries the current that passes through the circuit breaker.

The current sensing unit (normally just referred to as the sensing unit) of a hydraulic magnetic circuit breaker is shown in Figure 2.3 .

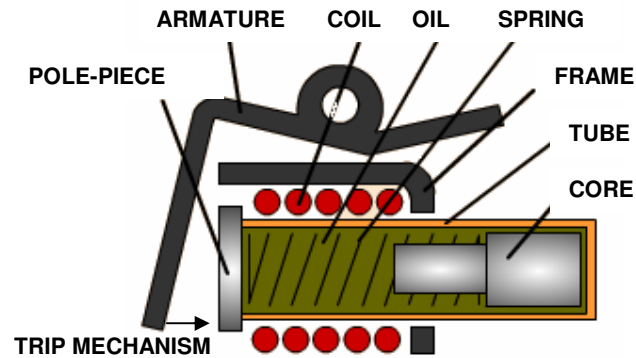


Figure 2.3: The Current Sensing Unit of a Hydraulic Magnetic Circuit Breaker.

At the heart of the sensing unit is a brass tube that contains a mild-steel ferromagnetic core, which is held in position at the back of the tube by a spring (as indicated in Figure 2.3) [1].

As the current through the core increases, the electromagnetic force acting on the core increases. If the current keeps on increasing there will be a point where the magnitude of the electromagnetic force will be larger than the opposing spring force and the core will move into the coil towards the pole-piece.

As the core moves forward the air gap between the pole-piece and the core decreases. This reduction in air gap will cause a dramatic drop in the reluctance of the complete electromagnetic circuit formed by the ferromagnetic components (core, pole-piece, armature and frame). As the reluctance drops, the flux through the circuit increases, and as a result the electromagnetic force acting to close the armature angle will also increase. If the electromagnetic force on the armature exceeds a minimum value (determined by a torsion spring) the armature will close, tripping the circuit breaker.

If the motion of the core is not damped this will happen instantaneously ($\pm 10\text{ms}$). Thus, in order to have the right time-delay characteristics the brass tube is filled with silicone oil of known viscosity. The viscous damping of the oil on the core will result in heavily damped core movement. The core velocity, and as a result the time-delay of the circuit breaker can be changed by adjusting the oil viscosity value.

2.3 Sensing Unit Performance Measures

The performance of a circuit breaker has to comply with certain specifications (e.g. IEC 947-2), and the demands of the market. Driven by these external influences there are five major criteria that will completely describe sensing unit performance. These five criteria are the must hold point, the must trip point, the overload characteristics, the instantaneous point and the impulse tolerance of the circuit breaker.

2.3.1 *Must-Hold-Point*

All circuit breakers have a nominal current rating (I_n) and should be able to hold their nominal current indefinitely without tripping. The maximum current (specified as a percentage of the nominal current) at which the circuit breaker is not allowed to trip is known as the must-hold-point. To ensure that nuisance tripping does not occur, most specifications specify the must-hold-point as $1.05I_n$.

2.3.2 *Must-Trip-Point*

The must-trip-point can be defined as the lowest current at which the circuit breaker should always trip. In the case of IEC 947-2 this point is specified as $1.25I_n$. The current range between the must-hold-point and the must-trip-point ($1.05I_n$ to $1.25I_n$) is not defined in terms of tripping, meaning the breaker is allowed to trip, or not to trip, at any current in this region. In all other current regions the circuit breaker should either trip, or not trip, depending on the characteristics of that region.

2.3.3 *Overload Characteristics*

The overload region of a circuit breaker can be defined as all the currents between the must-trip-point and the instantaneous point. This is the region in which the time-delay characteristics of the circuit breaker are the most crucial, and are forced to fall within very well defined boundaries. These boundaries will differ from time-delay curve to curve.

2.3.4 *Instantaneous Point*

The instantaneous point of a circuit breaker is the lowest current at which the circuit breaker will trip in 0.1 seconds or less. In thermal magnetic circuit breakers this point is typically defined as the point where the circuit breaker is tripped by the solenoid plunger (magnetic trip) and not the bimetal actuator. In hydraulic magnetic circuit breakers the instantaneous point is that current at which the core does not have to move or move very

little (0.3mm) before the armature will experience a large enough electromagnetic force to trip the circuit breaker.

2.3.5 Impulse Tolerance

Depending on the application, a circuit breaker should be able to withstand a current pulse of a very short duration without tripping. According to specifications the impulse tolerance is tested with a 10ms current pulse. The highest current peak at which the circuit breaker does not trip is known as its impulse tolerance value (typically $8I_n$ to $24I_n$).

2.4. Must-hold-Point and Must-Trip-Point

The must-hold-point and the must-trip-point of a hydraulic magnetic circuit breaker are realized by specifying the force values of the springs contained in the sensing unit. These springs are:

1. The core spring, which needs to be overcome by the electromagnetic core forces in order for the core to close the gap between itself and the pole-piece.
2. The armature spring, which needs to be overcome by the electromagnetic force acting on the armature, in order to close the gap between the armature and the pole-piece. Closing this will trip the circuit breaker.

The lowest current at which the core force will overcome the apposing core spring force, with the core gap at a maximum and the armature in its fully open position, is referred to as the core-pull-in point (CPP).

The lowest current at which the armature will overcome the opposing armature spring force with the core touching the pole-piece (zero core-gap), and the armature in its fully open position is referred to the armature-response-point (ARP).

The must-hold and must-trip points of a circuit breaker are always guaranteed by specifying the core spring value so that the CPP is between $1.05I_n$ and $1.25I_n$ and the armature spring such that the ARP is always less than the lowest possible value of the CPP. With these two conditions met, the core will start to move towards the pole-piece at a current between $1.05I_n$ and $1.25I_n$, and if the core reaches the pole-piece, the electromagnetic force acting on the armature will always be large enough to overcome the opposing armature spring force.

2.4.1 Factors Influencing the Core-Pull-In Point

In practice the CPP and the ARP can vary from sensing unit to sensing unit because of manufacturing tolerances of spring forces, variations of component dimensions affecting the maximum core-gap and maximum armature angles, slight changes in coil geometry and coil position which will affect the electromagnetic forces acting on the armature and core, as well as material properties which will also have an affect on the electromagnetic forces.

2.4.2 Factors Influencing the Armature Response Point

The ARP is sensitive to the same variables the CPP is sensitive to. The operation of the circuit breaker however, is less sensitive to variations of the ARP than variations of the CPP. The circuit breaker operation will not be compromised by normal variations in ARP, if a sensing unit is designed to have an ARP of $0.95I_n$ or less.

2.5. Overload Characteristics

The overload region of a hydraulic magnetic sensing unit is all currents higher than the CPP, which will result in a tripping time of more than 0.1 seconds. At these currents the core will move forward under the influence of the net core force (electromagnetic core force – core spring force) acting to close the core gap. This movement is damped by the viscous friction induced by displacing the oil through the gap between the outside of the core and the inside of the tube.

2.6 Instantaneous Region

Examining the time-delay curve shown in Figure 2.1, it is clear that the transition between the overload region and the instantaneous region for a hydraulic magnetic sensing unit is not a well defined point, but rather a gradual reduction in trip times as the trip-gap approaches the maximum core gap.

Under the influence of very high electromagnetic core force, the core movement is very fast and the trip-gap is very close (less than a 1mm), to the maximum core gap. For currents in the region of the instantaneous point the core and armature motion always need to be solved simultaneously in order to predict accurate results. In this region the circuit breaker and the calculations are much more sensitive to variations in armature spring forces and electromagnetic forces acting on the armature as this will cause a change in the trip-gap.

2.7. Prediction of Sensing Unit behaviour

The previous sections describe conceptually how the various elements that make up a hydraulic magnetic sensing unit would interact to result in time-delay behaviour shown in Figure 2.1. Conceptually the equations of motion for the various moving parts can be solved to predict the behaviour of the electromagnetic sensing unit if the forces acting on these components are known accurately.

2.8 Conclusion

Basic hydraulic magnetic circuit breaker behaviour is discussed in this section, and mention is made of the various components that make up a hydraulic magnetic sensing unit. The intent of this chapter is not to serve as complete reference to hydraulic magnetic circuit breakers, their design, construction or operation. Further details are provided in Chapter 5 and Chapter 6.

CHAPTER 3

FORCE MEASUREMENT APPARATUS

3.1 Introduction

Since the hydraulic magnetic sensing unit is a device that operates under the influence of electromagnetic forces, the prediction of its behaviour is heavily dependant on knowing these forces. A piece of equipment that is specifically designed to measure these forces has been developed, and is described in this chapter. In this report this piece of equipment is referred to as the Force Measurement Apparatus (FMA). The FMA is designed to fulfil three main functions:

1. Control the position of the core and the armature.
2. Control the current flowing through the sensing unit.
3. Measure the electromagnetic forces acting on both the core and the armature.

3.2 Physical Description

The FMA consists of two load cells mounted on stepper motor controlled positioning stages [2]. One load cell [3] is connected to the core while the other is connected to the armature via a specially prepared carbon fibre rope. The positioning stages position the core and armature, while the load cells will measure the electromagnetic forces acting on the core and armature respectively.

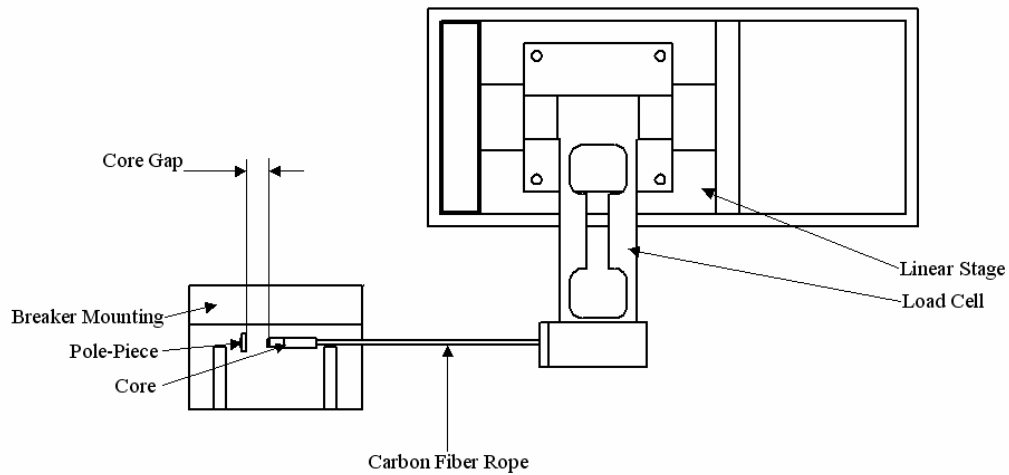


Figure 3.1: Load Cell Connection to Core (some circuit breaker components omitted)

The current through the sensing unit is controlled by controlling a DC switch mode power supply.

The entire system is controlled by means of a microprocessor, which control all the functionality of the system and is responsible for controlling the timing between the events comprising the measurement sequence.

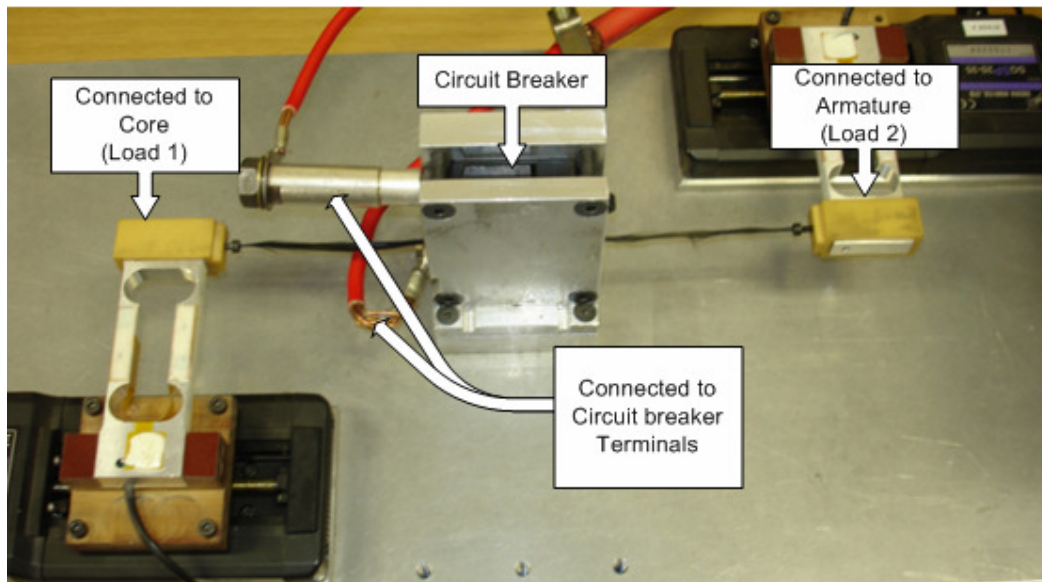


Figure 3.2: Force Measurement Apparatus

3.3 Functional Description

The function of the Force Measurement Apparatus (FMA) is to measure the electromagnetic forces acting on both the core and the armature of hydraulic magnetic sensing units. This goal is achieved by breaking the measurement process down into different subsections that are executed in sequence.

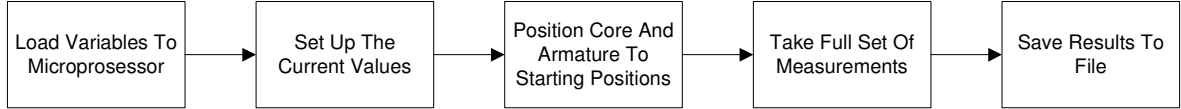


Figure 3.3: FMA Subsections

Each one of these subsections requires user input or is initialized by the user. These subsections can be further reduced to a sequence of tasks, which allow the achievement of the goal of each subsection. The next sections discuss the subsections and their functions in more detail.

3.3.1 Load Measurement Parameters

The first step in the measurement process is to load the measurement parameters. These parameters consist of the following:

1. The number of core positions at which core and armature forces are to be measured
2. The step size by which the core gap has to increase with every measurement
3. Armature positioning parameters
4. The number of times the measurements should be repeated at I_n
5. The type of circuit breaker, which implies a set of hard coded armature angles

Figure 3.4 shows a flowchart for the loading of measurement parameters. The user, by means of the user interface application, enters these parameters on the control PC. After acceptance of the parameters by the user, they are loaded in the microprocessor, which controls the measurement process.

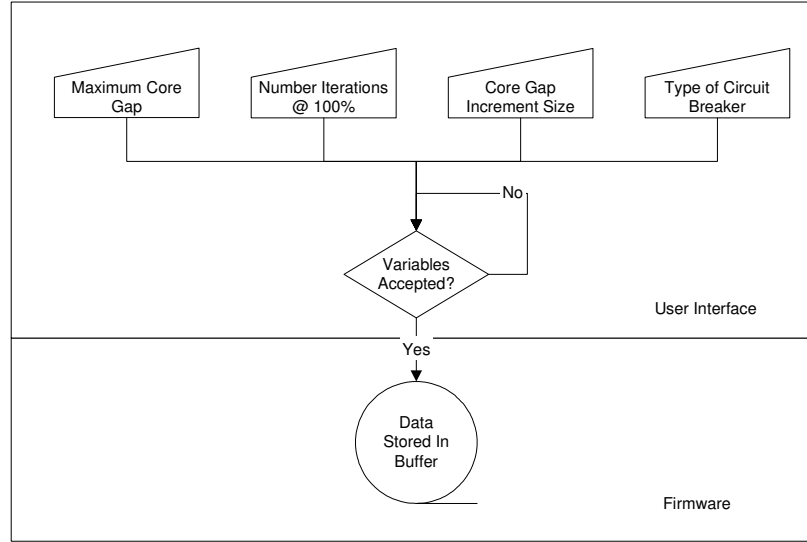


Figure 3.4: Subsection Responsible for the Loading of Measurement Parameters.

3.3.2 Load Current Settings

Core and armature force measurements have to be taken at currents up to 1000% of the circuit breaker rating (I_n), starting at I_n . These measurements are done at multiples of I_n from I_n up until $10I_n$. However, before the measurements can be taken these current settings need to be set up and saved inside the microprocessor [4]. The process for achieving this is described in Figure 3.5.

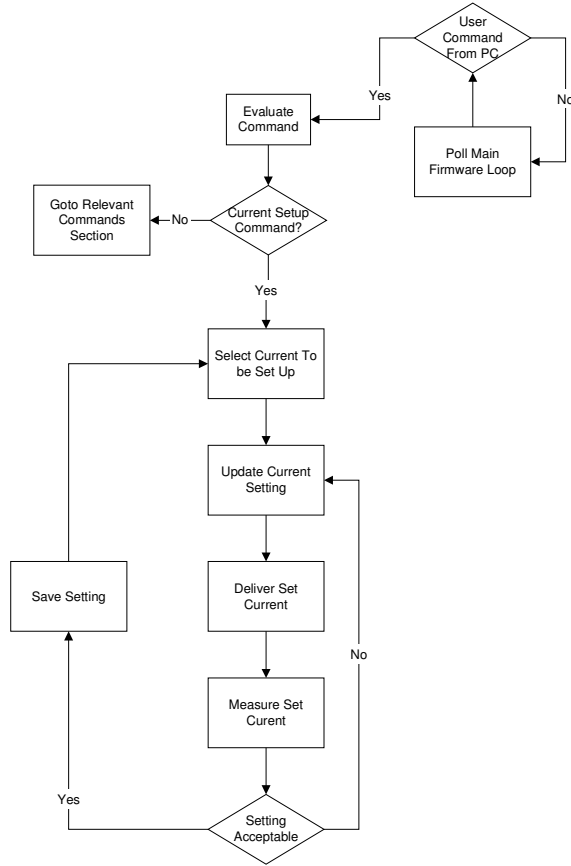


Figure 3.5: Current Setup Procedure

3.3.3 Position the Core and Armature in Known Positions

After setting up the measurement parameters as well as the currents at which the measurements have to be taken the setup has to be reset to a default starting state. This default state is:

1. Current setting set to 100% I_n value.
2. The core set to its zero position (touching the pole-piece).
3. The armature set to its fully open position (12° in the case of the circuit breakers used in this study).

The process for resetting the core and armature to their measurement starting positions is shown in Figure 3.6.

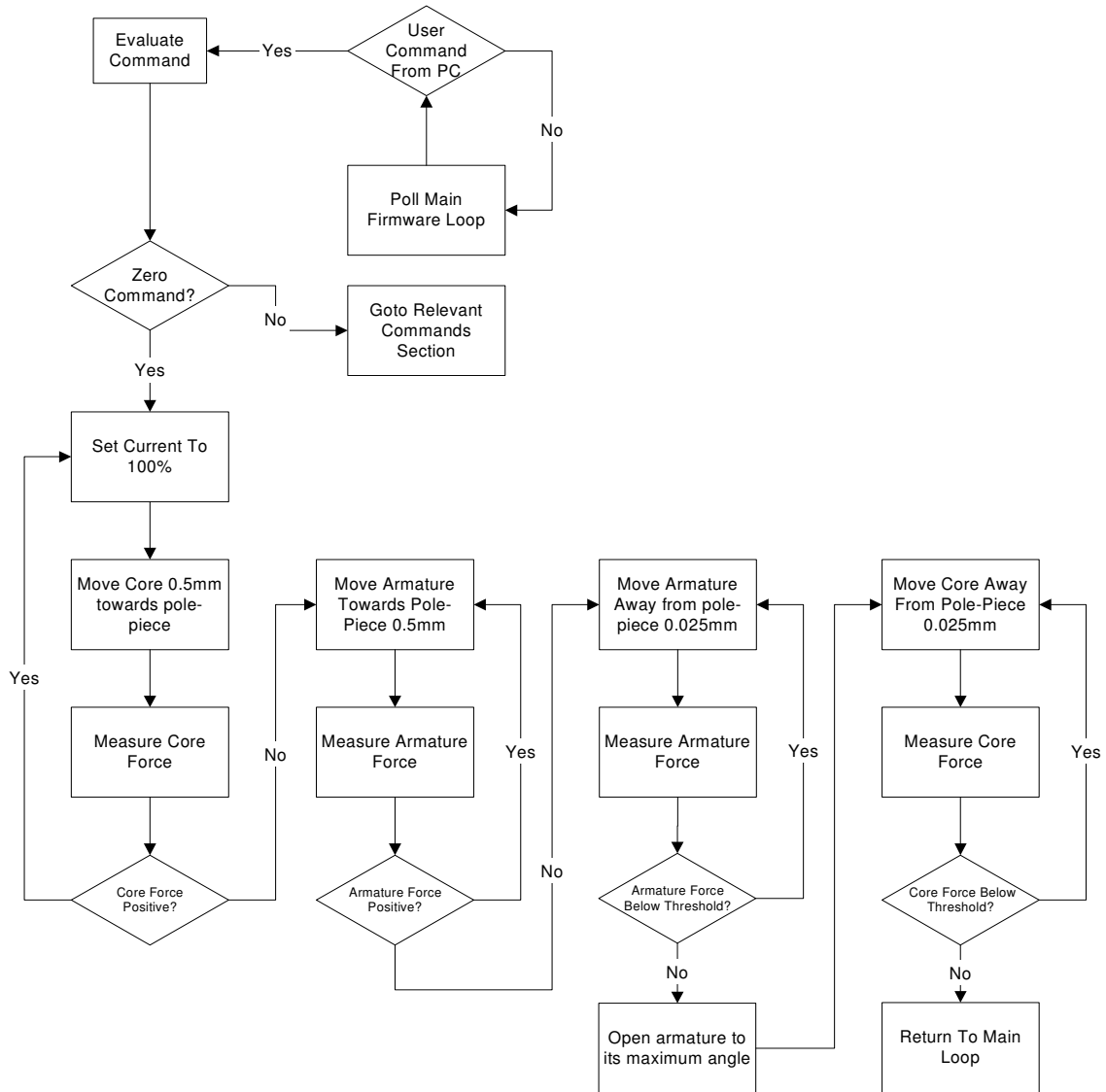


Figure 3.6: Reset Core and Armature to their default Measurement Starting Positions.

3.3.4 Measurement

After completion of the above-mentioned steps the measurement system is ready to take a set of measurements. A complete set of measurements consists of the data shown in Table 3.1.

Table 3.1: Complete Set of Measurement Data.

Current (% of Circuit Breaker Rating)	Core Force Measurements	Armature Torque Measurements	Notes
100%	0mm to the maximum core gap in 1mm or 0.5mm steps.	3 armature angles with the core at 0mm	These are repeated a number of times (usually 10) in order to get a representative average.
200%	0mm to the maximum core gap in 1mm or 0.5mm steps.	Torque measurements are taken at each core gap with the maximum armature angle. As well as 3 armature angles with the core at its maximum gap.	From 200% to 1000% the measurements are done only once
300% & 400%	Same as 200%	Same as 200%	These are done only once. The core force measurements are done using a 600gf load cell.
500% to 1000%	2mm to the maximum core gap in 1mm or 0.5mm steps.	Same as 200%	At 0mm and 1mm the core forces are very high but of little interest, thus they are not measured.

The flow diagram in Figure 3.7 shows the sequence of events and decisions that allows the FMA to measure the set of data described in Table 3.1.

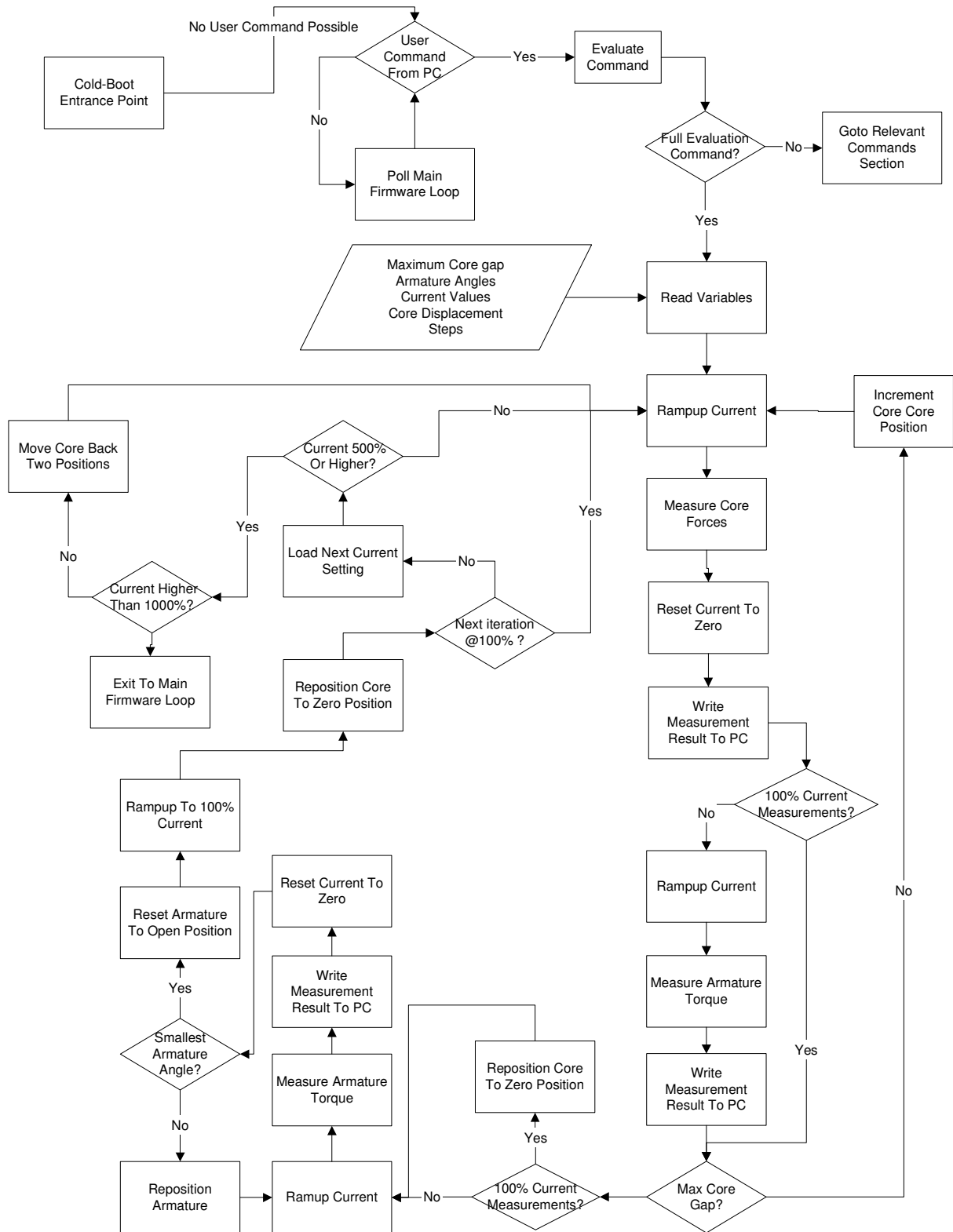


Figure 3.7: Measurement Sequence

3.3.5 Saving of Results to File

The final step in the measurement process is to save the results to a file, which will be used in calculating the time-delay characteristics of the circuit breaker. In Figure 3.7 it is shown that the measurements results are written to a memory location on PC after they are taken. The saving of the measurement results to a file only involves writing these results, from PC memory, to a text file.

3.4 Conclusion

This section discusses the FMA hardware and firmware in very brief detail. The measurement and control sequences described in this chapter have been tailored to the measurements of the needed forces in hydraulic magnetic sensing units. If need be, they can be reconfigured for use in other applications.

CHAPTER 4

ACCURACY OF ELECTROMAGNETIC FORCE MEASUREMENTS

4.1 Introduction

The FMA fulfils three functions, described in Chapter 3. These functions are the measurement of the electromagnetic force, the control of the current at which the measurement is taken and the positioning of the armature and the core. The accuracy of each of these processes impacts directly or indirectly on the accuracy of the measured electromagnetic force values.

This chapter quantifies the impact of these accuracies on the measured electromagnetic force.

The approach taken is to evaluate the accuracy of each FMA function in isolation, followed by calculating the cumulative accuracy of the FMA based on these individual results.

4.2 Measurement Sensitivity

All digital measurement equipment is defined by its maximum possible resolution. In the case of the FMA, this resolution is 12 bits [5]. The significance of this is that all analogue signals measured will be digitised and represented as a 12 bit digital value. This “limitation” result in a digitisation error. The reason for this error is that only discrete results (any whole number between 0 and 2^{12} in the case of a 12 bit system) can be represented, and analogue signals measured very seldom correspond exactly to a digital value.

Assume, as is the case for the FMA, that a 300gf load cell is being used and that the full load output of the load cell is 5V. Further assume that the A/D converter measuring the load cell output operates within the range 0V to 4.096V. This would imply digitisation sensitivity in terms of input voltage as:

$$A/D_{\text{sensitivity}} = \frac{4.096V}{2^{12} AD_{\text{division}}} = 1mV / AD_{\text{division}}$$

The conversion of this sensitivity to grams of force is made as follows:

$$gf/V_{\text{ratio}} = \frac{300gf}{5V} = 60gf / V$$

thus, the measurement sensitivity in terms of grams of force can be expressed as:

$$Sensitivity = (1mV / AD_{division})(0.06gf / mV) = 0.06gf / AD_{division}$$

The specific A/D converter used is known as a SAR converter. This type of A/D converter has the ability to round the measured analogue signal to the closest digital value. This would imply that if the analogue signal is somewhere between two digital values, the A/D converter will represent that sample with the closest possible digital value. This has the effect of doubling the resolution.

In other words, the measurement system would be able to detect changes in force of no smaller than 0.03gf. Assuming perfect calibration and 100% repeatability, this will then be the absolute maximum accuracy of the measurement system.

4.3 Measurement System Repeatability

The next step in defining a measurement system is to characterise its repeatability. The repeatability is influenced by noise on the measured signal, and possible drift of that signal [9]. The noise and DC signal drift is a function of the transducer, the anti-aliasing filter used on the A/D input, the track layout on the PC board and external EMI sources.

In the case of the FMA the repeatability is established by loading the load cell with a known mass, followed by taking successive series of measurements. The results of these measurements are shown in Figure 4.1.

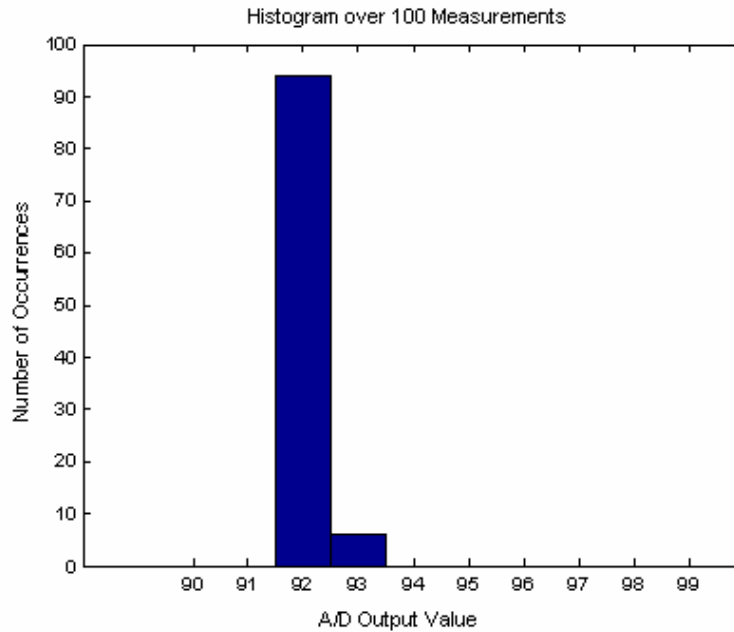


Figure 4.1: Measurement Repeatability

To obtain the results shown in Figure 4.1, the load cell was loaded with a mass of 5 grams and the A/D output was recorded for 100 successive measurements. The results from Figure 4.1 clearly show that the measured results vary between $92A/D_{divisions}$ and $93A/D_{divisions}$, with the majority of the measured results being $92A/D_{divisions}$. This implies that the system is not a true 12 bit measuring system, but an 11 bit system. The eleven most significant bits of the result never change during the measurements, with only the least significant bit (LSB) changing its logical state. Thus the measurement repeatability cannot be better than $2 \times 0.03gf = 0.06gf$ based on the measurement sensitivity value claimed.

4.4 Influence of Load Cell Calibration on Measurement Accuracy

The previous two sections define the measurement sensitivity and repeatability, only in terms of A/D sampling. In a complete measurement system that will give its output in terms of grams of force some calibration factor is needed to convert the A/D sampled results to grams of force.

As a result of the load cells used not being completely linear, especially at forces below 10gf, it is not sufficient to use only one conversion factor. Thus a table of calibration factors, calculated at discrete points, is used. A section of this calibration table is shown in Table 4.1

Table 4.1: Segment of the Load Cell Calibration Data

Weight applied (gf)	A/D Divisions	Conversion Factor	Conversion Factor
0	0		
1	18	18	18
2	36	18	18
3	55	18.33	18.3
4	73	18.25	18.3
5	92	18.4	18.4

The table is populated by loading the load cell with a known mass, noting the A/D sampled value. A calibration factor is then calculated by which the A/D sampled value needs to be divided. This process introduces inaccuracies, impacting on the measured results on three levels:

1. The A/D sampled value on which the calibration is based is uncertain.
2. The calibration factors are only defined at specific points, introducing an error if a measurement between two points needs to be scaled.
3. The calibration factors are stored in RAM, which force rounding errors as only one decimal is allowed.

4.4.1 Effect of LSB Uncertainty

The uncertainty of the least significant bit (LSB) in the 12 bit A/D result is due to the measurement repeatability discussed previously [11]. The effect of this in terms of grams force will become less important at high forces as $1A/D_{\text{division}}$ equates to 0.06gf. This will cause a negligible percentage error all forces higher than 5gf. The effect of this source of inaccuracy is illustrated below:

Consider the 4gf calibration point, and assume the A/D converter result that represents 4gf is $74A/D_{\text{division}}$ and not $73A/D_{\text{division}}$. Converting an A/D result to grams of force using the calibration factor of 18.25 will result in grams force value of 4.06gf, instead of 4gf. This results in a 1.25% error margin around the 4gf calibration.

4.4.2 Effect of Discreet Calibration Points

When converting a measured value a decision on which calibration point to use has to be made. This is done by finding the closest calibration point to that specific sampled result. As a result a calibration factor which is either slightly too high or too low will be used. As in the

previous case the effect of this source of inaccuracy will diminish dramatically as the measured forces increase. The reason for this is that the load cell is more linear than at low force values, and the percentage error will diminish. This is again illustrated by means of the values in Table 4.1.

Assume a measured force of 4.5gf. Assuming the load cell output to be linear between 4gf and 5gf will result in an A/D value of either 82 or 83 depending on the state of the LSB, which will not be consistent. If the A/D value is 82 the calibration factor at the 4gf point will be used, if the A/D value is 83 the calibration factor at the 5gf point will be used. Thus the total possible error in grams of force at this point can be calculated as:

$$\left| \frac{82}{18.25} - \frac{83}{18.4} \right| = 0.02gf$$

4.4.3 Effect of Calibration Factor Rounding

The calibration factors are allowed only one decimal value, due to microprocessor constraints. This implies that the calibration factor corresponding to the 4gf calibration point needs to be rounded to either 18.2 or 18.3. The convention followed throughout populating the calibration table is that the rounding will be done to the closest decimal, or in the case of a value perfectly between two one decimal numbers, the value will be rounded upwards. Thus the factor 18.25 will be rounded to 18.3. The error in grams of force due to this rounding is calculated as follows:

$$\left| \frac{73}{18.25} - \frac{73}{18.3} \right| = 0.01gf$$

4.4.4 Cumulative Measurement Error

The cumulative measurement error as a result of all the influences described above can now be calculated as [7]:

$$E_{measure} = \sqrt{0.06^2 + 0.02^2 + 0.01^2} = 0.064gf$$

4.5 Control Accuracy

The previous sections described the accuracy and repeatability of the FMA that can be expected, measuring a calibrated weight in a controlled environment, ignoring the effect of all other variables. Additional variables are introduced by the inclusion of the other measurement related functions.

These additional functions are:

1. The control of the current through the circuit breaker.
2. The control of the core and armature position.

4.5.1 Current Control and Regulation

A circuit breaker is a current sensitive device, and as such it stands to reason that the accuracy, to which the current can be controlled and regulated, will influence the overall accuracy of the measurement of electromagnetic forces. The current is influenced by two criteria:

1. The accuracy to which the current can be controlled
2. The current regulation

4.5.1.1 Current Control Sensitivity

The current control sensitivity is a function of the control circuit and its interface with the DC Switch Mode Power Supply (SMPS). This is explained as follows:

1. The output current of the DC supply is controlled by means of a 0V-5V analogue signal.
2. This signal is generated by a digital control system, which can only allow discrete current settings.

This is best analysed by means of the control circuit.

The current control signal is generated by two 8 bit digital potentiometers, of which the combination allows for 16 bit current control resolution. This implies that the 0V to 5V control signal can take on any one of 2^{16} discrete states. Thus, one increment of the current control register (16 bit register), will cause the current control signal to increment by

$$\frac{5V}{2^{16}} = 0.076mV$$

In the case of the 1500A DC SMPS used, where a current control signal of 5V will result in a current of 1500A, this current control signal resolution results in a current resolution of

$$\left(\frac{1500A}{5V} \right) (0.000076V) = 0.023A$$

Thus, the output current can be controlled in multiples of 23mA.

4.5.1.2 Current Control Repeatability

The current control repeatability is a function of the digital potentiometers used, and from the datasheets of these devices it can be deduced that the current control system is only a 14 bit repeatable system. This implies that the state of the two least significant bits is unknown. The two least significant bits uncertainty correspond to an uncertainty of 3 ($11_2 - 00_2 = 11_2 = 3_{10}$), resolution intervals. As a result the current control repeatability is limited to $(3)(0.023A) = 0.069A$. This value indicates the maximum accuracy to which the current can be controlled to, assuming the rest of the system is ideal.

4.5.1.3 Current Regulation

The current regulation is a function of the DC SMPS, and is specified by the manufacturer as $\pm 1\%$. Thus, one would expect the current output to vary by $\pm 1\%$ around the nominal controlled output current. As the sensitivity and the repeatability as a result of the control methodology cause very small current variation, and could be neglected (except for the case of small currents), current regulation is the dominant cause for variations in SMPS output current.

The error due to the current regulation (previously derived as $\pm 1\%$) can be calculated using the equation

$$\frac{F_1}{F_2} = \left(\frac{I_1}{I_2} \right)^2$$

which is described in more detail in Chapter 5.

Solving this equation for a typical case of a measured force of 5.5gf measured at I_m , results in a measurement error of $\pm 0.11gf$, as a result of current regulation.

4.5.2 Core and Armature Position Control

The final control function of the FMA that will impact the accuracy of the measured electromagnetic forces is the position of the core and armature at specific core gaps and armature angles. This positioning is done by means of highly accurate positioning stages under microprocessor control.

4.5.2.1 Positioning Stages – Sensitivity, Repeatability & Accuracy

The positioning stages are controlled by pulses sent to the stage drivers. One pulse results in a positioning table displacement of 25 μ m. The manufacturers specify the repeatability of this displacement as $\pm 0.02\mu$ m. In the case of the FMA the stage will receive 4000 pulses to effect a displacement of 1mm. The compounded error over 4000 displacement steps is calculated below.

$$E = \sqrt{(pulses)(0.02\mu m)^2}$$

$$\begin{aligned} \therefore E_{1mm} &= \sqrt{(4000)(0.02\mu m)^2} \\ &= 1.265\mu m \end{aligned}$$

This indicates that the positioning error due to positioning stage characteristics is negligible.

4.5.2.2 Positioning accuracy due to load cell deflection

The core and armature position is not solely controlled by the positioning stage. The core and armature are attached to their respective load cells, and the load cell position is controlled. The primary function of the load cell is to convert the force applied to it to a voltage. This is done by deflecting the load cell slightly, and the load cell output voltage is generated based on the magnitude of this deflection.

This being said, it is clear that the load cell is not ideal for the secondary function (positioning) it is asked to fulfil, as these deflections will influence the core and armature positioning. The deflection of the load cells is given by the manufacturer as 0.2mm at full load. Having a maximum load capacity of 300gf, one will expect the load cell to deflect at a rate of:

$$\frac{0.2mm}{300gf} = 6.67 \times 10^{-4} mm / gf$$

Thus, the maximum error that can be made in position due to the load cell deflection is 0.2mm, assuming a force of 300gf is being measured. As shown in Figure 4.2, this positioning error will reduce as the measured force is reduced.

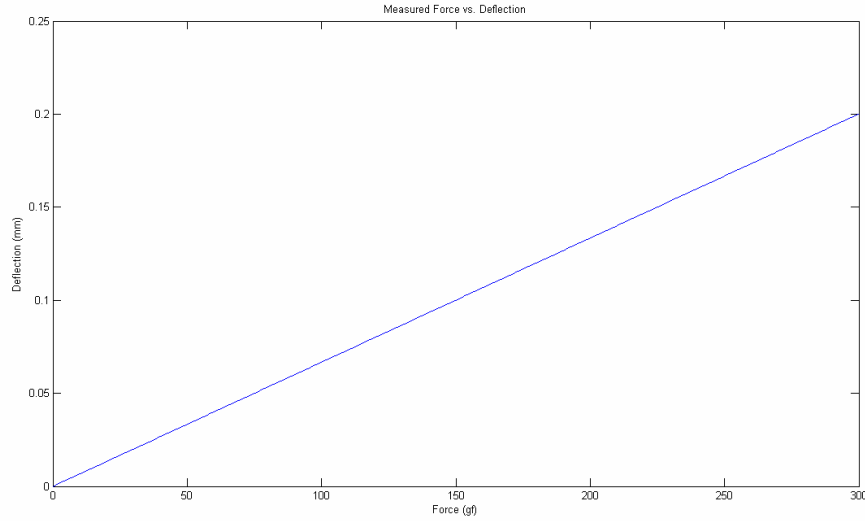


Figure 4.2: Load Cell Deflection vs. Measured Force

4.5.2.2 Core Reference Position Inaccuracy

The next very important step in positioning, is defining a reference position. In terms of core position the obvious point for this reference position is with the core touching the pole-piece (zero core-gap). Positioning the core to the reference point is achieved by setting the stage position so the core touches the pole-piece then, with a current of I_n flowing through the sensing unit coil, adjusting the position of the positioning table in very small steps away from the pole-piece. The steps in which the positioning table is moved away from the pole-piece are 0.1mm in magnitude. During this action the force acting on the load cell is monitored continuously. This is done to tension the carbon fiber rope connecting core to the load cell. When the force reaches a specific threshold value (70gf) the carbon fiber rope is assumed to be taut.

A load cell deflection of 0.046mm can be calculated for a load of 70gf. This is then compensated for by moving the positioning table 0.04mm in the direction of the pole-piece, leaving a resultant “zero position error” of 0.006mm.

4.5.2.3 Armature Reference Position Inaccuracy

The same process is repeated to position the armature in its reference position. This position is similarly defined as the point where the armature touches the pole-piece.

4.5.2.4 Effect of Load Cell Deflection during the Measurement Sequence

The error in the reference position of both the armature and the core result in a very small DC offset in the positioning that is present at all positions. At these new positions a force measurement needs to be taken which will again cause some deflection of the load cell, resulting in position inaccuracies. This can be compensated for in the same manner as in the zeroing process, but is not done in the current version of FMA. The reason for this is two fold:

1. This will slow down the measurement process, as a measurement needs to be taken and the position adjusted based on that measurement. The force measurement will then be done at that “updated” position. This implies doubling the amount of measurements, and doubling the time taken for a measurement set.
2. The forces critical to the behaviour of a hydraulic magnetic sensing unit are small. These critical forces are similar to the opposing spring forces in magnitude (typically 3gf to 20gf). At these low forces the load cell deflection is typically less than 0.015mm, which is acceptable. The positioning inaccuracy at high forces is higher, but is much less critical. The accuracy improvement does not justify the time penalty that will be paid.

An error in measured electromagnetic force can be calculated by referring to a typical case. The most critical electromagnetic core forces are at the maximum core gap, as this is used for the CPP prediction.

Consider the case where the maximum core-gap is situated 6mm away from the pole-piece. An electromagnetic force experienced on the core at this gap and a current I_n is 5.5gf. The electromagnetic force on the core will increase by 1.5gf/mm between a core-gap of 5mm and 6mm.

Thus, at 5.5gf the load cell will deflect by

$$6.67 \times 10^{-4} \text{ mm / gf} * 5.5 \text{ gf} = 0.0037 \text{ mm}$$

this displacement will result in an error, in grams force, of

$$1.5 \text{ gf / mm} * 0.0037 \text{ mm} = 0.0056 \text{ gf}$$

Assuming the absolute maximum error in displacement is given the maximum load cell deflection of 0.2mm, the absolute maximum error in the case described above will be

$$1.5 \text{ gf / mm} * 0.2 \text{ mm} = 0.3 \text{ gf}$$

However from the previous discussion it is clear that this case should not happen in practice and only represents the absolute theoretical maximum error.

4.6 Total Measurement Error

The total measurement error can be calculated by calculating the cumulative effect of the measurement accuracy, the current control accuracy and the positioning accuracy. As mentioned previously this value will be influenced by the magnitude of the force and the current describing a specific measurement.

Again referring to the typical values given in the previous paragraph the total error at this critical point can be calculated.

The total error is then calculated as

$$E_{total} = \sqrt{E_{measrue}^2 + E_{positioning}^2 + E_{current}^2}$$

$$E_{total} = \sqrt{0.064^2 + 0.0056^2 + 0.11^2}$$

$$\therefore E_{total} = 0.13gf$$

4.7 Conclusion

This chapter discussed the measurement and control performance of the FMA. The results will obviously impact on the prediction process, but the total error is within the limits needed for accurate prediction of sensing unit behaviour.

CHAPTER 5

DC CIRCUIT BREAKER PERFORMANCE PREDICTION

5.1 Introduction

It is clear from Chapter 2, that there are very specific performance measures defining the behaviour of hydraulic magnetic sensing units. Of these the most important are:

1. The must-hold-point and the must-trip-point.
2. The time-delay behaviour.

The aim of this chapter is to describe the prediction of these performance measures based on physical sensing unit variables (e.g. component geometries and spring force values), and electromagnetic core and armature force measurements made using the force measurement equipment previously described.

5.2 Measured Electromagnetic Forces

The electromagnetic forces that serve as input in the prediction process are summarised in Table 5.1. The measurements taken have been tailored to the needs of the prediction process, and the relevance of the various measurements will become clear during the discussions that follow.

Table 5.1 Set of Measured Electromagnetic Forces

Current	Electromagnetic Core Force	Electromagnetic Armature Force	Note
I_n	0mm to max core-gap. 1mm intervals.	Measured at 3 armature angles	Measurements repeated 10 times and averaged
$2I_n$	0mm to max core-gap. 1mm intervals.	Measured as per Note 1	Measurements done only once.
$3I_n$	0mm to max core-gap. 1mm intervals.	Measured as per Note 1	Measurements done only once.
$4I_n$	0mm to max core-gap. 1mm intervals.	Measured as per Note 1	Measurements done only once.
$5I_n$	2mm to max core-gap. 1mm intervals.	Measured as per Note 1	Measurements done only once.
$6I_n$	2mm to max core-gap. 1mm intervals.	Measured as per Note 1	Measurements done only once.
$7I_n$	2mm to max core-gap. 1mm intervals.	Measured as per Note 1	Measurements done only once.
$8I_n$	2mm to max core-gap. 1mm intervals.	Measured as per Note 1	Measurements done only once.
$9I_n$	2mm to max core-gap. 1mm intervals.	Measured as per Note 1	Measurements done only once.
$10I_n$	2mm to max core-gap. 1mm intervals.	Measured as per Note 1	Measurements done only once.

Note 1: 3 armature angles with the core at the maximum core gap.

An armature force measurement, with the armature at its maximum angle for each core position.

The next sections describe the prediction of the mentioned sensing unit performances measured, for a DC excited electromagnetic sensing unit based on the DC measurements listed in Table 5.1.

5.3 CPP Prediction

As described in Chapter 2, the CPP of a hydraulic magnetic sensing unit should lie between $1.05I_n$ and $1.25I_n$.

The CPP is manipulated, during the sensing unit design stage by specifying a spring force that will oppose the electromagnetic core force. The electromagnetic core force should be sufficiently large to overcome this spring force only at a current higher than $1.05I_n$. In addition the opposing spring force should not be so high that a current of higher than $1.25I_n$ is needed before the electromagnetic core force will overcome the opposing spring force.

This is a simple calculation when the electromagnetic force acting on the core at these current limits is known.

Table 5.1 indicates that only the electromagnetic core force at current I_n is known. Thus, the core force at $1.05I_n$ and $1.25I_n$ needs to be calculated based on the forces measured at I_n .

5.3.1 Scaling of Electromagnetic Force Measurements

When the electromagnetic force (F_1) is known at a specific current (I_1) on a ferromagnetic component of an electromagnetic circuit, the electromagnetic force (F_2) that component will experience at a different current (I_2) can be calculated using the relation shown below.

$$\frac{F_1}{F_2} = \left(\frac{I_1}{I_2} \right)^2 \quad \text{Equation 5.1}$$

Equation 5.1 can be derived from the magnetomotive law, describing the force F acting in the air gap of a magnetic circuit. This is given by [8]:

$$F = \frac{1}{2\mu_0} \oint B^2 \cdot dA$$

where: μ_0 = permeability constant of the vacuum

B = magnetic induction

A = air gap area

For magnetic fields the formula becomes:

$$F(i) = \frac{\Phi^2}{2\mu_0 A} \quad \text{with } \Phi \sim i$$

where: Φ = magnetic flux

i = magnetic induction

From the equation above it can be deduced that the electromagnetic force is proportional to the square of the current. Thus, keeping the air gap constant, the ratio of two electromagnetic force values is equal the square of the ratio of the currents that produced these two forces. As expressed in Equation 5.1.

Equation 5.1 only holds in the linear region of the BH curve. When the flux density is high enough to cause saturation of the ferromagnetic material Equation 5.1 will result in forces, which are higher than what would be measured. For this reason, force measurements are made in intervals of I_n instead of using Equation 5.1 to calculate all needed forces based on

a set of measurements at one current. Figure 5.1 shows the discrepancy between the measured core force values and the forces predicted using Equation 5.1.

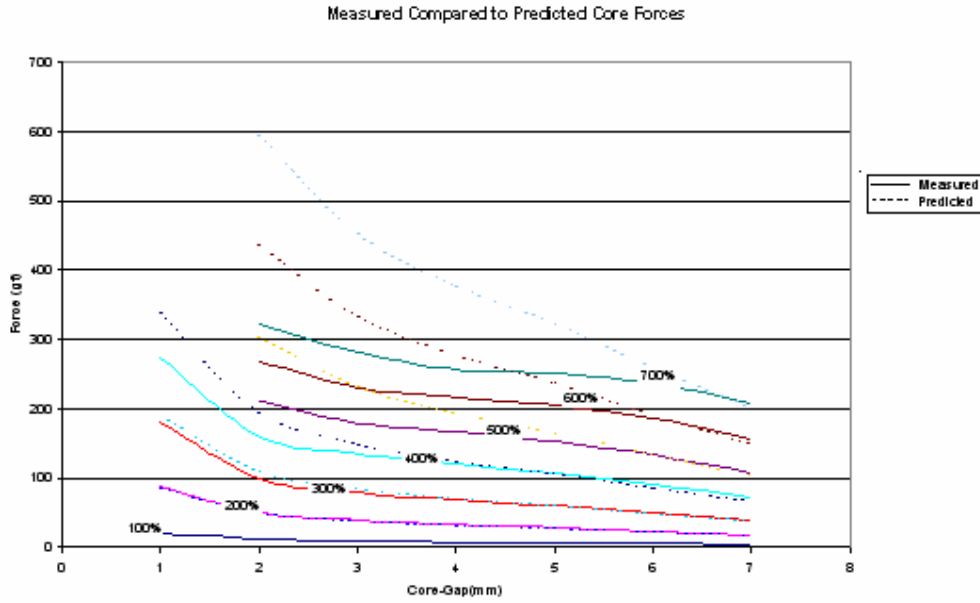


Figure 5.1: Measured vs. Calculated Core Force Values

In the case of the CPP a linear relationship BH curve relationship can be assumed. The reasons for this are:

1. The current is low, resulting in a low Ampere-Turn value for the MMF producing coil, which in turn results in low flux values.
2. The core-gap is at a maximum, resulting in a high reluctance electromagnetic circuit, also acting to keep the magnetic flux values low.

5.3.2 Maximum and Minimum CPP Prediction

The following variables influence the CPP:

1. The variation in the core, tube and pole-piece dimensions lead to variations in the maximum core gap. The variation in core gap leads to variation in the spring length and the core force.
2. Manufacturing tolerances on the core spring.

These variables should be evaluated on a case-by-case basis, but the CPP variation can be illustrated for a typical case.

Consider the core spring data in Table 5.2. Assume a maximum core gap of 6.1mm compared to minimum gap size of 5.96mm. The electromagnetic core force at the maximum and minimum core gap, at current I_m is obtained from the core force measurements. The core force values at 6.1mm and 5.96mm are 6.2gf and 6.3gf respectively.

Table 5.2: Published Core Spring Data

Spring Data			
L1 (mm)	F1 (gf)	L2 (mm)	F2 (gf)
15	5.2 - 6.2	6.6	13.1 - 14.3

The spring force values at the maximum and minimum care gaps can be calculated from the data in Table 5.2 and is shown in Table 5.3.

Table 5.3 Maximum and Minimum Spring Force values

Core Gap	Max Spring Force	Min Spring Force
5.96mm	8.85gf	7.5gf
6.1mm	8.7gf	7.35gf

Assuming a tolerance on the electromagnetic core force of $\pm 0.3\text{gf}$ (this value is obtained by calculating the electromagnetic forces with the coil in its extreme positions), the maximum and minimum CPP can be calculated as follows:

$$CPP_{\max} = I_n * \sqrt{\frac{F_{s_{\max}}}{F_{m_{\min}}}} = I_n * \sqrt{\frac{8.9\text{gf}}{5.9\text{gf}}} = 1.22I_n$$

$$CPP_{\min} = I_n * \sqrt{\frac{F_{s_{\min}}}{F_{m_{\max}}}} = I_n * \sqrt{\frac{7.35\text{gf}}{6.6\text{gf}}} = 1.07I_n$$

From the results shown above it is clear that, assuming tolerance of $\pm 0.3\text{gf}$ on the core force, the CPP will be just within its allowable band in terms of absolute maximum and minimum values. This leaves no margin for error as a result of measurement and control accuracies.

5.4 ARP Calculation

The calculation of the ARP is similar to that of the CPP. The electromagnetic forces acting on the armature at current I_n with the core touching the pole-piece are known. As with the CPP the electromagnetic armature forces can then be scaled using Equation 5.1 to find the current at which it would match the armature spring force.

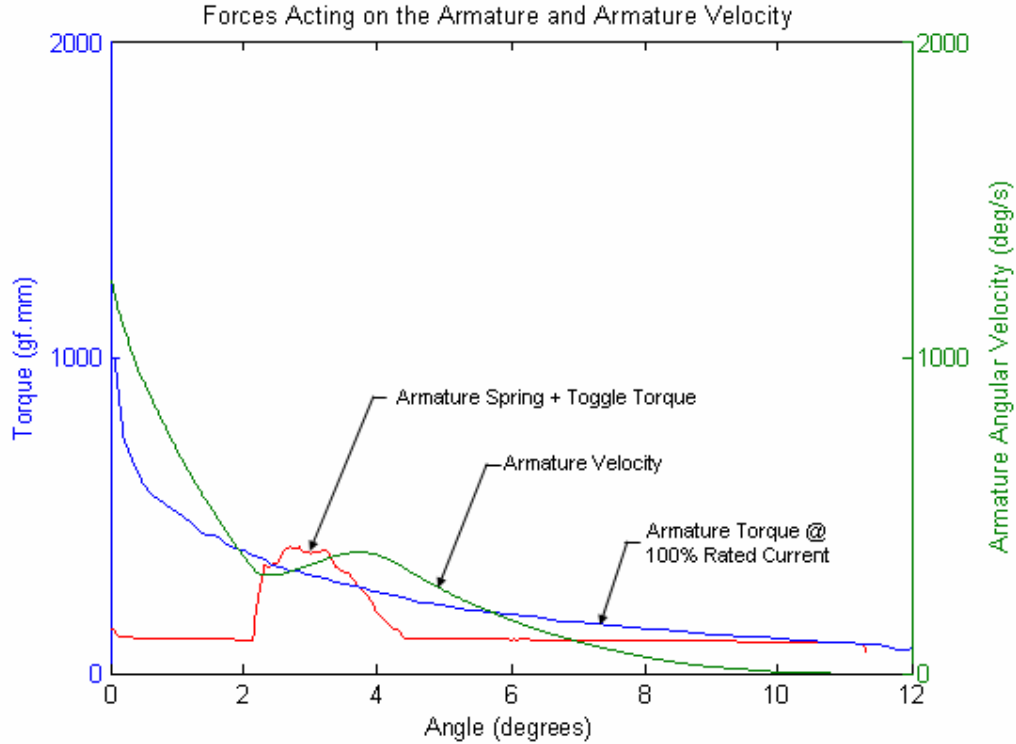


Figure 5.2: Armature Motion at the ARP.

Calculating the current at which the electromagnetic force and the spring force match is not necessarily the correct result. It needs to be verified that the armature will close the gap between itself and the pole-piece (armature gap) completely, before the ARP current can be accepted as correct.

The equation that describes the motion of the armature, based on the net torque it experiences is:

$$I \frac{d^2 \theta}{dt^2} = (T_m - T_s) \theta - k_a \frac{d\theta}{dt} \quad \text{Equation 5.2}$$

where I = moment of inertia of the armature

θ = the armature angle

T_m = electromagnetic torque acting on the armature

T_s = opposing mechanical torque

k_a = lumped friction coefficient on the armature rotation point

t = time

The solution to Equation 5.2 is graphically illustrated in Figure 5.2. In general k_a is assumed to be zero, which causes the last term in Equation 5.2 to reduce to zero.

The opposing torque line represents all the forces acting to oppose the electromagnetic spring force for the total travel of the armature. The area indicated as the “armature/toggle interface” is the mechanical force that needs to be transferred to the mechanism before the mechanism will release and trip the circuit breaker. By comparing the spring/toggle forces to the electromagnetic armature forces in Figure 5.2 it becomes clear that the electromagnetic armature forces dip below the toggle force at about 4° . This would imply that, if the armature starts moving from a 4° angle, at that specific current there would not be enough force available to move through the toggle interface region. The graph representing the armature velocity, in Figure 5.2 however indicates that the armature will have enough momentum to overcome the forces due to the toggle interface when it starts to move at a maximum armature angle of 11° .

Thus, for every ARP calculated through force balance the movement of the armature needs to be verified through its complete angular displacement.

5.5 Time-Delay Calculation

The time-delay behaviour of the circuit breaker is calculated by means of equations of motion for both the armature and the core. And can be divided into four steps:

1. Determine the trip-gap (as described in Chapter 2) for each current ($1.25I_m$, $2I_m$, $3I_m$ etc.)
2. Solve the equation describing core motion for t_c between the maximum core gap and the trip-gap.
3. For core gaps smaller than the trip gap, the equations of motion for both the armature and the core are solved simultaneously for t_a . This calculation terminates the instant the armature gap becomes zero.

4. The times calculated above in steps 2 and 3 are added together to form the total time ($t = t_a + t$) it took for the circuit breaker to trip.

5.5.1 Determination of the Trip-Gap

As the gap between the core and the pole-piece is reduced, the electromagnetic force on the armature increases. This will continue as long as there is a current of a value higher than the CPP flowing through the coil.

For every current higher than the CPP there is some critical core gap for which the electromagnetic force acting on the armature will just exceed the opposing armature spring force. This specific core gap is referred to as the trip-gap, and will approach the maximum core gap as the current is increased.

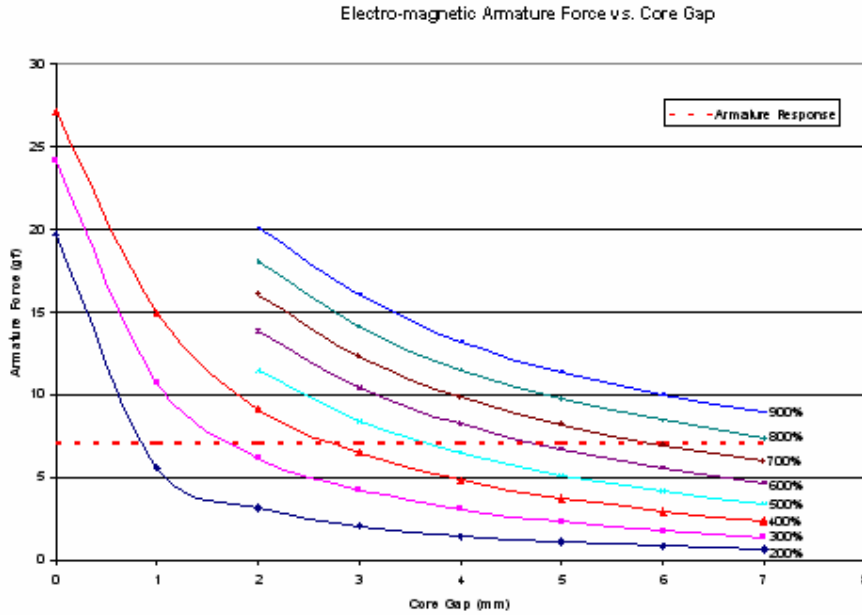


Figure 5.3: Electromagnetic Forces Acting on the Armature at Different Core Gaps and Currents.

Figure 5.3 shows the electromagnetic forces acting on the armature for currents ranging from $2I_n$ to $9I_n$ as a function of the core gap (7mm being the maximum core gap with 0mm the point where the core touches the pole-piece). The dotted “Armature Response” line indicates the armature spring force with the armature in the fully open position. The core gaps at which the electromagnetic armature force lines (solid lines) is equal to the “Armature Response” line indicates the trip-gap for that current.

For electromagnetic force values below the “Armature Response” line there will be a net force on the armature forcing the armature to stay open. For electromagnetic forces higher than the “Armature Response” line the situation will be reversed with the net force on the armature acting to close the armature.

5.5.2 Equations of Motion

Equation 5.3, shown below, describes the movement of the core in a hydraulic magnetic sensing unit [8].

$$m \frac{d^2 x}{dt^2} = (F_m - F_s)x - k_v \frac{dx}{dt} \quad \text{Equation 5.3}$$

where m = the mass of the core

x = the core gap

F_m = electromagnetic force acting on the core

F_s = core spring force

k_v = viscous friction coefficient

t = time

Due to the tube being filled with silicone oil the viscous drag coefficient (k_v), in Equation 5.2, cannot be zero. The theory and concepts describing the calculation of the viscous drag coefficient are described in [8].

5.6 Conclusion

This chapter outlines the mathematics and methods for the calculation a DC sensing units' performance measures. Some detail has been omitted that is critical to the calculation process of sensing unit time-delay behaviour, but the outline of the prediction process should be clear.

CHAPTER 6

AC CIRCUIT BREAKER PERFORMANCE PREDICTION

6.1 Introduction

Chapter 5 described the prediction of DC circuit breaker performance based on DC electromagnetic force measurements. The same approach and mathematics is used for predicting the behaviour of AC hydraulic magnetic sensing units. The driving electromagnetic force in the AC case will obviously be time varying. As only DC electromagnetic force measurements are available, the time varying electromagnetic forces need to be calculated from the DC measurement results. In addition the response of the armature and core to these time-varying driving forces needs to be calculated.

This is more complicated than the DC predictions, as the frequency response of the system needs to be taken into account. Time-varying electromagnetic forces are influenced by additional variables like eddy current and hysteresis losses, the effect of these losses needs to be quantified for accurate AC performance prediction.

6.2 Electromagnetic Forces

The electromagnetic forces available to base the predictions on are DC measurements. The equivalent AC electromagnetic forces need to be predicted based on these DC force measurement results.

6.2.1 Calculation Based on DC Measurements

In order to predict a time varying electromagnetic force based on the DC measurements the following approach has been taken:

1. Assume the DC force measurements represent the RMS force of the equivalent AC force to be calculated.
2. Further assume that an equivalent RMS current produces this RMS electromagnetic force.

The following can be deduced using these two assumptions and its impact on Equation 5.1:

From Equation 5.1:

$$F_{AC} = F_{DC} \left(\frac{I_{AC}}{I_{DC}} \right)^2$$

The AC current can be expressed as: $I_{AC} = \sqrt{2} I_{DC} \sin(\omega t)$

$$F_{AC} \text{ can then be expressed as: } F_{AC} = F_{DC} * (\sqrt{2} \sin(\omega t))^2$$

This relationship does not take hysteresis and eddy current losses into account.

6.2.2 Hysteresis Losses

Under AC excitation, the ferromagnetic material undergoes continual hysteresis. There is energy lost in each hysteresis cycle. The energy loss in the ferromagnetic core is in the form of heat caused by the movement of the magnetic dipoles as the excitation field oscillates back and forth. The hysteresis loss (P_h) can be written as:

$$P_h = K_h B_{\max}^n f$$

where K_h and n are empirically determined constants dependent on the characteristics of the core material and the core volume. Note that the hysteresis loss varies linearly with the operating frequency [10].

6.2.3 Eddy Current Losses

Given that the ferromagnetic core in most magnetic circuits is also a good conductor of current, the time-varying magnetic flux passing through the core can induce circulating currents by Faraday induction. These currents are known as eddy currents. Eddy currents can also heat the core due to the ohmic losses in the conductor. The eddy current loss (P_e) in the ferromagnetic core can be written as:

$$P_e = K_e B_{\max}^2 f^2$$

where K_e is a constant dependent on the characteristics of the core material. Note that the eddy current loss varies as the square of the operating frequency [10].

6.2.4 Temperature Measurement

Hysteresis and eddy current losses act to increase the temperature of the ferromagnetic components exposed to time-varying magnetic flux. It stands to reason, that by measuring the temperature of the ferromagnetic components an idea of the energy loss due to hysteresis and eddy currents can be formed under various excitation frequencies.

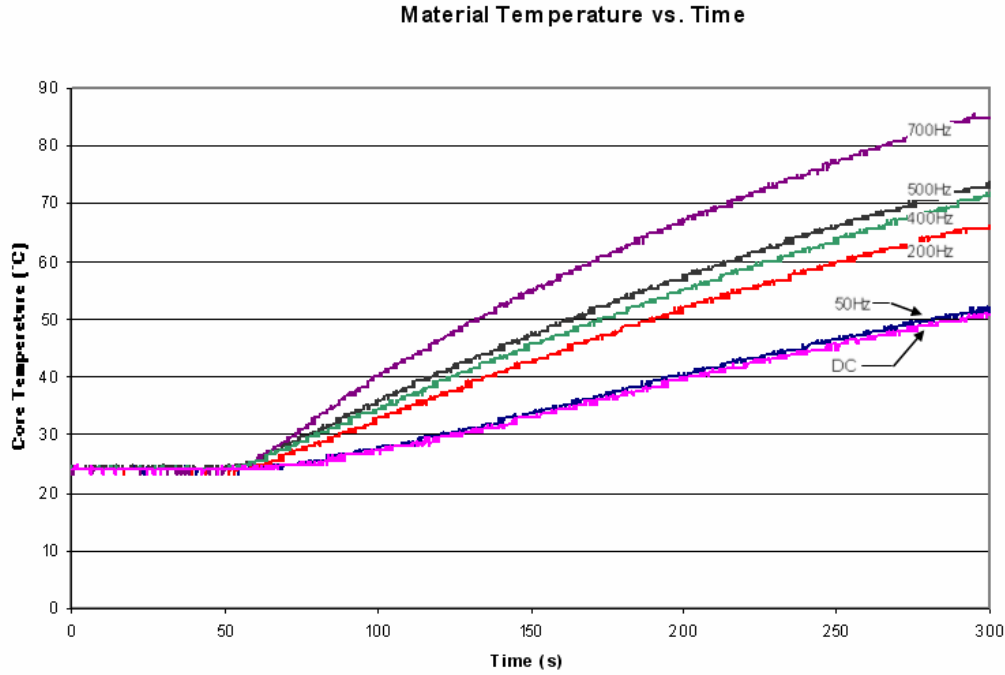


Figure 6.1: Core Temperature Measurements

Figure 6.1 shows the results of core temperature measurements. The measurements were made on an electromagnetic sensing unit with a nominal current (I_n) of 1A. The excitation current through the coil was set to 1A RMS, with the frequency varied.

Two observations can be made from the results in Figure 6.1:

1. The temperature difference between the DC measurement and the 50Hz measurements are negligibly small. This indicates very little hysteresis and eddy current loss at 50Hz.
2. As the frequency increases, the temperature difference increases dramatically.

Based on these results the impact of hysteresis and eddy current losses is assumed to be negligible at 50Hz excitation.

6.3 Core and Armature Motion under AC Conditions

As a result of the time-varying nature of the forces driving the motion of both the core and armature, together with the interconnectivity of the behaviour of the core and armature the differential equations describing the system need to be solved simultaneously. These equations are:

The motion of the armature, given by:

$$I \frac{d^2 \theta(t)}{dt^2} = (T_m - T_s) \theta(t) - k_a \frac{d\theta(t)}{dt}$$

where I = moment of inertia of the armature

θ = the armature angle

T_m = electromagnetic torque acting on the armature

T_s = armature spring torque

k_a = lumped friction coefficient on the armature rotation point

t = time

The motion of the core, given by:

$$m \frac{d^2 x(t)}{dt^2} = (F_m - F_s) x(t) - k_v \frac{dx(t)}{dt}$$

where m = the mass of the core

x = the core gap

F_m = electromagnetic force acting on the core

F_s = core spring force

k_v = viscous friction coefficient

t = time

The driving current, given by:

$$v(t) = R * i(t) + L \frac{di(t)}{dt}$$

where v = supply voltage

R = total resistance

i = total current

L = circuit inductance

t = time

In order to be solved using conventional methods (e.g. Runga-Kutta Formula or Gear's method [10]), these second order differential equations need to be rewritten as a set of first order differential equations. This is achieved by defining:

The core linear velocity as:

$$v_c(t) = \frac{dx(t)}{dt}$$

and the armature rotational velocity as:

$$v_a(t) = \frac{d\theta(t)}{dt}$$

Substituting these into the equations of motion given above yields:

$$I \frac{dv_a(t)}{dt} = (T_m - T_s)\theta(t) - k_a v_a(t)$$

$$m \frac{dv_c(t)}{dt} = (F_m - F_s)x(t) - k_v v_c(t)$$

$$v(t) = R * i(t) + L \frac{di(t)}{dt}$$

These equations are now in a form that can be solved simultaneously using conventional methods.

6.4 Conclusion

The prediction of AC circuit breaker behaviour is the same as the prediction of DC circuit breaker behaviour. The only additional complication is that the AC electromagnetic driving force needs to be calculated from the DC measured forced values. The results obtained solving the equations mentioned above are discussed in Chapter 8.

CHAPTER 7

METHOD OF TESTING AND TEST EQUIPMENT

7.1 Introduction

This chapter describes the test method and the equipment used for the evaluation of circuit breaker time-delay behaviour. By their very nature, circuit breakers are current sensitive devices, and as such the variation of the current during the tests and the influence on the test results will be discussed.

In addition no measurement is perfectly accurate, and some uncertainty in the measured results is to be expected. This is also briefly touched on in this chapter.

7.2 Description of the Test Method

The test methodology involves applying a specific current to the terminals of a functional circuit breaker. The time-delay between the first instant the current is applied and the instant at which the circuit breaker trips is measured.

7.2.1 DC Test Setup

A schematic of the DC test setup is shown in Figure 7.1. The test setup consists of a 10V 250A Switch-Mode-Power-Supply (SMPS), a calibrated shunt (high wattage resistor of known resistance), a switch, and the circuit breaker under test.

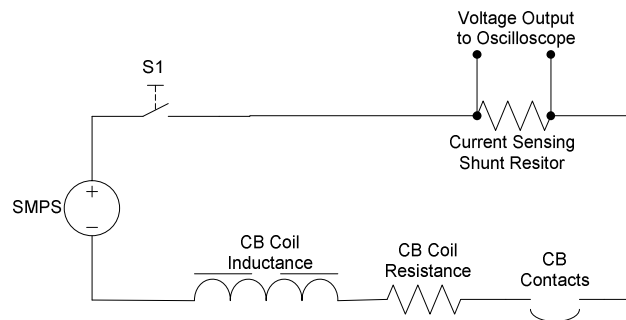


Figure 7.1 DC Test Setup

The current is measured by measuring the voltage drop over the calibrated resistor, and the time measurement is done, by evaluating the differential output voltage on an oscilloscope.

7.2.2 AC Test Setup

Figure 7.2 shows a schematic of the AC test setup. The setup is identical to that of the DC setup, with the exception of replacing the SMPS with a transformer. The transformer will step down the primary supply voltage (220V AC) to a safe secondary voltage of 10V. Current control is achieved by connecting a Variac to the transformer's secondary winding.

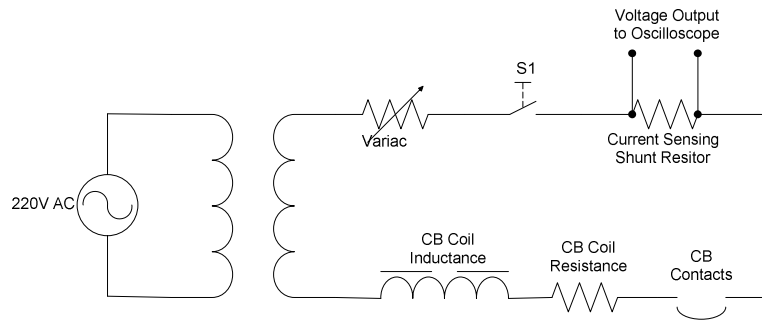


Figure 7.2: AC Test Setup

7.3 Current Measurement

The current measurement is done indirectly by measuring the differential voltage over a calibrated resistor of very low resistance and high wattage. This differential voltage is measured on an oscilloscope.

Two calibrated resistors were used during the testing process.

The first had a resistance of 0.002Ω and a maximum wattage rating of 5W. This implies that a maximum current of 50A can be measured using this shunt. The maximum differential voltage measured over the resistance will then be 100mV.

The second shunt used had a resistance of 0.1Ω and a maximum wattage rating of 20W. This implies that a maximum current of 200A can be measured resulting in a differential voltage over the shunt resistance of 200mV.

7.4 Measurement Uncertainties

Inaccuracies in the measured time-delays will result from the inherent limitations of the testing method, and the equipment comprising the test setup. Another source for inaccuracies is the uncertainty of measurements, especially the measurement of current and

time. The source of these uncertainties is equipment calibration errors and the human interface with the test and measurement equipment.

There are four sources of for uncertainties in the time-delay measurements:

1. Calibration of the shunt resistance
2. Accuracy of the oscilloscope
3. AC and DC test dynamics
4. Human interface with the test setup

7.4.1 Current Measuring Resistance Calibration

The manufacturer of the shunt resistance specified its accuracy as $\pm 1\%$ of the nominal resistance. Thus, there is a $\pm 1\%$ uncertainty in the measured current.

7.4.2 Oscilloscope Accuracy

The output voltage of the current measuring resistor is measured on an oscilloscope. The vertical scale accuracy on the oscilloscope is given by the manufacturer as $\pm 5\%$.

7.4.3 Test Dynamics

During the testing process the circuit breaker undergoes certain changes, due to its nature. Firstly the core will move into the coil changing the total test circuit inductances. This is of no concern in the DC case but influences AC test conditions. Secondly the conductor temperature will increase as a result of I^2R losses. This increase in temperature causes an increase in resistance, also acting to reduce the test current.

7.4.4.1 DC Test Dynamics

During DC tests, the heating of the conductors, especially the coil, cause an increase in resistance. This resistance increase results in a reduction in the current when the supply voltage is kept constant. Setting up the SMPS in constant current mode compensates for this effect. In this mode the SMPS will vary the output voltage so that the output current is kept constant.

7.4.4.2 AC Test Dynamics

The increase of resistance due to the heating of conductors, mainly the coil, also plays a role in the AC test procedure. In addition the increase in inductance of the circuit breaker,

previously described, will also act to reduce the current under constant supply voltage. The AC test setup used has no facility to automatically control the driving voltage to keep the current constant. During the testing procedure this control was done manually by adjusting the Variac.

7.4.5 Human Interface

In all tests involving a human interface there is some degree of error due to human reaction and interpretation. In this particular case these errors are introduced by:

1. Setting the current based on the voltage drop across the current sensing resistor.
2. Measuring the time from the oscilloscope output.
3. Adjustment of the Variac in the AC case.

These errors are extremely hard to define accurately. A concerted effort has been made to keep these errors to a minimum.

7.5 Conclusion

From the discussions above it is clear that inherent circuit breaker behaviour and the interplay of that behaviour with both the AC and the DC test setups will cause inaccuracies in the measured results. As such, the results should be analysed with this background knowledge kept in mind.

A possible improvement for future work will be to reconfigure the test setups, especially in the AC case to reduce the amount of human interface in the testing process.

CHAPTER 8

SUMMARY OF RESULTS

8.1 Introduction

The prediction, of both AC and DC circuit breaker behaviour, based on only DC electromagnetic force measurements is evaluated in the following manner:

1. The DC electromagnetic forces acting on the core and armature were measured for a number of sensing units.
2. Based on these forces, component dimensions, a core spring, an armature spring and silicone oil viscosity was specified.
3. The CPP, the ARP and the time-delay behaviour were calculated, based on the variables predicted above.
4. The circuit breakers were manufactured and tested under both AC and DC conditions, without changing the construction of the circuit breakers.
5. Finally the predicted results were compared to the measured results.

The process described above implies that three sets of results need to be evaluated. These results are:

1. DC electromagnetic force measurements
2. The predicted circuit breaker behaviour
3. The measured circuit breaker behaviour, and its correlation to the predicted behaviour.

8.2 Test Sample Description

The test sample consisted of circuit breakers of six different current ratings and three different curves. The current ratings used in this test sample were $I_n = 2.5\text{A}$, 4A, 5A, 12A, 12.5A and 15A, with long, medium and fast time-delay curves developed for the 2.5A, 4A, 12A and 12.5A circuit breakers. Only long and medium time-delay curves were developed for the 5A and 15A circuit breakers.

Ten circuit breakers of each current rating and curve were manufactured and tested.

8.3 Electromagnetic Force Measurements

The accuracy, and the repeatability, of the force measurement equipment are described in Chapter 4. As the electromagnetic force values are not perfectly known, it is impossible to compare the measured electromagnetic forces with a perfect reference. Thus, the accuracy is evaluated indirectly by the success in predicting performance measures like the CPP of the test samples.

The repeatability of the electromagnetic force measurements can be derived from a set of measurements. This derivation and the impact on the predictions are discussed in the next section.

8.3.1 Measurement Repeatability

In order to get a value for the repeatability of a set of measurements, the measurements need to be attached to a statistical distribution. And it must be proven that the statistical distribution is representative of the data set. The repeatability does not however give any indication regarding the accuracy of the measurements, although repeatability is a prerequisite for accuracy.

To create the dataset on which the repeatability will be calculated the FMA was set up to do measurements at one current (I_n) value and seven core positions, and this was repeated 30 without any operator interference. The distribution of these measurements is proven to be normal using the “probplot” function in the statistics toolbox in Matlab (See Figure 8.1). This function will compare a dataset to the theoretical normal distribution and give a graphical representation of the correlation. In this case it is clear that the measured data correlate well with the theoretical distribution. Thus, the measurements produced by the FMA are always assumed to be normal and as a result normal probability statistics can be used to define the repeatability of the measurements [11].

The first step in this process is to calculate the sample standard deviation given by:

$$\sigma^2 = \frac{1}{N-1} \sum_{i=0}^{N-1} (x_i - \mu)^2$$

With σ the standard deviation, N is the number of samples; x_i is the i -th measurement and μ the sample mean of the signal, given by:

$$\mu = \frac{1}{N} \sum_{i=0}^{N-1} x_i$$

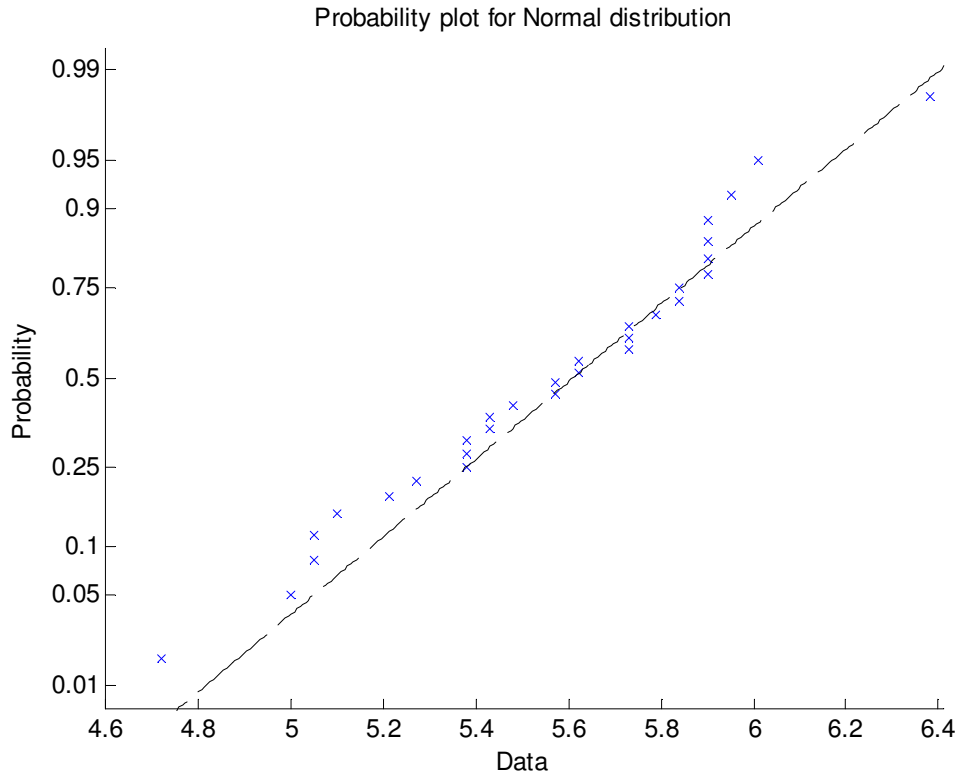


Figure 8.1: Output of the Matlab Function ‘proplot’ Applied to a Set of Core Force Measurements

The Standard Error is defined as:

$$Std_Error = \frac{\sigma}{N}$$

where σ is the standard deviation with N the number of measurements. This Standard Error can then be used to calculate a Confidence Interval. A Confidence Interval is a measure for how certain one can be that the true mean of a data set is in the interval.

For instance, from the mean calculated over the ten measurements and the Standard Deviation of those measurements a Standard error can be calculated. Adding and subtracting two Standard Errors from the mean gives a 95% confidence interval. This means that one can be 95% sure that the true mean of the measurement set will lie between these two values.

This is done on the data set in Table 8.1 and is given in Table 8.2.

Table 8.1:100% I_n Measurement Results of a 12A C-Frame Sample

Core Gap	Core Force Measurements (gf)										Std Dev. (gf)	Avg. (gf)
	Set 1	Set 2	Set 3	Set 4	Set 5	Set 6	Set 7	Set 8	Set 9	Set 10		
1mm	20	20.27	21.28	20.27	19.88	20.33	21.06	20.39	20.67	20.89	0.458	20.504
2mm	12.3	12.41	12.47	11.7	11.92	11.97	11.97	11.86	11.86	11.92	0.260	12.038
3mm	9.5	9.39	9.23	9.5	9.18	9.23	9.39	9.5	9.28	9.61	0.146	9.381
4mm	7.88	8.09	8.15	8.04	7.93	7.93	7.98	7.98	7.93	7.88	0.089	7.979
5mm	7.01	7.11	6.84	6.84	6.79	6.79	6.84	6.79	6.9	6.84	0.106	6.875
6mm	5.62	5.73	5.79	5.62	5.68	5.62	5.57	5.68	5.57	5.48	0.088	5.636
7mm	4.48	4.42	4.48	4.48	4.48	4.31	4.31	4.31	4.2	4.26	0.105	4.351

Table 8.2: 95% Confidence Interval Calculated from Table 8.1

Gap	Std. Deviation (gf)	Average (gf)	Standard Error	95% Confidence Interval	
				Min Limit	Max Limit
1mm	0.458	20.504	0.145	20.215	20.793
2mm	0.260	12.038	0.082	11.874	12.202
3mm	0.146	9.381	0.046	9.289	9.473
4mm	0.089	7.979	0.028	7.922	8.036
5mm	0.106	6.875	0.033	6.808	6.942
6mm	0.088	5.636	0.028	5.580	5.692
7mm	0.105	4.351	0.033	4.285	4.417

Thus for a core gap of 6mm one can be 95% sure that the mean of the measured data would be between 5.58gf and 5.692gf. In this case these values are of particular importance because the CPP calculation will be effected by it in the following way:

Assume the spring force at 6mm counteracting the magnetic force at that core gap is 6.7gf.

The nominal CPP calculated using the average value in Table 1 is:

$$\frac{F_{CPP}}{F_{100\%}} = \left(\frac{I_{CPP}}{I_n} \right)^2$$

substituting F_{CPP} with the spring force of 6.7gf, I_{CPP} can be calculated as:

$$I_{CPP_avg} = \sqrt{\frac{6.7}{5.636}}$$

$$\therefore I_{CPP_avg} = 109\%$$

Following the same logic the maximum and minimum CPP over the 95% confidence interval can be calculated as:

$$I_{CPP_min} = 108.5\%$$

$$I_{CPP_max} = 109.5\%$$

From this it can be deduced that a tolerance of $\pm 0.5\%$ should be placed on the CPP calculation as a result of measurement repeatability.

8.4 Predicted Core Movement under AC and DC Conditions

Solving the system of equations described for the AC and DC cases for core position as a function of time results in the graphs shown in Figure 8.2.

It is clear that the AC and DC core movement are virtually identical. The only difference is a very small frequency (100Hz) component superimposed on the core movement in the AC case.

This implies that the RMS current dominates the core movement. This is expected as the viscous oil heavily damps the core movement.

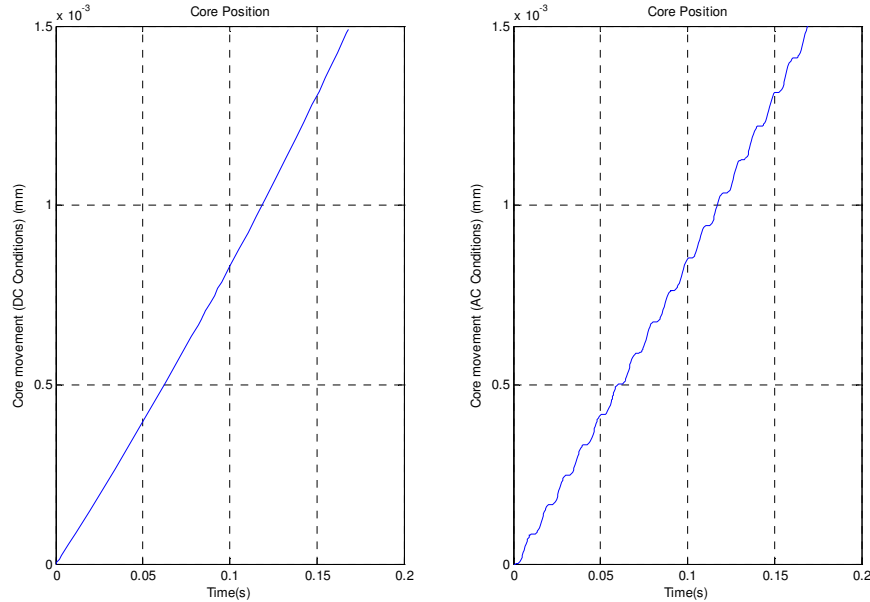


Figure 8.2 AC and DC Core Movement

8.5 Predicted Armature Response under AC and DC Conditions

Figure 8.3 and Figure 8.4 shows both AC and DC armature responses compared to the same time reference. The responses were calculated by solving all the system of equations described in Chapter 6 under equivalent driving conditions. Thus, the core will have to reach a certain position before the armature experiences enough force to overcome the opposing spring force.

From Figure 8.3 and Figure 8.4 certain observations can be made:

1. The AC time delay is faster than the DC time-delay (0.35s versus 0.45s).
2. It can be deduced that the core needed to move less in the AC case than the DC case for the armature to react.
3. The armature velocity is greater in the DC case than the AC case
4. The difference in time-delay is in the vicinity of 0.1s.

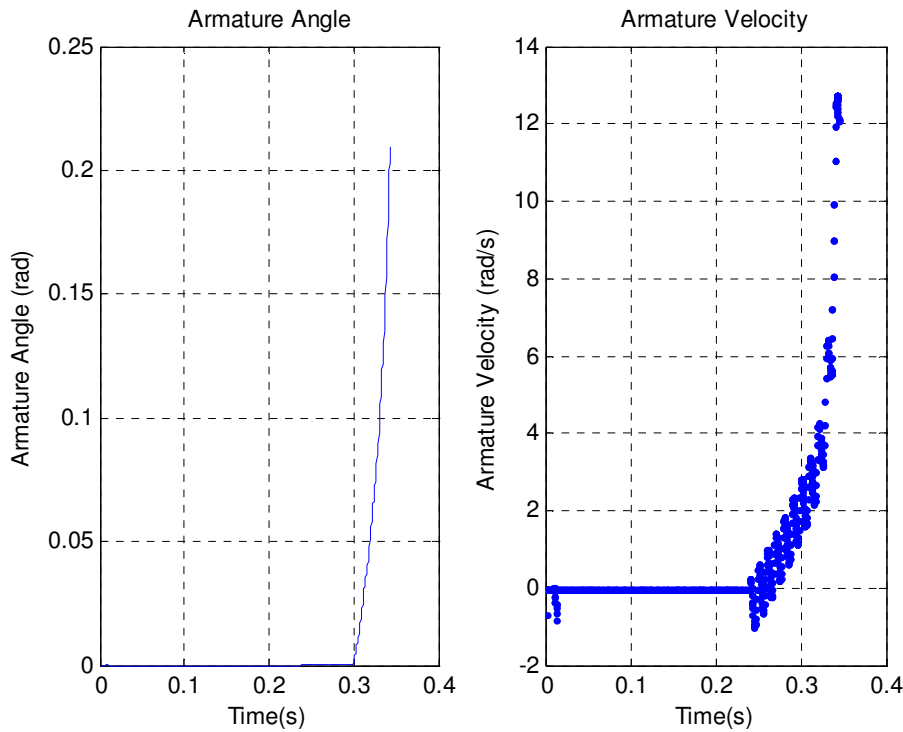


Figure 8.3: Armature Response under AC Excitation

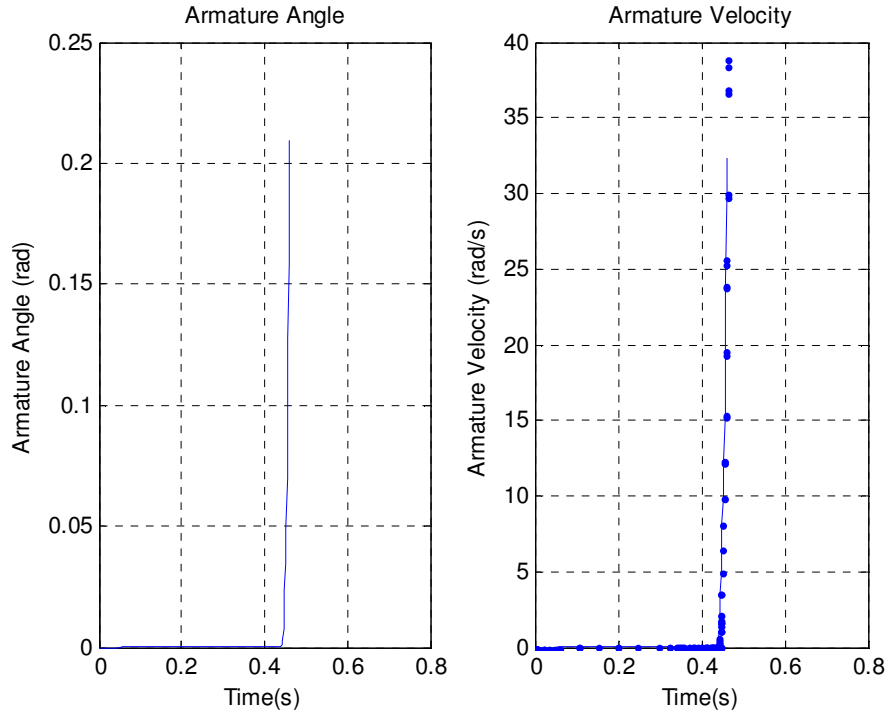


Figure 8.4: Armature response under DC conditions

8.6 AC vs. DC Time-Delays

From the section above it is clear that faster time-delay values are expected when a circuit breaker is tested under AC conditions, compared to a circuit breaker tested under equivalent DC conditions. This reduction in time is due to an increase in the trip-gap. The reduction in trip-gap is to some extent but not totally, counteracted by the lower armature velocity.

The difference between AC and DC circuit breaker performance, described in the previous sections, should be put into context regarding its effect on the circuit breaker time-delay. The following will assist in this:

1. The time-delay behaviour in the overload region is dominated by core movement, which is proven to be the same for both the AC and the DC case.
2. The core velocity will always be high as the core approaches the trip-gap. This will diminish the effect the difference in trip-gap between the AC and DC case will have on the total time-delay, as the time taken to make up the difference in trip-gap will be a relatively small portion of the total time-delay.
3. The lower armature velocity in the AC case will further act to reduce the effect of the different trip-gaps.

4. The total time-delay of the circuit breaker is influenced by many other variables to a much larger extent than the differences shown between the AC and the DC case.

From the above, the assumption is made that AC and DC circuit breakers will produce very similar time-delay behaviour, with circuit breakers tested under AC conditions producing marginally faster time-delays.

8.7 CPP Results

The CPP of the various samples were not tested individually as it is an extremely time consuming process, since core movement is very slow at currents just above I_{cp} and difficult to detect inside the oil filled brass tube of the sensing unit. However, all circuit breakers were tested at $1.05I_n$ and $1.25I_n$ to ensure that the must-hold-points and must-trip-points are specified within the allowable tolerance.

Figure 8.5 and Figure 8.6 give an indication of the accuracy of the CPP prediction. A theoretical Monte Carlo analysis, over 1000 samples was done randomly assigning values to all circuit breaker variables affecting the CPP, within their specified maximum and minimum limits. Using these randomly assigned variables the CPP was calculated producing the histograms shown in Figure 8.5 and Figure 8.6. These predictions were then compared to CPP measured on circuit breakers specifically built to produce maximum and minimum CPPs. From Figure 8.5 and Figure 8.6 below it is clear that the correlation between the measured and predicted results regarding CPP is very good.

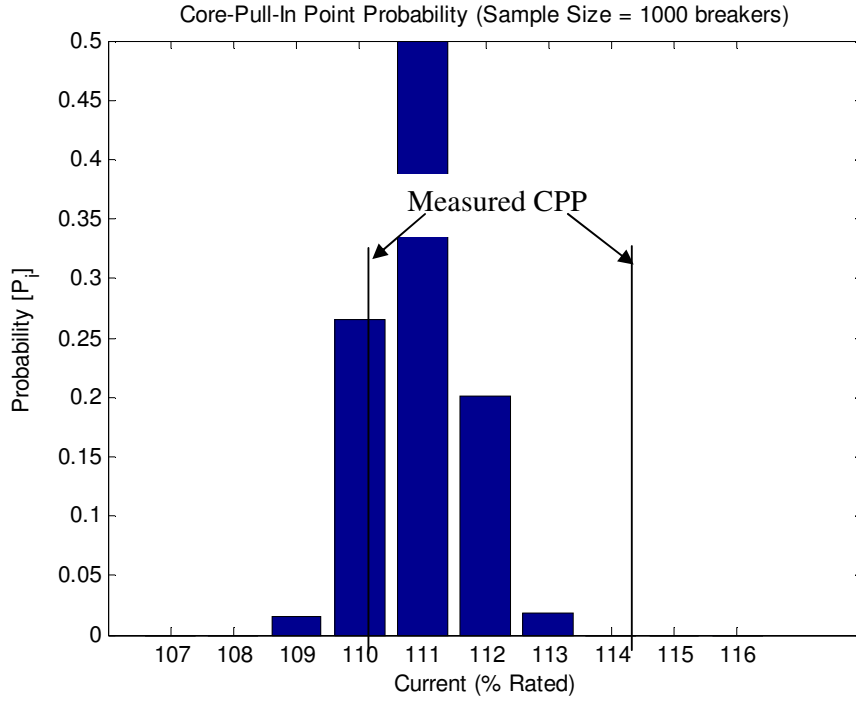


Figure 8.5: Monte Carlo Analysis on the CPP of 15A Circuit Breaker Compared to Measurement Results

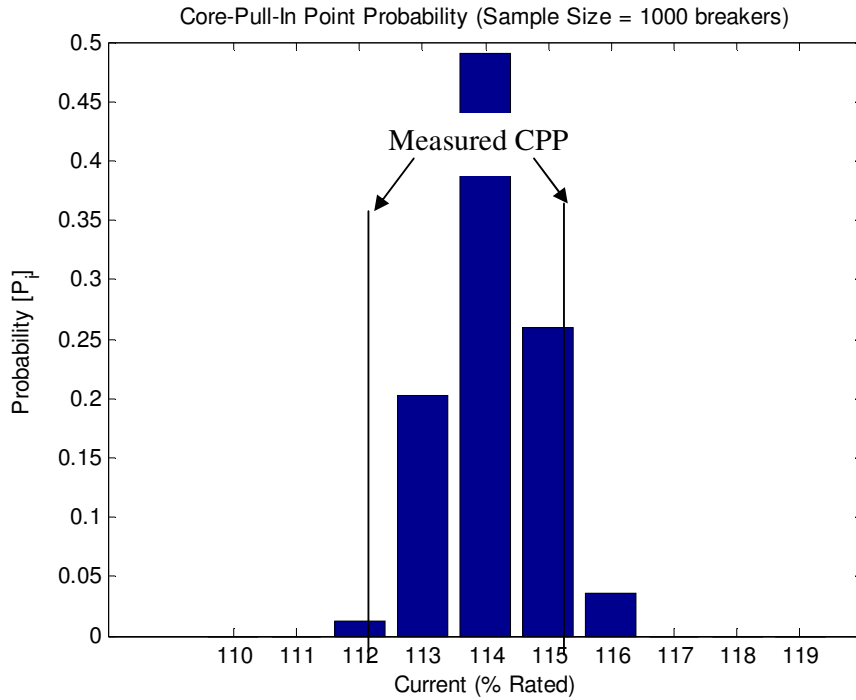


Figure 8.6: Monte Carlo Analysis on the CPP of 5A Circuit Breaker Compared to Measurement Result

8.8 ARP Results

As predicted from the AC results described in Chapter 6 the ARP measurements differ between the AC and the DC case.

Table 8.3 AC and DC ARP Results

I_n	DC Measurement (% I_n)	AC Measurement (% I_n)	DC Predictions (% I_n)		AC Prediction (% I_n)	
			Min	Max	Min	Max
5A	86	81	86	93	78	84
12A	95	86	94	97	85	91
15A	91	83	97	100	80	87

Table 8.3 shows the measured and the predicted ARP values for both the AC and DC case. This is the only aspect in which AC and DC circuit breakers differ. It is clear that AC and DC circuit breakers will not have the same ARP, with the ARP of AC breakers always lower than that of DC circuit breakers. Thus, in terms of the must-trip-point of the circuit breaker, the DC ARP value will represent the worst-case value. The impact of these differences on the time-delay values is expected to be small.

8.9 Time-Delay Results

The predicted time-delay behaviour correlates well with both AC and DC measured results. A typical set of results is shown in Figure 8.7, Figure 8.8 and Figure 8.9.

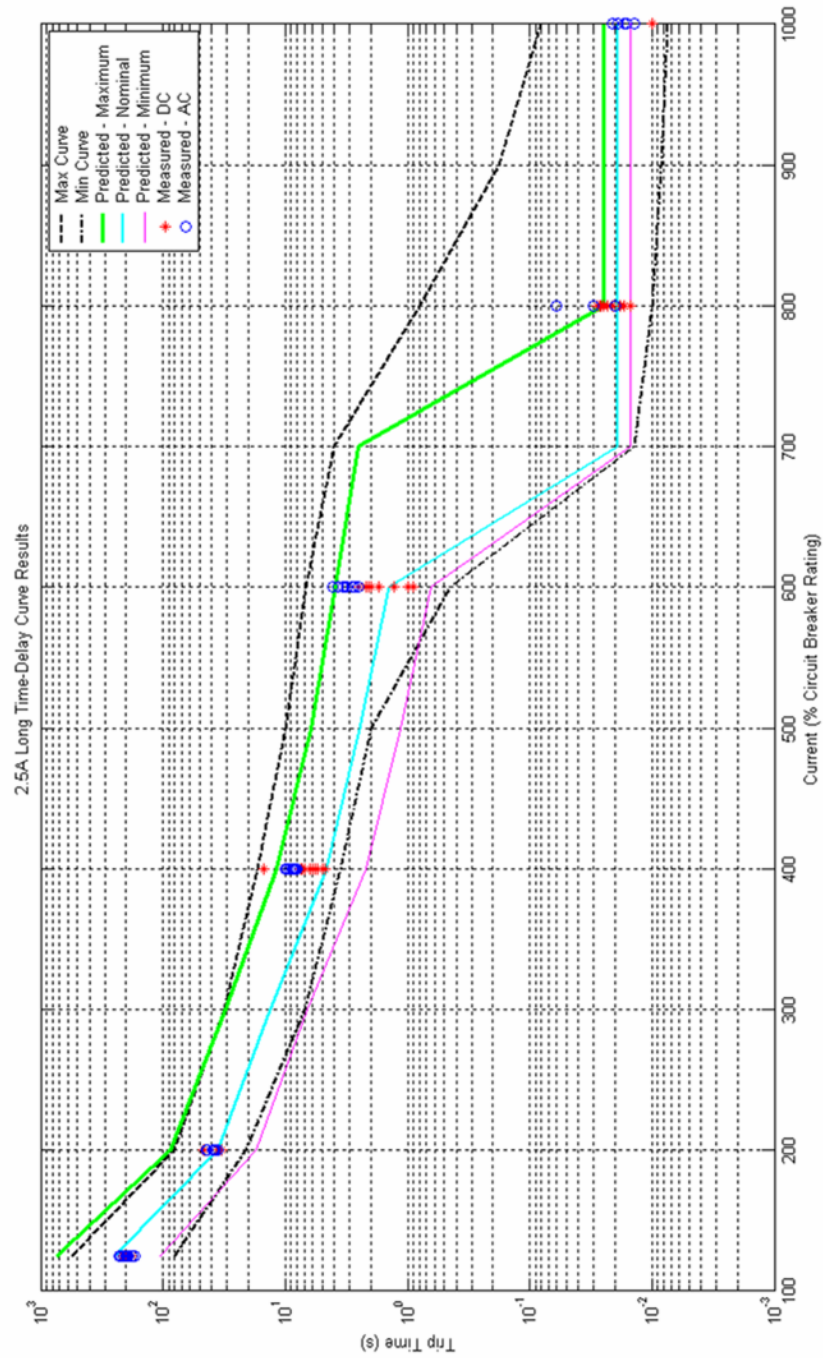


Figure 8.7: 2.5A Slow Time-Delay Curve Results

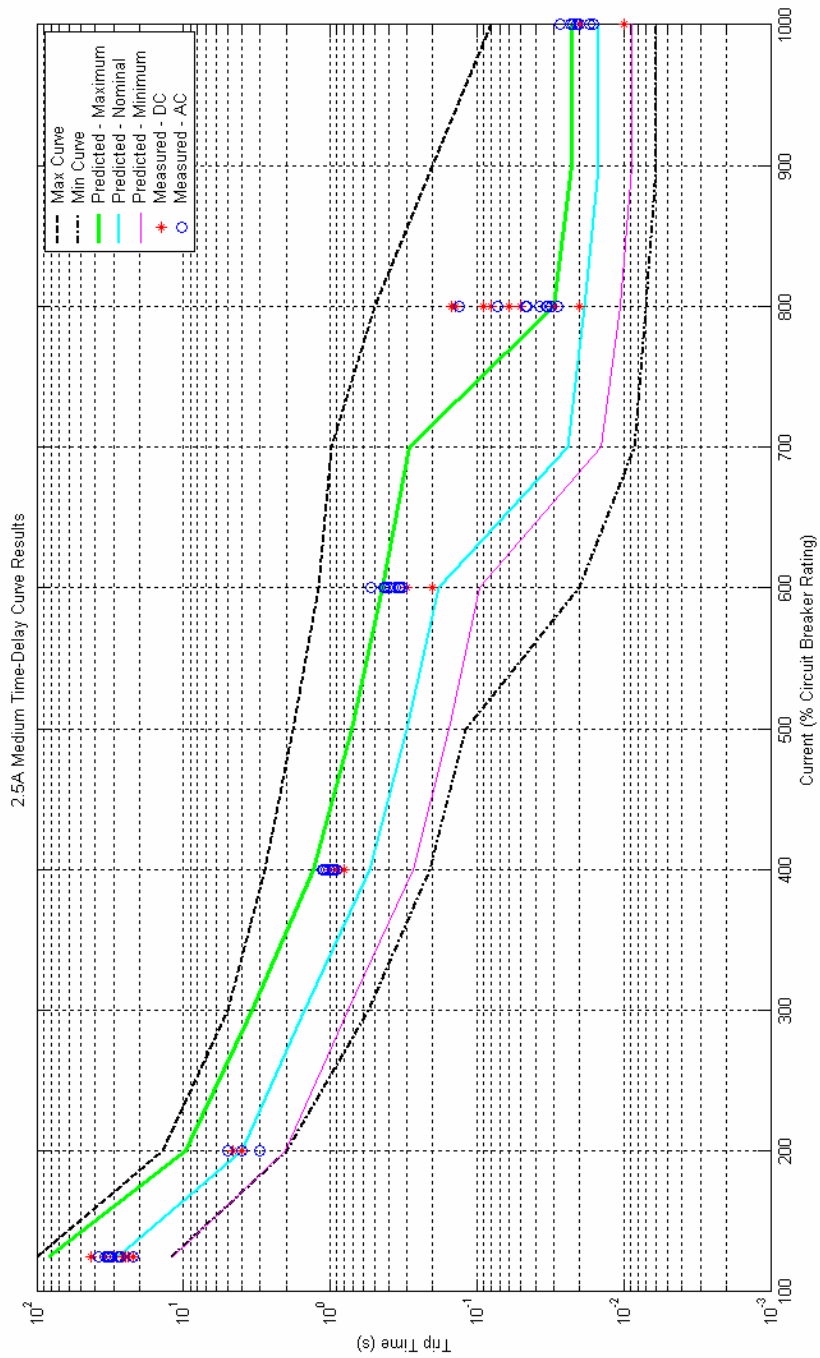


Figure 8.8 : 2.5A Medium Time-Delay Curve Results

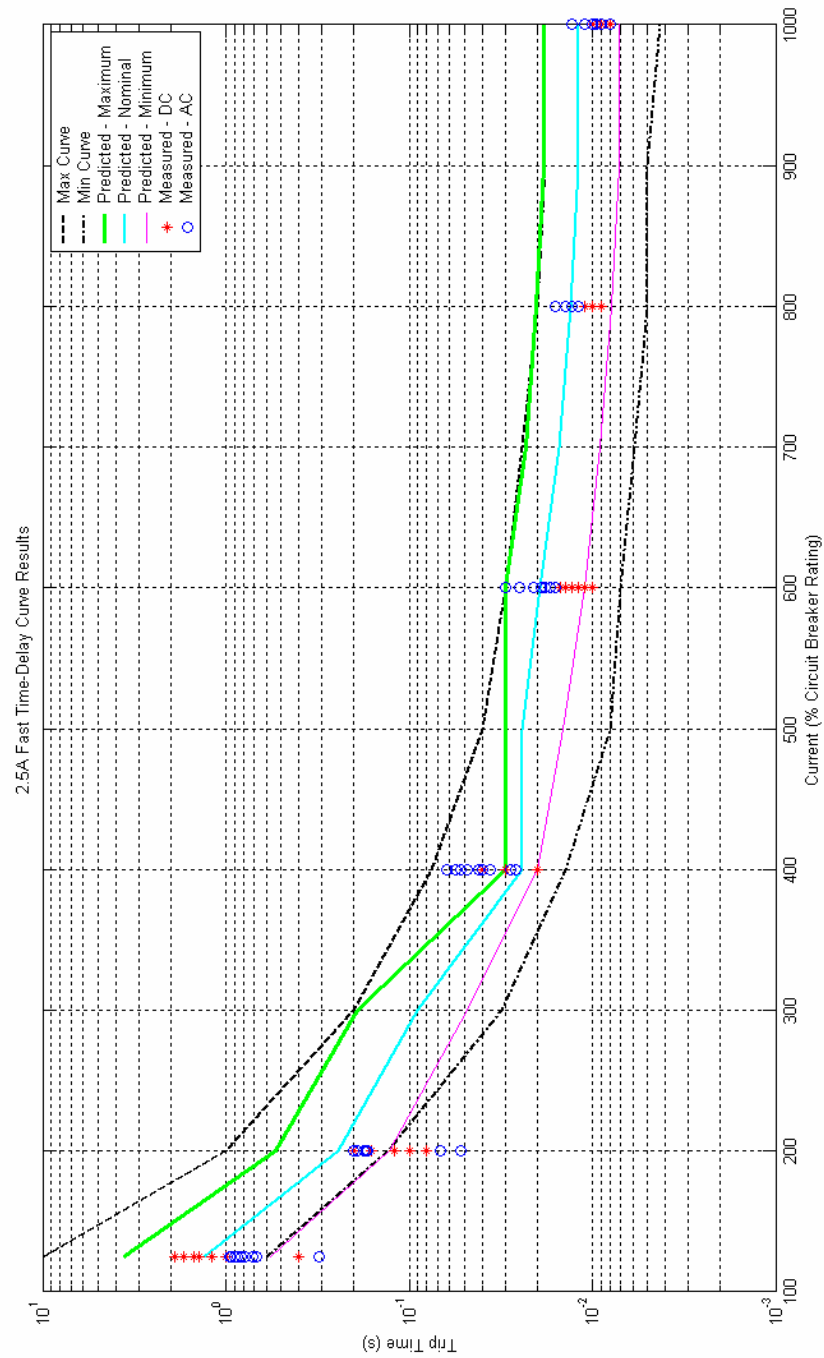


Figure 8.9: 2.5A Fast Time-Delay Curve Results

From Figure 8.7, Figure 8.8 and Figure 8.9 the following can be deduced:

The predicted maximum and minimum time-delay values follow the maximum and minimum published curve closely.

1. At $1.25I_n$ where the time-delay is dominated by relatively slow core movement, and as a result is very sensitive to tolerances, the measured time-delay values correspond well to the prediction.
2. At $8I_n$ where the time-delay is a combination of very fast core movement with simultaneous armature movement, the predicted time-delay values are conservative.
3. There is no clear pattern distinguishing AC measurements from DC measurements.

All the results from the other test samples follow the same pattern

8.10 Conclusion

This chapter briefly described the test sample, the electromagnetic force measurement results, the performance measure prediction results and the circuit breaker test results in general. The complete set of results is presented in Appendix A

CHAPTER 9

SUMMARY AND CONCLUSION

9.1 Introduction

This chapter summarises the objective, the methodology followed, and the results obtained in this dissertation. It will draw conclusions regarding the success of the proposed methodology, and suggest areas for future work.

9.2 The Aim

The aim of this work is to accurately determine the electromagnetic forces acting on ferromagnetic components as a result of an applied magnetic field, and to predict the movement of these components under the influence of these applied forces. The electromagnetic circuit chosen to test this methodology is the current sensing unit of low voltage hydraulic magnetic circuit breakers.

9.3 Summary

To predict the behaviour of ferromagnetic components under the influence of an electromagnetic force, the electromagnetic forces acting on the components need to be known to a high level of accuracy. As a complex interaction of factors influence these electromagnetic forces commercial FEM packages were found wanting in terms of accuracy and calculation speed. This is overcome by the design and commissioning of a piece of automated measurement equipment that accurately measures the electromagnetic forces acting on the components.

These forces were then used to predict the dynamic behaviour of the ferromagnetic components by solving the equations of motion of these components.

This work endeavours to predict the movement of said ferromagnetic components under the influence of both AC and DC excitation. To predict the behaviour under the influence of AC excitation, the equivalent AC electromagnetic forces were extrapolated based on the DC electromagnetic force measurements.

To evaluate the success of the predictions (for both AC and DC excitation), hydraulic magnetic circuit breakers, with all variables identical to the theoretical case, were built. These circuit breakers were tested and the results compared to the predictions.

9.4 Summary of Results

The measurement of the electromagnetic forces proved to be faster than FEM calculations. In addition, the accuracy of the electromagnetic force measurement proved to be superior to FEM calculations. This higher accuracy could be achieved as software modelling simplifications of the coil and electromagnetic circuit geometry is avoided.

The calculation of the dynamic behaviour of the ferromagnetic components based on the electromagnetic force measurement results were successful, as the predicted behaviour correlated well with measurements made on actual circuit breakers. The only instance where the prediction failed to predict the circuit breaker behaviour to satisfaction is in the instantaneous region of the time-delay curve (see Figure 2.1), where the predicted time-delay values are generally faster than the measurements.

9.5 Possible Improvements

Hydraulic magnetic circuit breakers, due to its very nature, are sensitive to manufacturing and testing variables. This is the reason for the relative width of the time-delay curves to which the circuit breakers have to conform. This obscures the test results too some extend.

As future improvement the current control in the circuit breaker test circuits can be improved, reducing tests variables and measurement uncertainties. In addition, this method can be evaluated on an electromagnetic system which is less sensitive to manufacturing tolerances.

The biggest discrepancies between the test and prediction are found at high currents ($8I_n$ to $10I_n$). At these currents, the time-delay is not dominated by core motion, as is the case for lower currents. As a result the armature behaviour is not negligible. A possible cause for this discrepancy is the inaccuracies in the modelling of the armature motion. As described in Chapter 5, the friction acting against the armature motion is assumed to be zero. Further work is necessary to verify the validity of this assumption.

9.6 Conclusion

In conclusion it can be stated that the measurement of electromagnetic forces is a success and in many respects is more suitable, in this case, than commercial FEM software packages used for calculating electromagnetic forces.

The methodology for predicting the behaviour of moving parts under the influence of electromagnetic force is deemed successful, and was proven to be so when evaluated on hydraulic magnetic circuit breakers.

REFERENCES

- [1] Cohen, V. *Application guide for the protection of LV distribution systems*, Fourth Edition, CBI Electric, 2006.
- [2] Opto Sigma, *SGSP/SGAM Series Datasheet*, Sigma Koki CO. Ltd.
- [3] Tidea 1004 Load Cell Datasheet
- [4] Microchip Corporation, *PIC18F2520 Datasheet*, 2005
- [5] Microchip Corporation, *MCP3201 2.7V 12-Bit A/D Converter with SPI™ Serial Interface Datasheet*, 2005
- [6] Griffiths, David J., *Introduction to Electrodynamics*, Second Edition, Prentice Hall, 1989
- [7] Vardeman, Stephen B., *Statistics for engineering problem solving*, PWS Publishing Company, 1994
- [8] Hibler R.C., *Engineering Mechanics, Dynamics*, Prentice Hall, 1997
- [9] Smith, Steven W., *The Scientist and Engineers guide to Digital Signal Processing*, California Technical Publishing, 1999
- [10] Kreutzig, *Advanced Engineering Mathematics*, Prentice Hall, 2001.
- [11] Microchip Corporation Inc, *Reduction of Noise in ADC Systems*, 2005
- [12] In-Mook Choi, Dong-June Choi, *The modelling and design of a mechanism for micro-force measurement*, KAIST, 2001

APPENDIX A

DETAIL DESCRIPTION OF PREDICTIONS & RESULTS

A.1 Introduction

This section shows a complete set of prediction and evaluation results used to verify the theoretical curve development method, based on the measurement of electromagnetic forces. The predictions and measurements were done utilizing the Force Measurement Apparatus and methods outlined in this thesis.

A.2 Prediction Results

Curve Development Results (Measurements: FMA v1 - Calculation: Tesla v10)			
10-Mar-2006 10:23:17			
Breaker Data			
Rating (A) =	2.50		
100% Test Current (A) =	2.55		
Curve =	Slow		
AC/DC =	DC		
Sensing Unit =	C_D		
Coil =	Short(no add info)		
Notch =	1 (2314234)		
Armature Bom no. =	2164293		
Frame Bom no. =	2204756		
Magnetic Data File =	C:\Program Files\MATLAB71\work\2_5A_Results.xls		
Tube Data (no add info)			
	Minimum	Nominal	Maximum
Tube Length =	29.46	29.48	29.50
Tube Inside Diameter =	4.40	4.42	4.44
Pip dimension =	0.45	0.50	0.55
Core Data(no add info)			
	Minimum	Nominal	Maximum
Core diameter =	4.28	4.29	4.30
Core Length (X) =	16.90	16.95	17.00
Core thin Length (Y) =	6.50	6.55	6.60
Oil Data(no add info)			
	Minimum	Nominal	Maximum
Oil Viscosity =	475.00	500.00	525.00
Spring Data(no add info)			
	Minimum	Nominal	Maximum
L1 =		15.00	
L2 =		6.60	
F1 =	5.20	5.70	6.20
F2 =	13.10	13.70	14.30
Pole Piece Data(no add info)			
	Minimum	Nominal	Maximum
Pole Piece Length =	6.95	7.00	7.05
Pole Piece lpy =	0.90	1.00	1.10
Results			
Core Pull-in point			
	Minimum	Nominal	Maximum
CPP (% Rated =)	105.00	115.00	123.00
Armature Response Point			
	Minimum	Nominal	Maximum
ARP (% Rated =)	97.00	98.00	100.00
Time Delay			
	Minimum	Nominal	Maximum
125% (s) =	105.519	251.283	743.746
200% (s) =	17.525	35.687	87.869
300% (s) =	6.5801	13.2853	31.1851
400% (s) =	2.1857	4.5758	11.9166
500% (s) =	1.1508	2.4743	6.1337
600% (s) =	0.6453	1.4335	3.8730
700% (s) =	0.0150	0.0190	2.5164
800% (s) =	0.0150	0.0190	0.0250
900% (s) =	0.0150	0.0190	0.0250
1000% (s) =	0.0150	0.0190	0.0250

DETAIL DESCRIPTION OF PREDICTIONS & RESULTS

Curve Development Results (Measurements: FMA v1 - Calculation: Tesla v10)
31-Oct-2006 12:26:23

Breaker Data

Rating (A) = 4.00
100% Test Current (A) = 4.17
Curve = Slow
AC/DC = DC
Sensing Unit = C_D
Coil = Short(no add info)
Notch = 1 (2314234)
Armature Bom no. = 2164293
Frame Bom no. = 2204756
Magnetic Data File = C:\Program Files\MATLAB\R2006a\work\4A_Measured Results.xls

Tube Data (2032012)

	Minimum	Nominal	Maximum
Tube Length =	29.46	29.48	29.50
Tube Inside Diameter =	4.40	4.42	4.44
Pip dimension =	0.45	0.50	0.55

Core Data(2234124)

	Minimum	Nominal	Maximum
Core diameter =	4.28	4.29	4.30
Core Length (X) =	16.90	16.95	17.00
Core thin Length (Y) =	6.50	6.55	6.60

Oil Data(1809382)

	Minimum	Nominal	Maximum
Oil Viscosity =	396.20	417.05	437.90

Spring Data(4304128)

	Minimum	Nominal	Maximum
L1 =		15.00	
L2 =		6.60	
F1 =	5.10	5.30	5.50
F2 =	12.70	12.95	13.20

Pole Piece Data(no add info)

	Minimum	Nominal	Maximum
Pole Piece Length =	6.95	7.00	7.05
Pole Piece lpy =	0.90	1.00	1.10

Results

Core Pull-in point

	Minimum	Nominal	Maximum
CPP (% Rated =)	107.00	114.00	120.00

Armature Response Point

	Minimum	Nominal	Maximum
ARP (% Rated =)	96.00	97.00	98.00

Time Delay

	Minimum	Nominal	Maximum
125% (s) =	89.711	217.009	660.138
200% (s) =	16.006	31.291	73.716
300% (s) =	6.5330	13.2485	30.5170
400% (s) =	2.1343	4.6017	11.3288
500% (s) =	1.2033	2.4281	5.9898
600% (s) =	0.6818	1.3933	3.5201
700% (s) =	0.0126	0.8708	2.2671
800% (s) =	0.0097	0.0163	0.0253
900% (s) =	0.0082	0.0137	0.0209
1000% (s) =	0.0073	0.0122	0.0189

DETAIL DESCRIPTION OF PREDICTIONS & RESULTS

Curve Development Results (Measurements: FMA v1 - Calculation: Tesla v10)
19-Jan-2007 08:28:50

Breaker Data

Rating (A) = 12.00
100% Test Current (A) = 12.10
Curve = Slow
AC/DC = DC
Sensing Unit = C_D
Coil = Short(no add info)
Notch = 2 (2314234)
Armature Bom no. = xxxxxxxx
Frame Bom no. = xxxxxxxx
Magnetic Data File = C:\Program Files\MATLAB\R2006a\work\12A_Measured_Results.xls

Tube Data (2032012)

	Minimum	Nominal	Maximum
Tube Length =	29.46	29.48	29.50
Tube Inside Diameter =	4.40	4.42	4.44
Pip dimension =	0.45	0.50	0.55

Core Data(2234124)

	Minimum	Nominal	Maximum
Core diameter =	4.28	4.29	4.30
Core Length (X) =	16.90	16.95	17.00
Core thin Length (Y) =	6.50	6.55	6.60

Oil Data(1809382)

	Minimum	Nominal	Maximum
Oil Viscosity =	396.20	416.95	437.70

Spring Data(4304128)

	Minimum	Nominal	Maximum
L1 =		15.00	
L2 =		6.60	
F1 =	2.80	3.30	3.80
F2 =	10.50	11.10	11.70

Pole Piece Data(no add info)

	Minimum	Nominal	Maximum
Pole Piece Length =	6.95	7.00	7.05
Pole Piece lpy =	0.90	1.00	1.10

Results

Core Pull-in point

	Minimum	Nominal	Maximum
CPP (% Rated =)	100.00	114.00	124.00

Armature Response Point

	Minimum	Nominal	Maximum
ARP (% Rated =)	95.00	96.00	98.00

Time Delay

	Minimum	Nominal	Maximum
125% (s) =	98.373	240.376	752.222
200% (s) =	17.253	34.178	81.842
300% (s) =	6.4604	12.7001	29.1045
400% (s) =	2.6576	5.6536	14.7625
500% (s) =	1.3369	2.8365	6.6204
600% (s) =	0.8087	1.7503	4.1277
700% (s) =	0.0134	1.0770	2.5699
800% (s) =	0.0104	0.0179	0.0291
900% (s) =	0.0085	0.0142	0.0216
1000% (s) =	0.0073	0.0123	0.0190

DETAIL DESCRIPTION OF PREDICTIONS & RESULTS

Curve Development Results (Measurements: FMA v1 - Calculation: Tesla v10)			
31-Oct-2006 12:36:22			
Breaker Data			
Rating (A) =	12.50		
100% Test Current (A) =	12.60		
Curve =	Slow		
AC/DC =	DC		
Sensing Unit =	C_D		
Coil =	Short(no add info)		
Notch =	2 (2314234)		
Armature Bom no. =	2164293		
Frame Bom no. =	2204756		
Magnetic Data File = C:\Program Files\MATLAB\R2006a\work\12_5A_Measured_Results.xls			
Tube Data (2032012)			
	Minimum	Nominal	Maximum
Tube Length =	29.46	29.48	29.50
Tube Inside Diameter =	4.40	4.42	4.44
Pip dimension =	0.45	0.50	0.55
Core Data(2234124)			
	Minimum	Nominal	Maximum
Core diameter =	4.28	4.29	4.30
Core Length (X) =	16.90	16.95	17.00
Core thin Length (Y) =	6.50	6.55	6.60
Oil Data(1809382)			
	Minimum	Nominal	Maximum
Oil Viscosity =	396.20	417.05	437.90
Spring Data(4304128)			
	Minimum	Nominal	Maximum
L1 =		15.00	
L2 =		6.60	
F1 =	5.10	5.30	5.50
F2 =	12.70	12.95	13.20
Pole Piece Data(no add info)			
	Minimum	Nominal	Maximum
Pole Piece Length =	6.95	7.00	7.05
Pole Piece lpy =	0.90	1.00	1.10
Results			
Core Pull-in point			
	Minimum	Nominal	Maximum
CPP (% Rated =)	110.00	117.00	123.00
Armature Response Point			
	Minimum	Nominal	Maximum
ARP (% Rated =)	94.00	96.00	97.00
Time Delay			
	Minimum	Nominal	Maximum
125% (s) =	102.895	260.963	898.450
200% (s) =	17.421	35.102	83.208
300% (s) =	5.8860	11.5044	26.5276
400% (s) =	2.2366	4.7775	11.7411
500% (s) =	1.1897	2.5193	5.9154
600% (s) =	0.7405	1.5076	3.5812
700% (s) =	0.4475	1.0079	2.4154
800% (s) =	0.0098	0.0167	0.0261
900% (s) =	0.0082	0.0135	0.0207
1000% (s) =	0.0070	0.0118	0.0184

DETAIL DESCRIPTION OF PREDICTIONS & RESULTS

Curve Development Results (Measurements: FMA v1 - Calculation: Tesla v10)
01-Nov-2006 08:55:11

Breaker Data

Rating (A) = 15.00
100% Test Current (A) = 15.20
Curve = Slow
AC/DC = DC
Sensing Unit = C_D
Coil = Short (no add info)
Notch = 2 (2314234)
Armature Bom no. = 2164293
Frame Bom no. = 2204756
Magnetic Data File = C:\Program Files\MATLAB\R2006a\work\15A_Results.xls

Tube Data (2032012)

	Minimum	Nominal	Maximum
Tube Length =	29.46	29.48	29.50
Tube Inside Diameter =	4.40	4.42	4.44
Pip dimension =	0.45	0.50	0.55

Core Data(2234124)

	Minimum	Nominal	Maximum
Core diameter =	4.28	4.29	4.30
Core Length (X) =	16.90	16.95	17.00
Core thin Length (Y) =	6.50	6.55	6.60

Oil Data(1809382)

	Minimum	Nominal	Maximum
Oil Viscosity =	396.80	417.00	437.20

Spring Data(4304128)

	Minimum	Nominal	Maximum
L1 =		15.00	
L2 =		6.60	
F1 =	5.10	5.30	5.50
F2 =	12.70	12.95	13.20

Pole Piece Data(no add info)

	Minimum	Nominal	Maximum
Pole Piece Length =	6.95	7.00	7.05
Pole Piece lpy =	0.90	1.00	1.10

Results

Core Pull-in point

	Minimum	Nominal	Maximum
CPP (% Rated =)	109.00	115.00	121.00

Armature Response Point

	Minimum	Nominal	Maximum
ARP (% Rated =)	94.00	95.00	97.00

Time Delay

	Minimum	Nominal	Maximum
125% (s) =	91.944	225.950	717.470
200% (s) =	16.452	32.842	76.275
300% (s) =	5.8376	11.8370	27.0213
400% (s) =	3.0435	5.9915	14.5744
500% (s) =	1.5694	3.2259	7.9737
600% (s) =	0.6889	1.5848	4.1095
700% (s) =	0.2387	0.6771	2.1604
800% (s) =	0.0091	0.0152	0.0232
900% (s) =	0.0076	0.0127	0.0195
1000% (s) =	0.0066	0.0113	0.0177

DETAIL DESCRIPTION OF PREDICTIONS & RESULTS

Curve Development Results (Measurements: FMA v1 - Calculation: Tesla v10)
31-Oct-2006 12:54:22

Breaker Data

Rating (A) = 2.50
100% Test Current (A) = 2.55
Curve = Medium
AC/DC = DC
Sensing Unit = C_D
Coil = Short (no add info)
Notch = 1 (2314234)
Armature Bom no. = 2164293
Frame Bom no. = 2204756
Magnetic Data File = C:\Program Files\MATLAB\R2006a\work\2_5A_Results.xls

Tube Data (2032012)

	Minimum	Nominal	Maximum
Tube Length =	29.46	29.48	29.50
Tube Inside Diameter =	4.40	4.42	4.44
Pip dimension =	0.45	0.50	0.55

Core Data(2234124)

	Minimum	Nominal	Maximum
Core diameter =	4.28	4.29	4.30
Core Length (X) =	16.90	16.95	17.00
Core thin Length (Y) =	6.50	6.55	6.60

Oil Data(1809382)

	Minimum	Nominal	Maximum
Oil Viscosity =	53.20	56.00	58.80

Spring Data(4304128)

	Minimum	Nominal	Maximum
L1 =		15.00	
L2 =		6.60	
F1 =	5.20	5.70	6.20
F2 =	13.10	13.70	14.30

Pole Piece Data(no add info)

	Minimum	Nominal	Maximum
Pole Piece Length =	6.95	7.00	7.05
Pole Piece lpy =	0.90	1.00	1.10

Results

Core Pull-in point

	Minimum	Nominal	Maximum
CPP (% Rated =)	105.00	115.00	123.00

Armature Response Point

	Minimum	Nominal	Maximum
ARP (% Rated =)	97.00	98.00	100.00

Time Delay

	Minimum	Nominal	Maximum
125% (s) =	11.822	28.147	83.303
200% (s) =	2.039	4.019	9.582
300% (s) =	0.7553	1.5098	3.4196
400% (s) =	0.2747	0.5344	1.3104
500% (s) =	0.1547	0.2990	0.7142
600% (s) =	0.0961	0.1824	0.4365
700% (s) =	0.0142	0.0240	0.2892
800% (s) =	0.0106	0.0185	0.0300
900% (s) =	0.0088	0.0147	0.0224
1000% (s) =	0.0088	0.0147	0.0224

DETAIL DESCRIPTION OF PREDICTIONS & RESULTS

Curve Development Results (Measurements: FMA v1 - Calculation: Tesla v10)			
31-Oct-2006 12:57:59			
Breaker Data			
Rating (A) =	4.00		
100% Test Current (A) =	4.17		
Curve =	Medium		
AC/DC =	DC		
Sensing Unit =	C_D		
Coil =	Short(no add info)		
Notch =	2 (2314234)		
Armature Bom no. =	2164293		
Frame Bom no. =	2204756		
Magnetic Data File = C:\Program Files\MATLAB\R2006a\work\4A_Measured Results.xls			
Tube Data (2032012)			
	Minimum	Nominal	Maximum
Tube Length =	29.46	29.48	29.50
Tube Inside Diameter =	4.40	4.42	4.44
Pip dimension =	0.45	0.50	0.55
Core Data(2234124)			
	Minimum	Nominal	Maximum
Core diameter =	4.28	4.29	4.30
Core Length (X) =	16.90	16.95	17.00
Core thin Length (Y) =	6.50	6.55	6.60
Oil Data(1809382)			
	Minimum	Nominal	Maximum
Oil Viscosity =	53.20	56.00	58.80
Spring Data(4304128)			
	Minimum	Nominal	Maximum
L1 =		15.00	
L2 =		6.60	
F1 =	5.10	5.30	5.50
F2 =	12.70	12.95	13.20
Pole Piece Data(no add info)			
	Minimum	Nominal	Maximum
Pole Piece Length =	6.95	7.00	7.05
Pole Piece lpy =	0.90	1.00	1.10
Results			
Core Pull-in point			
	Minimum	Nominal	Maximum
CPP (% Rated =)	107.00	114.00	120.00
Armature Response Point			
	Minimum	Nominal	Maximum
ARP (% Rated =)	94.00	95.00	96.00
Time Delay			
	Minimum	Nominal	Maximum
125% (s) =	12.049	29.143	88.645
200% (s) =	2.124	4.254	10.026
300% (s) =	0.9088	1.7673	4.0427
400% (s) =	0.2942	0.6224	1.4670
500% (s) =	0.1712	0.3320	0.7975
600% (s) =	0.0958	0.1966	0.4733
700% (s) =	0.0098	0.0166	0.3052
800% (s) =	0.0082	0.0136	0.0208
900% (s) =	0.0073	0.0122	0.0189
1000% (s) =	0.0066	0.0113	0.0178

DETAIL DESCRIPTION OF PREDICTIONS & RESULTS

Curve Development Results (Measurements: FMA v1 - Calculation: Tesla v10)
31-Oct-2006 13:02:08

Breaker Data

Rating (A) = 12.00
100% Test Current (A) = 12.10
Curve = Medium
AC/DC = DC
Sensing Unit = C_D
Coil = Short(no add info)
Notch = 2 (2314234)
Armature Bom no. = 2164293
Frame Bom no. = 2204756
Magnetic Data File = C:\Program Files\MATLAB\R2006a\work\12A_Measured_Results.xls

Tube Data (2032012)

	Minimum	Nominal	Maximum
Tube Length =	29.46	29.48	29.50
Tube Inside Diameter =	4.40	4.42	4.44
Pip dimension =	0.45	0.50	0.55

Core Data(2234124)

	Minimum	Nominal	Maximum
Core diameter =	4.28	4.29	4.30
Core Length (X) =	16.90	16.95	17.00
Core thin Length (Y) =	6.50	6.55	6.60

Oil Data(1809382)

	Minimum	Nominal	Maximum
Oil Viscosity =	53.20	56.00	58.80

Spring Data(4304128)

	Minimum	Nominal	Maximum
L1 =		15.00	
L2 =		6.60	
F1 =	2.80	3.30	3.80
F2 =	10.50	11.10	11.70

Pole Piece Data(no add info)

	Minimum	Nominal	Maximum
Pole Piece Length =	6.95	7.00	7.05
Pole Piece lpy =	0.90	1.00	1.10

Results

Core Pull-in point

	Minimum	Nominal	Maximum
CPP (% Rated =)	100.00	113.00	124.00

Armature Response Point

	Minimum	Nominal	Maximum
ARP (% Rated =)	95.00	96.00	98.00

Time Delay

	Minimum	Nominal	Maximum
125% (s) =	13.213	32.288	101.056
200% (s) =	2.265	4.611	11.021
300% (s) =	0.8565	1.7265	3.9358
400% (s) =	0.3744	0.7494	1.9393
500% (s) =	0.1969	0.3829	0.9153
600% (s) =	0.1259	0.2419	0.5805
700% (s) =	0.0759	0.1549	0.3712
800% (s) =	0.0104	0.0179	0.0291
900% (s) =	0.0085	0.0142	0.0216
1000% (s) =	0.0073	0.0123	0.0190

DETAIL DESCRIPTION OF PREDICTIONS & RESULTS

Curve Development Results (Measurements: FMA v1 - Calculation: Tesla v10)			
19-Jan-2007 08:49:24			
Breaker Data			
Rating (A) =	12.50		
100% Test Current (A) =	12.60		
Curve =	Medium		
AC/DC =	DC		
Sensing Unit =	C_D		
Coil =	Short(no add info)		
Notch =	2 (2314234)		
Armature Bom no. =	xxxxxxxxxx		
Frame Bom no. =	xxxxxxxxxx		
Magnetic Data File =	C:\Program Files\MATLAB\R2006a\work\12_5A_Measured_Results.xls		
Tube Data (2032012)			
	Minimum	Nominal	Maximum
Tube Length =	29.46	29.48	29.50
Tube Inside Diameter =	4.40	4.42	4.44
Pip dimension =	0.45	0.50	0.55
Core Data(2234124)			
	Minimum	Nominal	Maximum
Core diameter =	4.28	4.29	4.30
Core Length (X) =	16.90	16.95	17.00
Core thin Length (Y) =	6.50	6.55	6.60
Oil Data(1809382)			
	Minimum	Nominal	Maximum
Oil Viscosity =	396.20	416.95	437.70
Spring Data(4304128)			
	Minimum	Nominal	Maximum
L1 =		15.00	
L2 =		6.60	
F1 =	5.10	5.30	5.50
F2 =	12.70	12.95	13.20
Pole Piece Data(no add info)			
	Minimum	Nominal	Maximum
Pole Piece Length =	6.95	7.00	7.05
Pole Piece lpy =	0.90	1.00	1.10
Results			
Core Pull-in point			
	Minimum	Nominal	Maximum
CPP (% Rated =)	110.00	117.00	123.00
Armature Response Point			
	Minimum	Nominal	Maximum
ARP (% Rated =)	94.00	96.00	97.00
Time Delay			
	Minimum	Nominal	Maximum
125% (s) =	102.895	260.901	898.039
200% (s) =	17.989	36.195	83.170
300% (s) =	5.8913	11.8598	27.3341
400% (s) =	2.2381	4.9808	12.1981
500% (s) =	1.1903	2.5187	5.9128
600% (s) =	0.7403	1.6008	3.7918
700% (s) =	0.0127	1.0076	2.4143
800% (s) =	0.0098	0.0167	0.0261
900% (s) =	0.0082	0.0135	0.0207
1000% (s) =	0.0070	0.0118	0.0184

DETAIL DESCRIPTION OF PREDICTIONS & RESULTS

Curve Development Results (Measurements: FMA v1 - Calculation: Tesla v10)
01-Nov-2006 08:57:51

Breaker Data

Rating (A) = 15.00
100% Test Current (A) = 15.20
Curve = Medium
AC/DC = DC
Sensing Unit = C_D
Coil = Short(no add info)
Notch = 2 (2314234)
Armature Bom no. = 2164293
Frame Bom no. = 2204756
Magnetic Data File = C:\Program Files\MATLAB\R2006a\work\15A_Results.xls

Tube Data (2032012)

	Minimum	Nominal	Maximum
Tube Length =	29.46	29.48	29.50
Tube Inside Diameter =	4.40	4.42	4.44
Pip dimension =	0.45	0.50	0.55

Core Data(2234124)

	Minimum	Nominal	Maximum
Core diameter =	4.28	4.29	4.30
Core Length (X) =	16.90	16.95	17.00
Core thin Length (Y) =	6.50	6.55	6.60

Oil Data(1809382)

	Minimum	Nominal	Maximum
Oil Viscosity =	53.20	56.00	58.80

Spring Data(4304128)

	Minimum	Nominal	Maximum
L1 =		15.00	
L2 =		6.60	
F1 =	5.10	5.30	5.50
F2 =	12.70	12.95	13.20

Pole Piece Data(no add info)

	Minimum	Nominal	Maximum
Pole Piece Length =	6.95	7.00	7.05
Pole Piece lpy =	0.90	1.00	1.10

Results

Core Pull-in point

	Minimum	Nominal	Maximum
CPP (% Rated =)	109.00	115.00	121.00

Armature Response Point

	Minimum	Nominal	Maximum
ARP (% Rated =)	94.00	95.00	97.00

Time Delay

	Minimum	Nominal	Maximum
125% (s) =	12.331	30.347	96.498
200% (s) =	2.223	4.431	10.284
300% (s) =	0.8000	1.6104	3.6601
400% (s) =	0.4254	0.8254	1.9861
500% (s) =	0.2277	0.4540	1.0984
600% (s) =	0.1054	0.2336	0.5787
700% (s) =	0.0420	0.1093	0.3165
800% (s) =	0.0091	0.0152	0.0232
900% (s) =	0.0076	0.0127	0.0195
1000% (s) =	0.0066	0.0113	0.0177

DETAIL DESCRIPTION OF PREDICTIONS & RESULTS

Curve Development Results (Measurements: FMA v1 - Calculation: Tesla v10)
31-Oct-2006 15:51:34

Breaker Data

Rating (A) = 2.50
100% Test Current (A) = 2.55
Curve = Fast
AC/DC = DC
Sensing Unit = C_D
Coil = Short(no add info)
Notch = 3 (2314234)
Armature Bom no. = 2164293
Frame Bom no. = 2204756
Magnetic Data File = C:\Program Files\MATLAB\R2006a\work\2_5A_Results.xls

Tube Data (2032012)

	Minimum	Nominal	Maximum
Tube Length =	29.46	29.48	29.50
Tube Inside Diameter =	4.40	4.42	4.44
Pip dimension =	0.45	0.50	0.55

Core Data(2234124)

	Minimum	Nominal	Maximum
Core diameter =	4.28	4.29	4.30
Core Length (X) =	19.50	19.55	19.60
Core thin Length (Y) =	6.50	6.55	6.60

Oil Data(1809382)

	Minimum	Nominal	Maximum
Oil Viscosity =	5.90	6.20	6.50

Spring Data(4304128)

	Minimum	Nominal	Maximum
L1 =		15.00	
L2 =		6.60	
F1 =	6.30	6.90	7.50
F2 =	14.30	15.00	15.70

Pole Piece Data(no add info)

	Minimum	Nominal	Maximum
Pole Piece Length =	6.95	7.00	7.05
Pole Piece lpy =	0.90	1.00	1.10

Results

Core Pull-in point

	Minimum	Nominal	Maximum
CPP (% Rated =)	105.00	112.00	117.00

Armature Response Point

	Minimum	Nominal	Maximum
ARP (% Rated =)	91.00	93.00	94.00

Time Delay

	Minimum	Nominal	Maximum
125% (s) =	0.573	1.317	3.627
200% (s) =	0.128	0.244	0.532
300% (s) =	0.0481	0.0898	0.1919
400% (s) =	0.0200	0.0240	0.0300
500% (s) =	0.0145	0.0240	0.0300
600% (s) =	0.0110	0.0192	0.0300
700% (s) =	0.0091	0.0151	0.0230
800% (s) =	0.0079	0.0131	0.0201
900% (s) =	0.0071	0.0119	0.0185
1000% (s) =	0.0071	0.0119	0.0185

DETAIL DESCRIPTION OF PREDICTIONS & RESULTS

Curve Development Results (Measurements: FMA v1 - Calculation: Tesla v10)
31-Oct-2006 15:55:39

Breaker Data

Rating (A) = 4.00
100% Test Current (A) = 4.17
Curve = Fast
AC/DC = DC
Sensing Unit = C_D
Coil = Short(no add info)
Notch = 3 (2314234)
Armature Bom no. = 2164293
Frame Bom no. = 2204756
Magnetic Data File = C:\Program Files\MATLAB\R2006a\work\4A_Measured Results.xls

Tube Data (2032012)

	Minimum	Nominal	Maximum
Tube Length =	29.46	29.48	29.50
Tube Inside Diameter =	4.40	4.42	4.44
Pip dimension =	0.45	0.50	0.55

Core Data(2234124)

	Minimum	Nominal	Maximum
Core diameter =	4.28	4.29	4.30
Core Length (X) =	19.50	19.55	19.60
Core thin Length (Y) =	6.50	6.55	6.60

Oil Data(1809382)

	Minimum	Nominal	Maximum
Oil Viscosity =	5.90	6.20	6.50

Spring Data(4304128)

	Minimum	Nominal	Maximum
L1 =		15.00	
L2 =		6.60	
F1 =	6.80	7.40	8.00
F2 =	14.80	15.50	16.20

Pole Piece Data(no add info)

	Minimum	Nominal	Maximum
Pole Piece Length =	6.95	7.00	7.05
Pole Piece lpy =	0.90	1.00	1.10

Results

Core Pull-in point

	Minimum	Nominal	Maximum
CPP (% Rated =)	110.00	117.00	123.00

Armature Response Point

	Minimum	Nominal	Maximum
ARP (% Rated =)	90.00	92.00	93.00

Time Delay

	Minimum	Nominal	Maximum
125% (s) =	0.790	1.950	6.043
200% (s) =	0.137	0.263	0.578
300% (s) =	0.0589	0.1059	0.2225
400% (s) =	0.0200	0.0240	0.0300
500% (s) =	0.0140	0.0240	0.0300
600% (s) =	0.0104	0.0178	0.0285
700% (s) =	0.0086	0.0143	0.0218
800% (s) =	0.0075	0.0125	0.0193
900% (s) =	0.0068	0.0115	0.0180
1000% (s) =	0.0062	0.0108	0.0171

DETAIL DESCRIPTION OF PREDICTIONS & RESULTS

Curve Development Results (Measurements: FMA v1 - Calculation: Tesla v10)
31-Oct-2006 15:59:58

Breaker Data

Rating (A) = 12.00
100% Test Current (A) = 12.10
Curve = Fast
AC/DC = DC
Sensing Unit = C_D
Coil = Short(no add info)
Notch = 3 (2314234)
Armature Bom no. = 2164293
Frame Bom no. = 2204756
Magnetic Data File = C:\Program Files\MATLAB\R2006a\work\12A_Measured_Results.xls

Tube Data (2032012)

	Minimum	Nominal	Maximum
Tube Length =	29.46	29.48	29.50
Tube Inside Diameter =	4.40	4.42	4.44
Pip dimension =	0.45	0.50	0.55

Core Data(2234124)

	Minimum	Nominal	Maximum
Core diameter =	4.28	4.29	4.30
Core Length (X) =	19.50	19.55	19.60
Core thin Length (Y) =	6.50	6.55	6.60

Oil Data(1809382)

	Minimum	Nominal	Maximum
Oil Viscosity =	5.90	6.20	6.50

Spring Data(4304128)

	Minimum	Nominal	Maximum
L1 =		15.00	
L2 =		6.60	
F1 =	4.30	4.90	5.50
F2 =	11.90	12.60	13.30

Pole Piece Data(no add info)

	Minimum	Nominal	Maximum
Pole Piece Length =	6.95	7.00	7.05
Pole Piece lpy =	0.90	1.00	1.10

Results

Core Pull-in point

	Minimum	Nominal	Maximum
CPP (% Rated =)	104.00	112.00	119.00

Armature Response Point

	Minimum	Nominal	Maximum
ARP (% Rated =)	92.00	93.00	95.00

Time Delay

	Minimum	Nominal	Maximum
125% (s) =	0.677	1.602	4.615
200% (s) =	0.136	0.250	0.573
300% (s) =	0.0580	0.1046	0.2169
400% (s) =	0.0200	0.0240	0.0621
500% (s) =	0.0197	0.0240	0.0300
600% (s) =	0.0136	0.0240	0.0300
700% (s) =	0.0108	0.0188	0.0300
800% (s) =	0.0090	0.0150	0.0228
900% (s) =	0.0077	0.0129	0.0197
1000% (s) =	0.0068	0.0115	0.0180

DETAIL DESCRIPTION OF PREDICTIONS & RESULTS

Curve Development Results (Measurements: FMA v1 - Calculation: Tesla v10)
31-Oct-2006 16:04:01

Breaker Data

Rating (A) = 12.50
100% Test Current (A) = 12.60
Curve = Fast
AC/DC = DC
Sensing Unit = C_D
Coil = Short(no add info)
Notch = 3 (2314234)
Armature Bom no. = 2164293
Frame Bom no. = 2204756
Magnetic Data File = C:\Program Files\MATLAB\R2006a\work\12_5A_Measured_Results.xls

Tube Data (2032012)

	Minimum	Nominal	Maximum
Tube Length =	29.46	29.48	29.50
Tube Inside Diameter =	4.40	4.42	4.44
Pip dimension =	0.45	0.50	0.55

Core Data(2234124)

	Minimum	Nominal	Maximum
Core diameter =	4.28	4.29	4.30
Core Length (X) =	19.50	19.55	19.60
Core thin Length (Y) =	6.50	6.55	6.60

Oil Data(1809382)

	Minimum	Nominal	Maximum
Oil Viscosity =	5.90	6.20	6.50

Spring Data(4304128)

	Minimum	Nominal	Maximum
L1 =		15.00	
L2 =		6.60	
F1 =	5.80	6.40	7.00
F2 =	13.80	14.50	15.20

Pole Piece Data(no add info)

	Minimum	Nominal	Maximum
Pole Piece Length =	6.95	7.00	7.05
Pole Piece lpy =	0.90	1.00	1.10

Results

Core Pull-in point

	Minimum	Nominal	Maximum
CPP (% Rated =)	107.00	115.00	121.00

Armature Response Point

	Minimum	Nominal	Maximum
ARP (% Rated =)	91.00	93.00	94.00

Time Delay

	Minimum	Nominal	Maximum
125% (s) =	0.701	1.678	4.926
200% (s) =	0.145	0.278	0.614
300% (s) =	0.0548	0.0974	0.2018
400% (s) =	0.0200	0.0240	0.0482
500% (s) =	0.0181	0.0240	0.0300
600% (s) =	0.0128	0.0240	0.0300
700% (s) =	0.0104	0.0179	0.0286
800% (s) =	0.0086	0.0143	0.0218
900% (s) =	0.0074	0.0124	0.0192
1000% (s) =	0.0065	0.0112	0.0176

A.3 Predicted Results Compared To Measurements

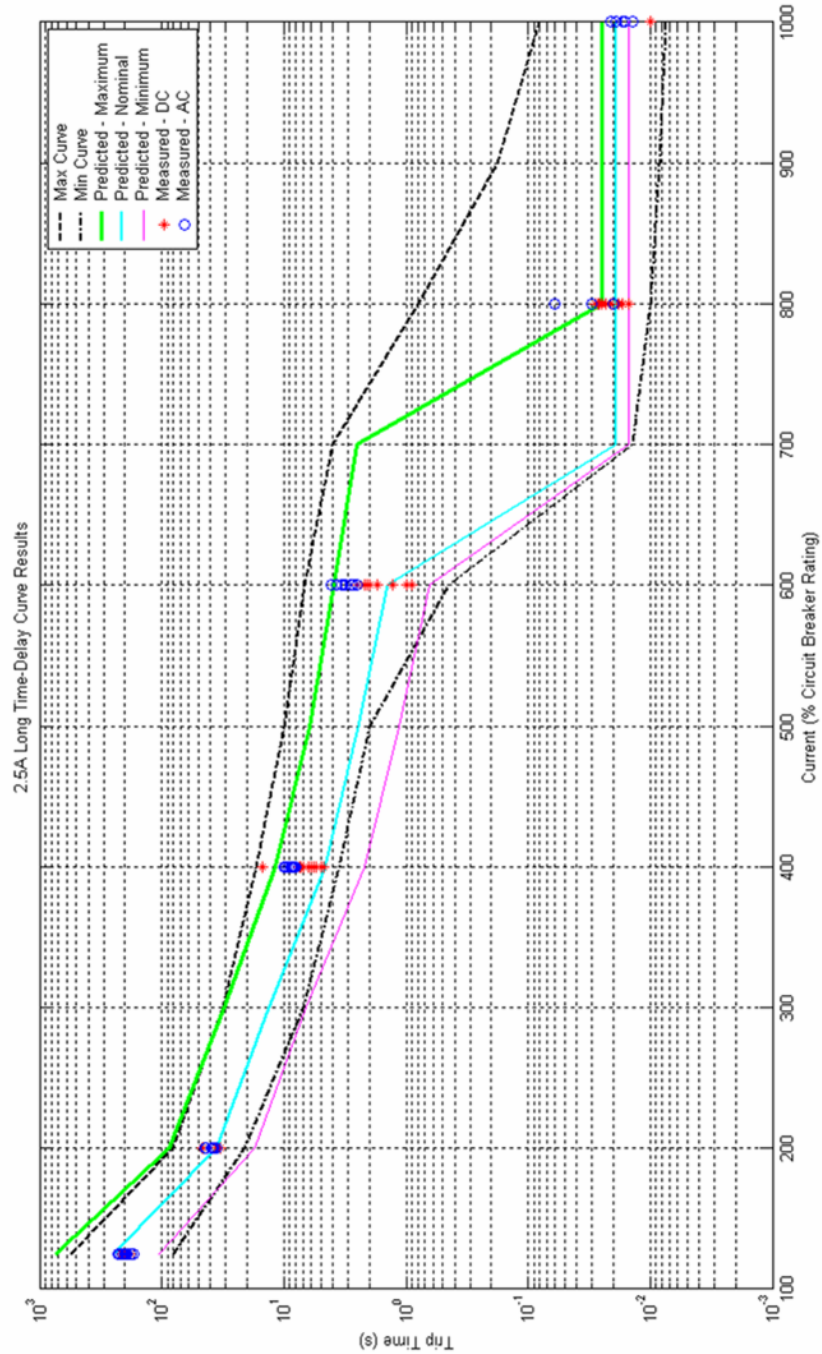


Figure A.1: 2.5A Circuit Breaker Long Time-Delay Curve Results

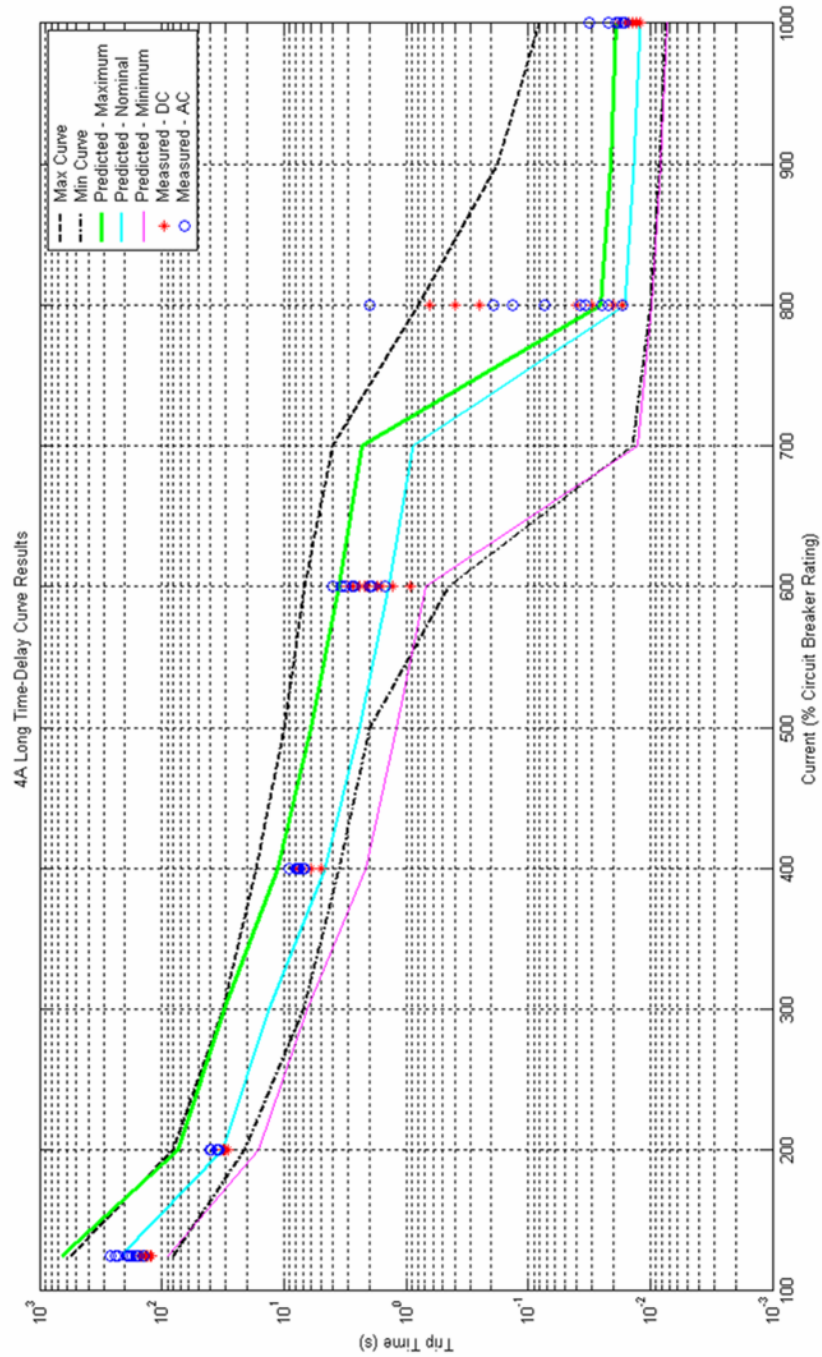


Figure A.2: 4A Circuit Breaker Long Time-Delay Curve Results

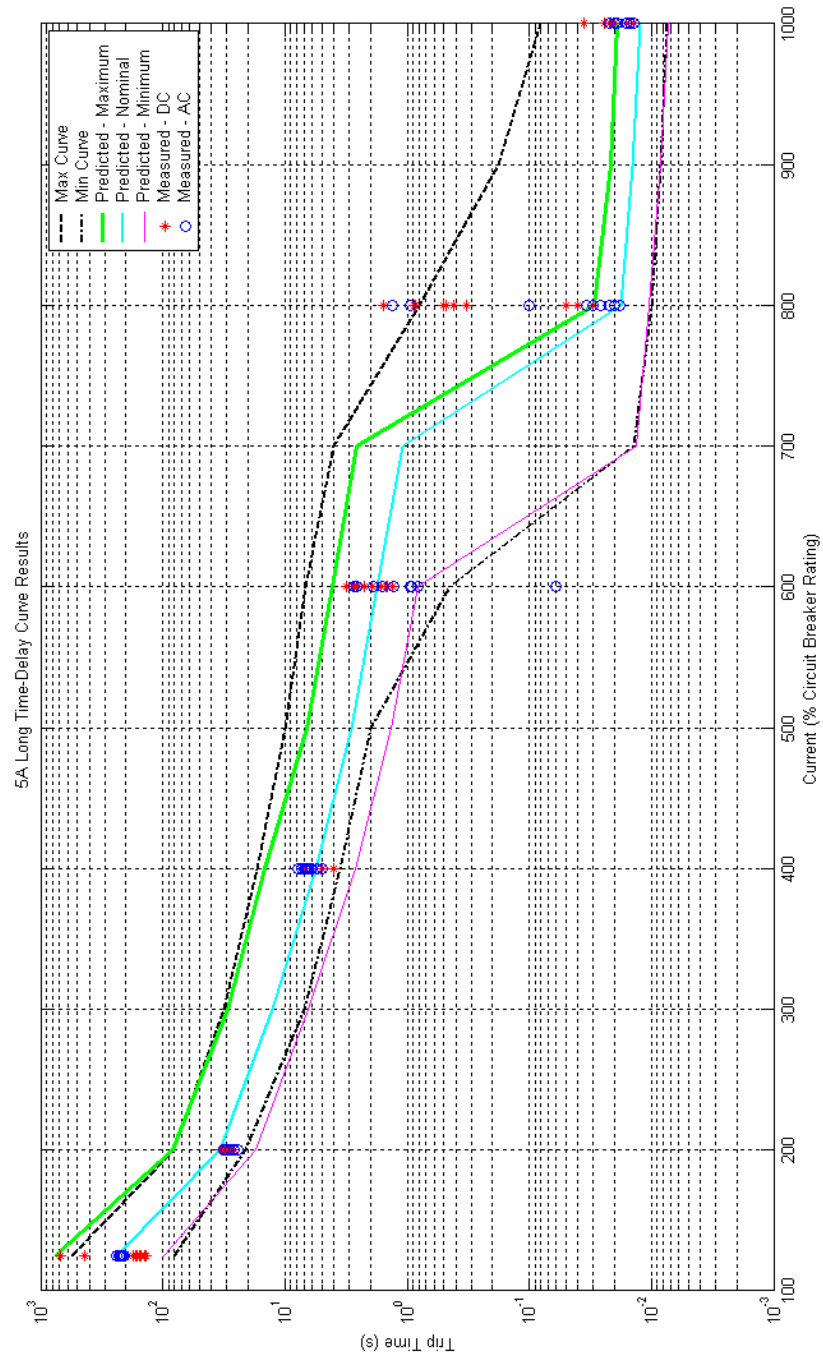


Figure A.3: 5A Circuit Breaker Long Time-Delay Curve Results

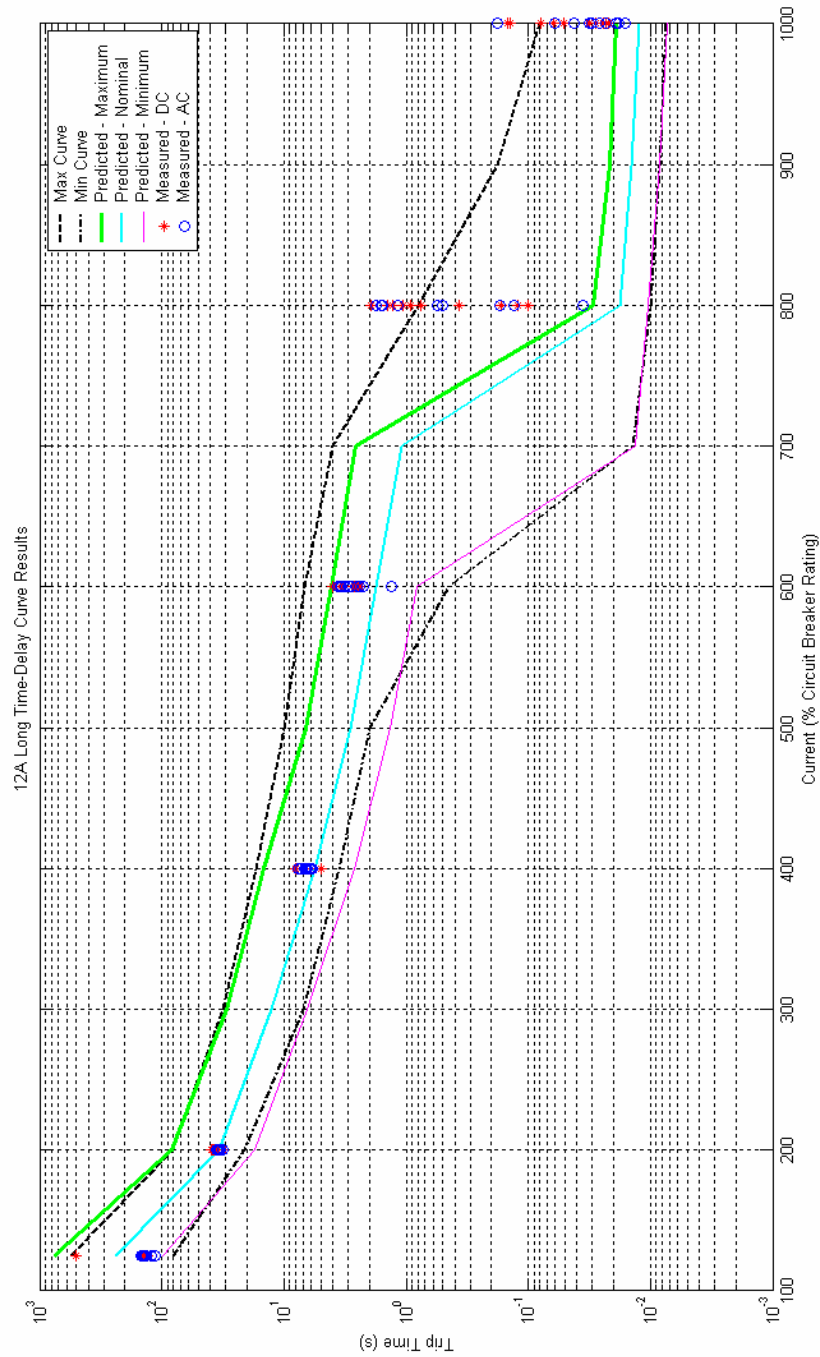


Figure A.4: 12A Circuit Breaker Long Time-Delay Curve Results

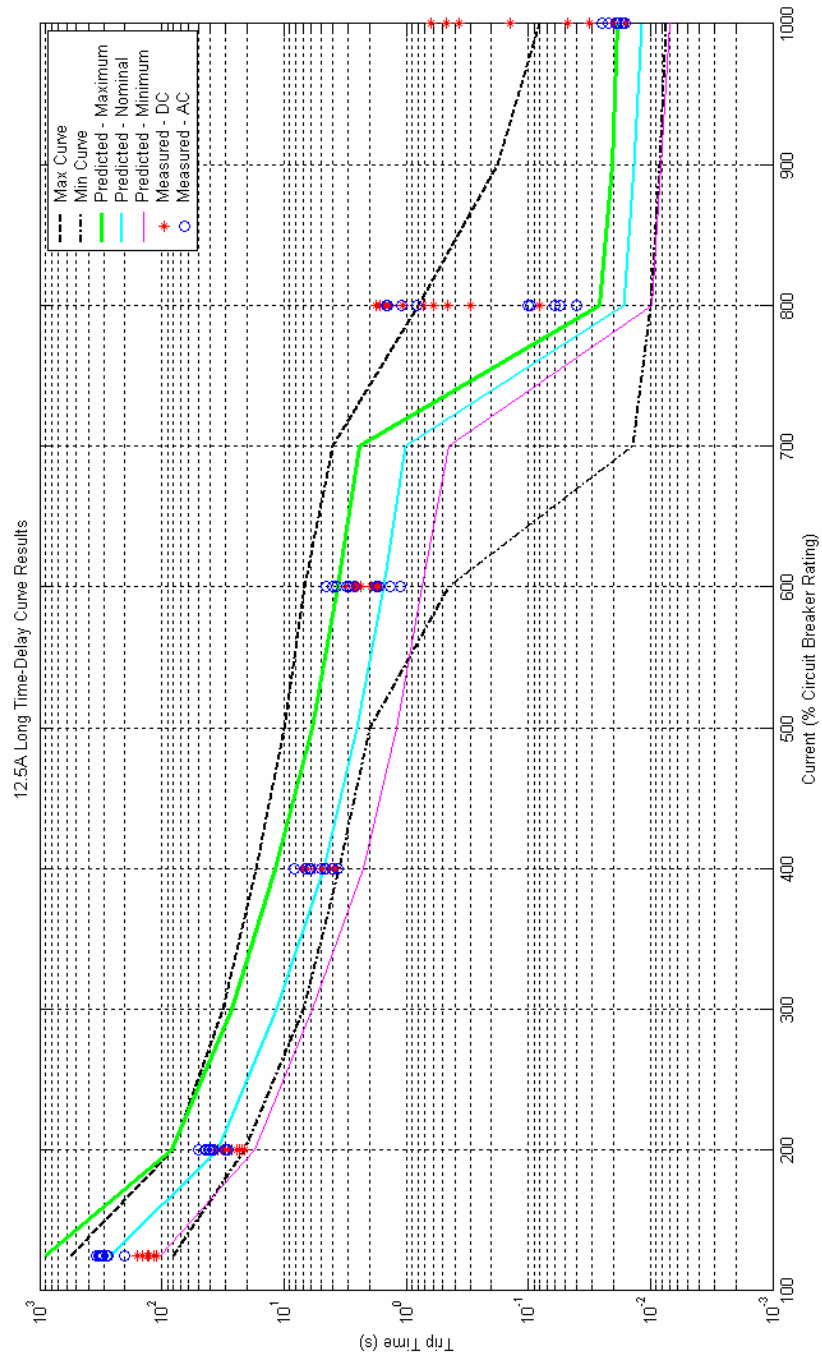


Figure A.5: 12.5A Circuit Breaker Long Time-Delay Curve Results

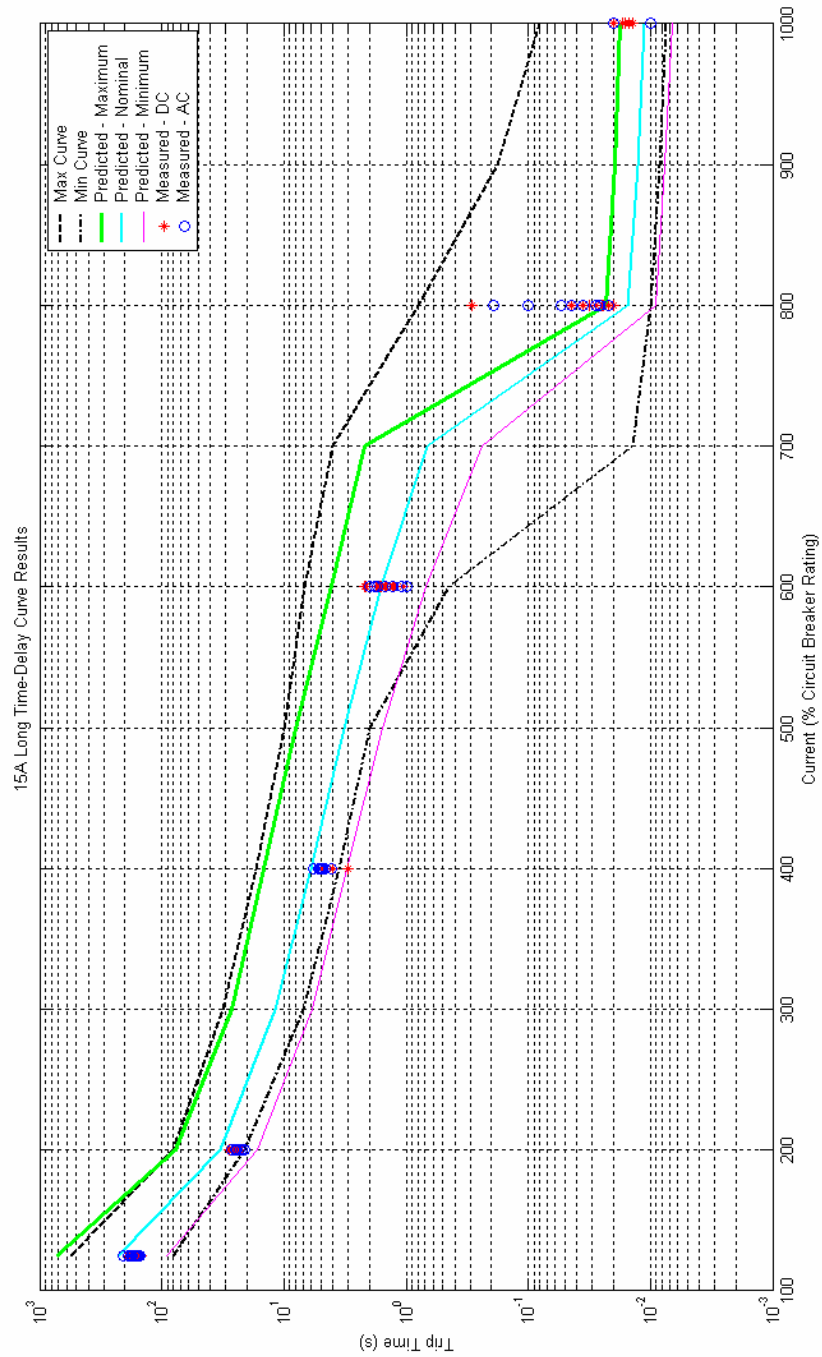


Figure A.6: 15A Circuit Breaker Long Time-Delay Curve Results

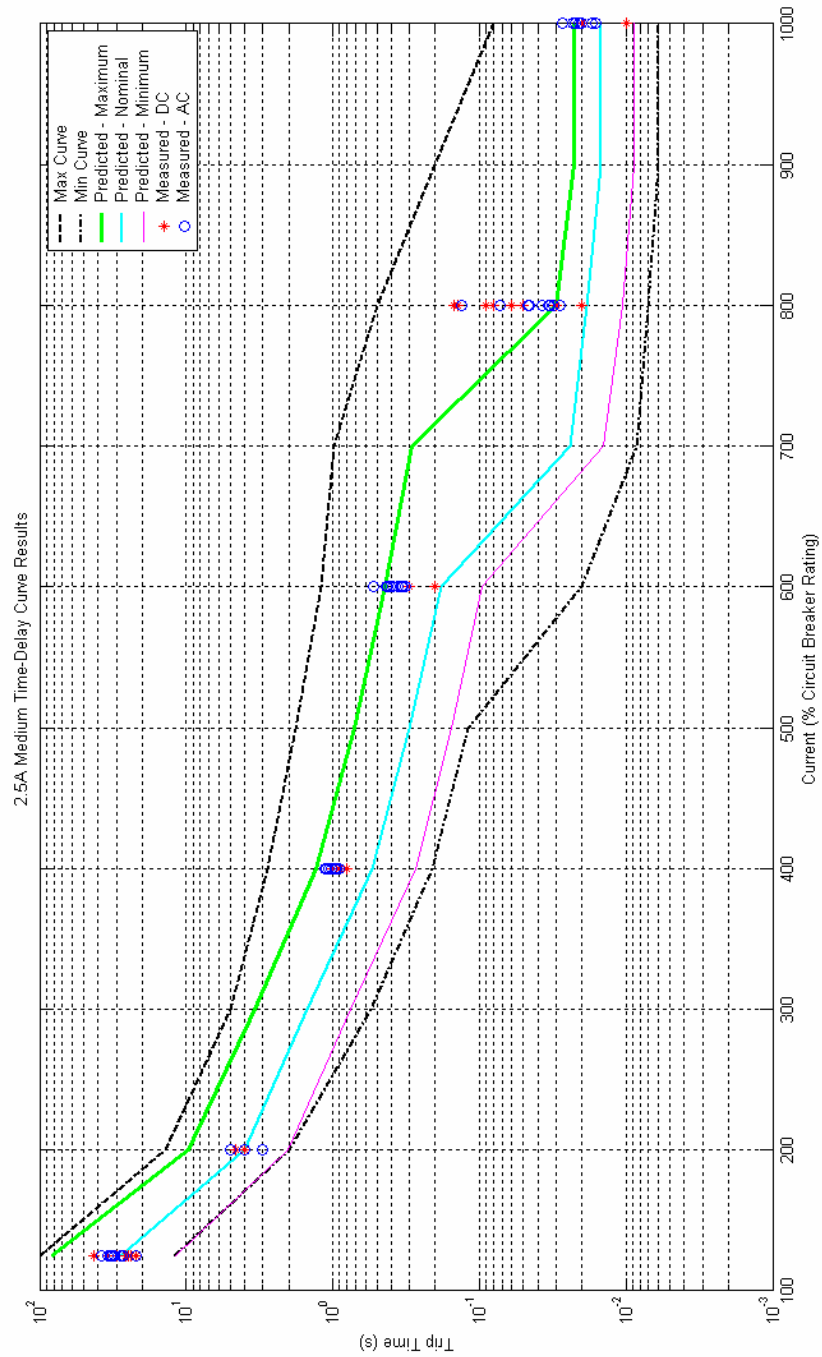


Figure A.7: 2.5A Circuit Breaker Medium Time-Delay Curve Results

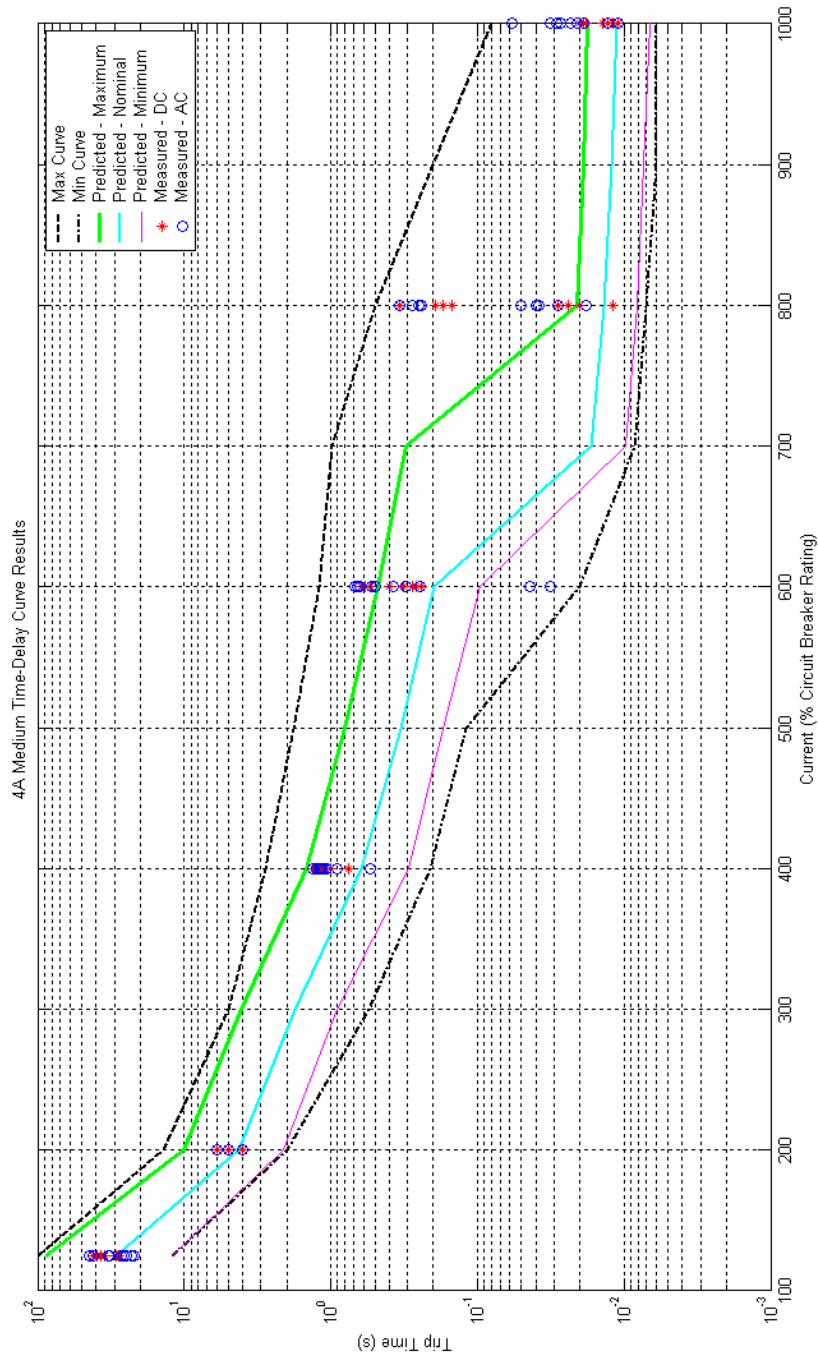


Figure A.8: 4A Circuit Breaker Medium Time-Delay Curve Results

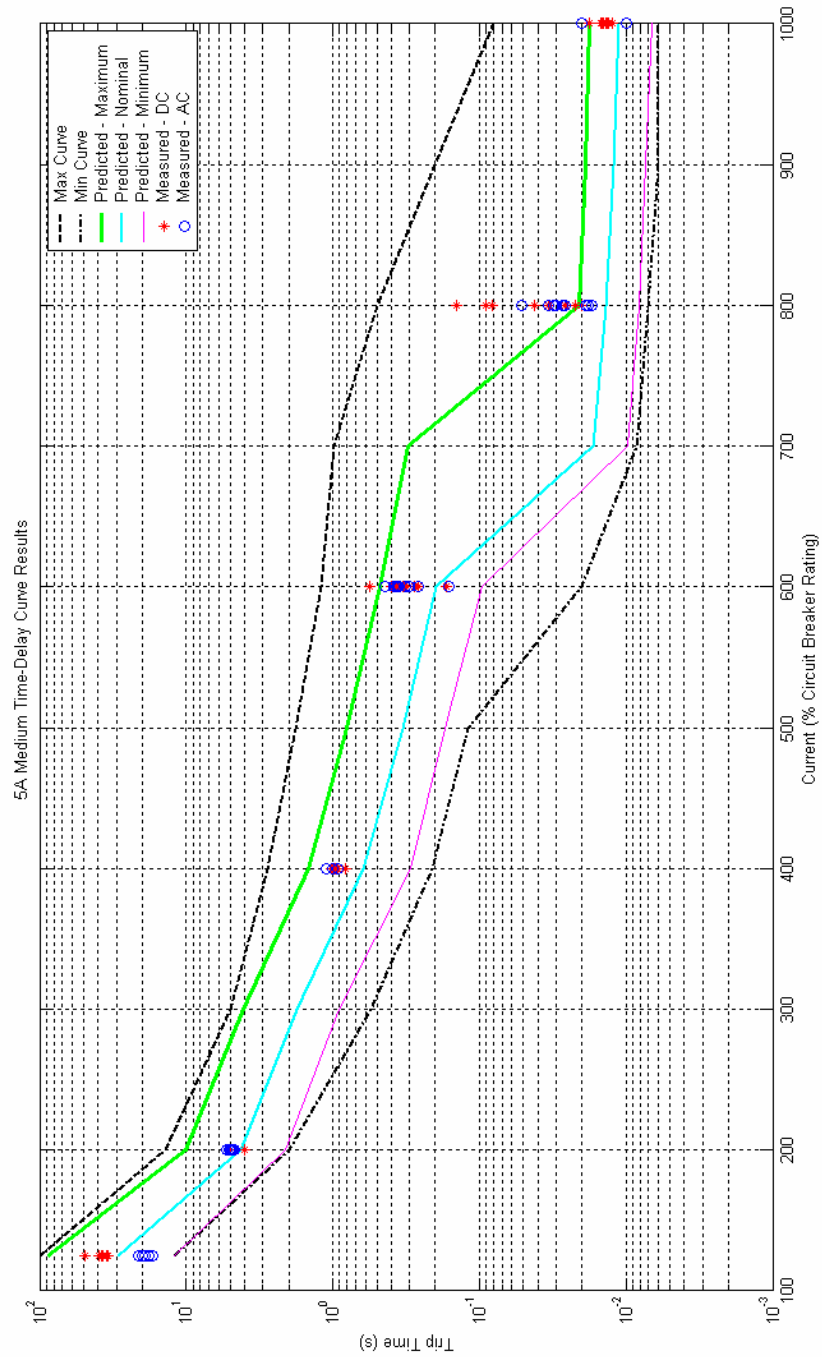


Figure A.9: 5A Circuit Breaker Medium Time-Delay Curve Results

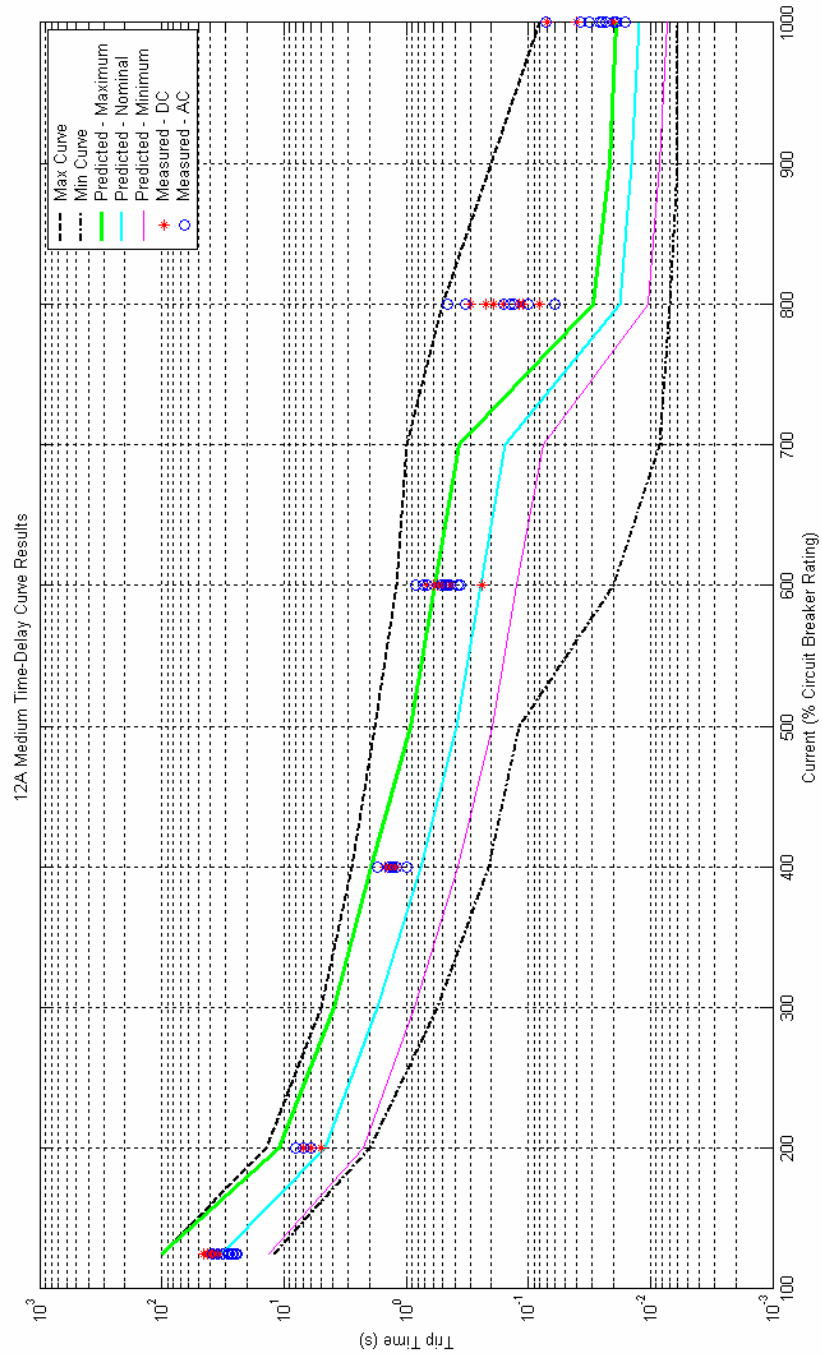


Figure A.10: 12A Circuit Breaker Medium Time-Delay Curve Results

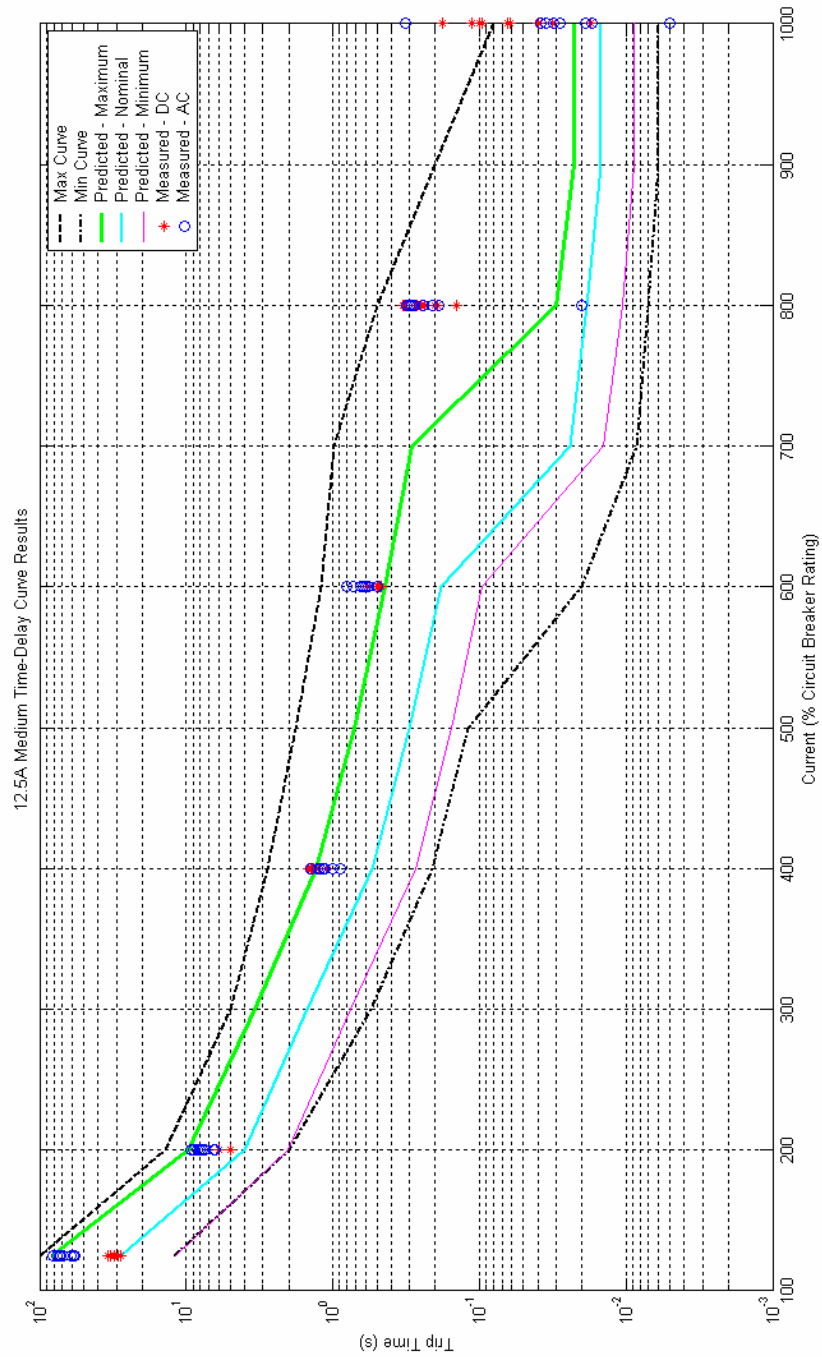


Figure A.11: 12.5A Circuit Breaker Medium Time-Delay Curve Results

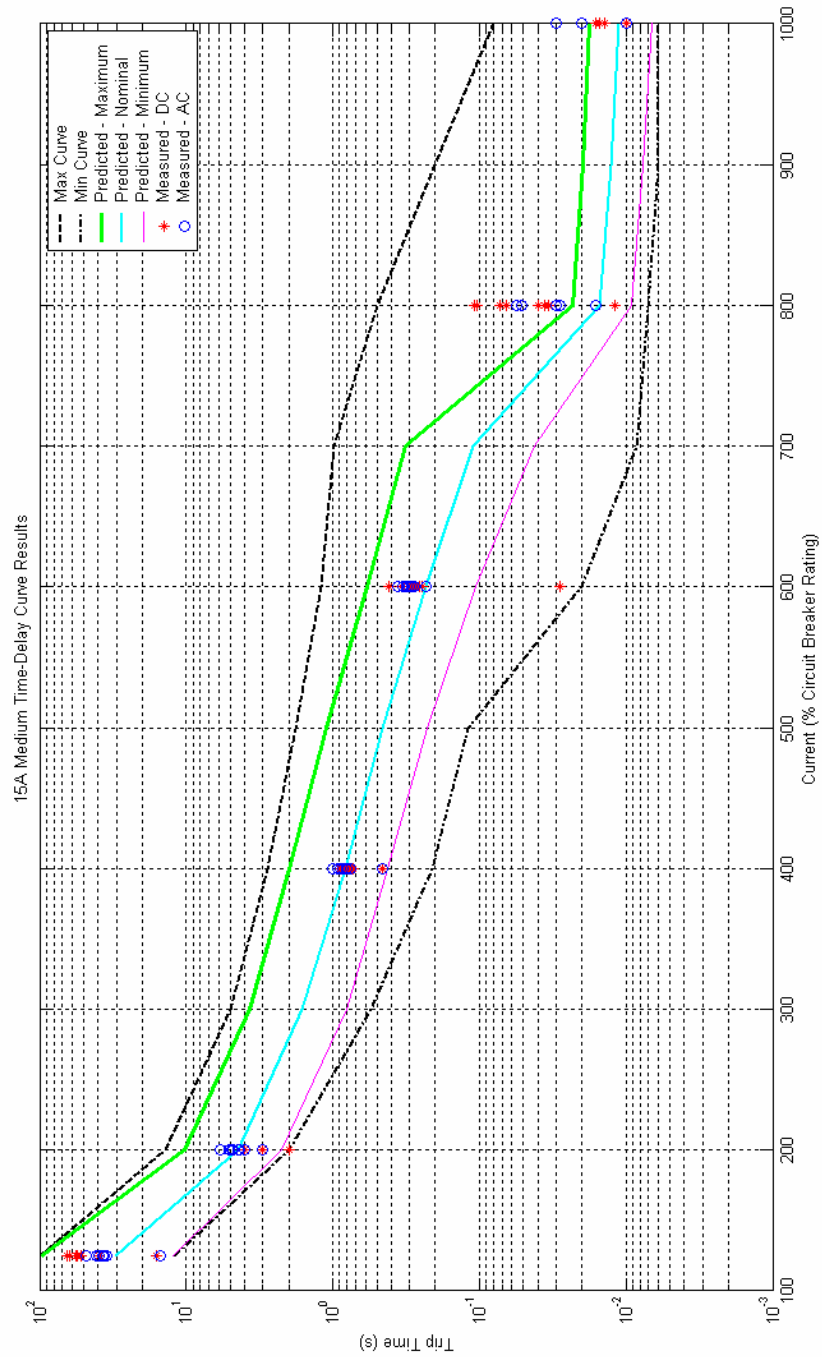


Figure A.12: 15A Circuit Breaker Medium Time-Delay Curve Results

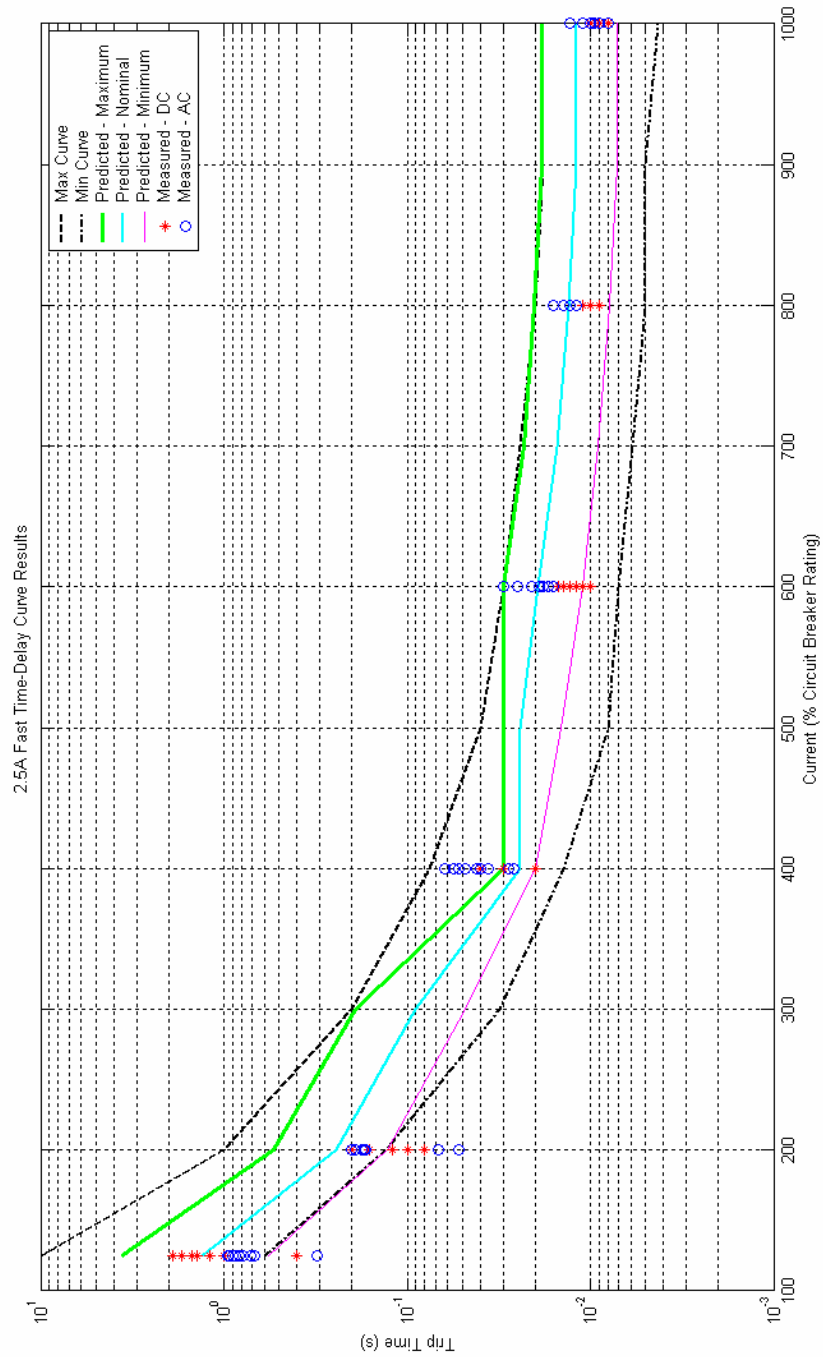


Figure A.13: 2.5A Circuit Breaker Short Time-Delay Curve Results

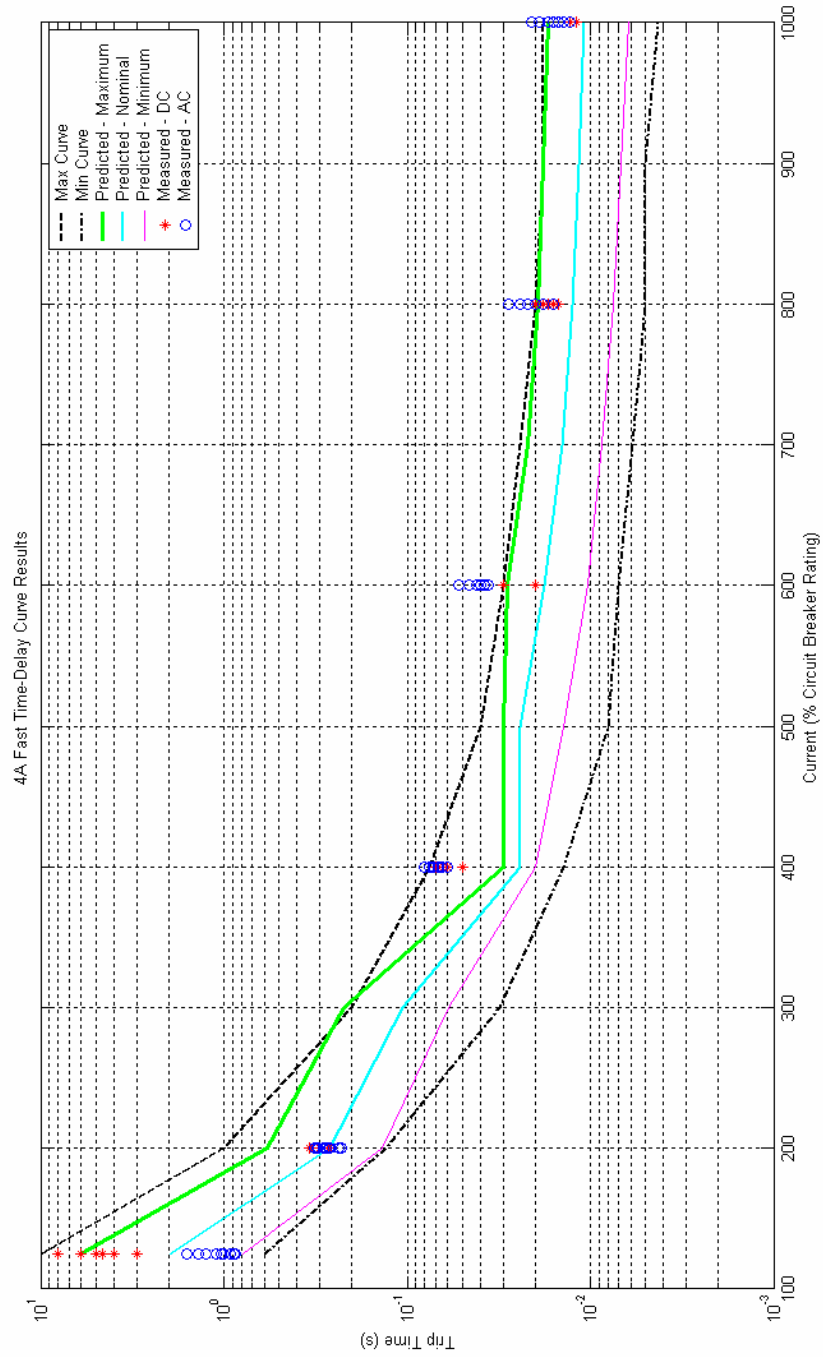


Figure A.14: 4A Circuit Breaker Short Time-Delay Curve Results

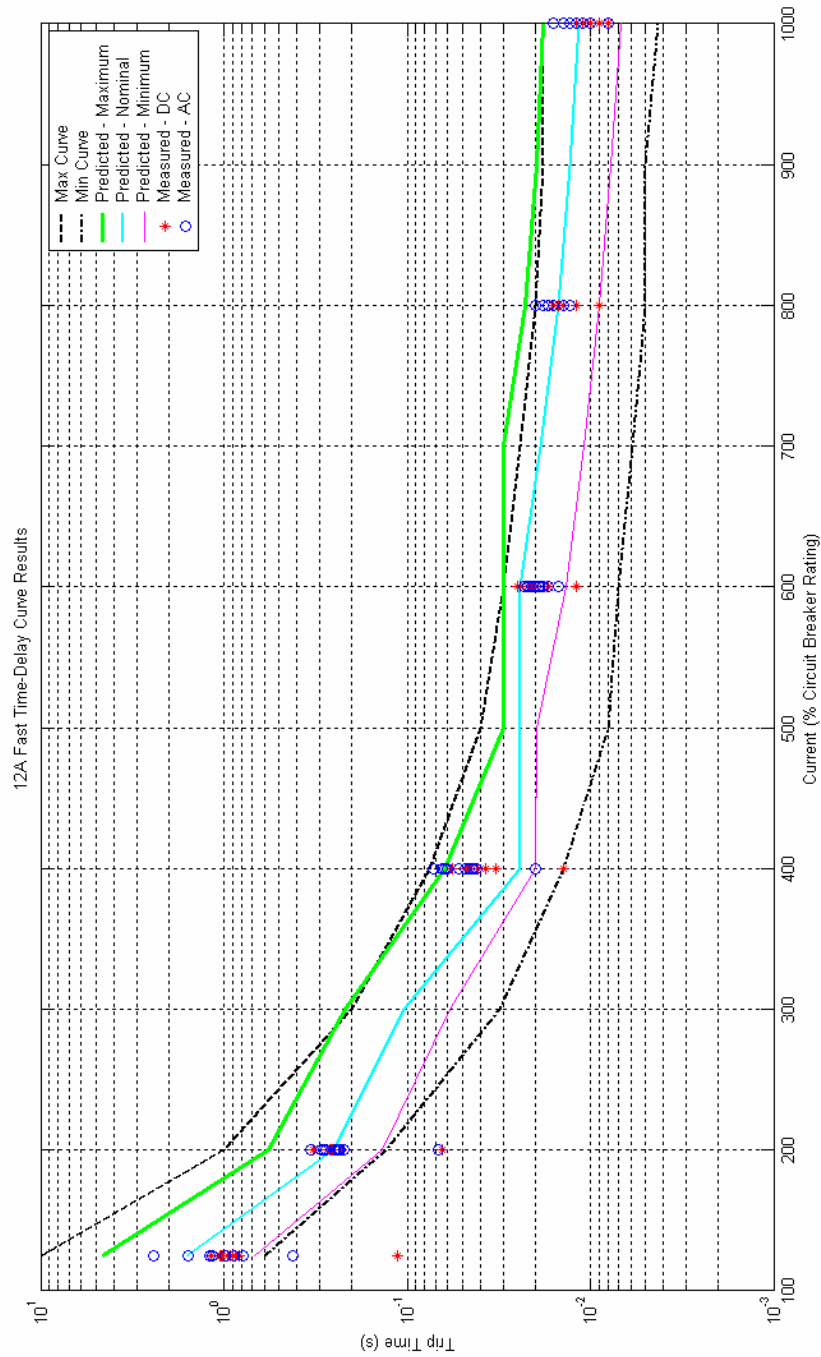


Figure A.15: 12A Circuit Breaker Short Time-Delay Curve Results

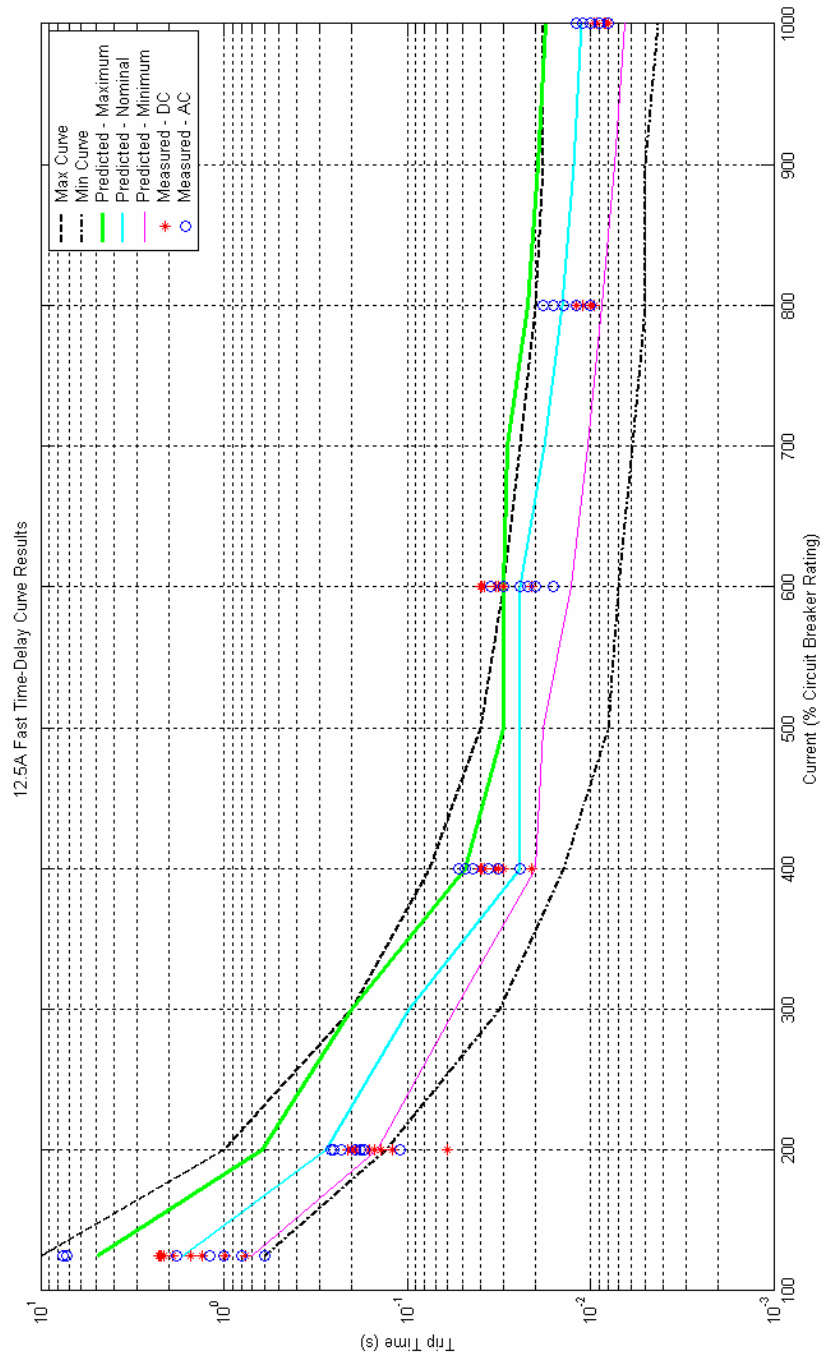


Figure A.16: 12.5A Circuit Breaker Short Time-Delay Curve Results